Chapter 2
General Forms of Limit Surface: Application for Isotropic Materials

Holm Altenbach and Vladimir A. Kolupaev

Abstract Limit surfaces are a tool used in theory of plasticity and failure analysis for dividing the safe from the unsafe regions. Their mathematical formulations are given by yield and strength criteria. The number of suggested criteria is unmanageable. By lack of the sufficient conditions only plausibility assumptions can limit this variety.

Typically, the TRESCA, VON MISES, and SCHMIDT-ISHLINSKY criteria are employed for the modeling of yielding. The effect of pressure-sensitivity is accounted for with the criteria of RANKINE and BURZYŃSKI-YAGN. Generalizations are obtained with linear combinations of these and further criteria. However, methods for the selection of efficient criteria for a particular application are still missing.

In this work, a nomenclature for isotropic yield criteria is introduced. Proposed systematization restricts the number of appropriate yield criteria. Global convexity limits for the yield criteria of trigonal and hexagonal symmetry are defined.

The basic idea is to find a general form of isotropic yield surface that satisfies the plausibility assumptions. This surface should contain possible yield surfaces lying between the lower and the upper bounds of the convexity restrictions. Any known or new criteria can then be considered as a special cases of the general criterion. The discussed yield criteria are extended for pressure-sensitive materials. The selection of the effective criterion for a particular application is simplified.

Key words: Equivalent stress, Deviatoric plane, Isogonal and isotoxal hexagon, Multi-axial loading

---

Holm Altenbach
Lehrstuhl für Technische Mechanik, Institut für Mechanik, Fakultät für Maschinenbau, Otto-von-Guericke-Universität Magdeburg, Universitätsplatz 2, 39106 Magdeburg, Germany,
e-mail: holm.altenbach@ovgu.de

Vladimir A. Kolupaev
Fraunhofer Institute for Structural Durability and System Reliability (LBF), Schloßgartenstr. 6, 64289 Darmstadt, Germany,
e-mail: Vladimir.Kolupaev@lbf.fraunhofer.de

H. Altenbach et al. (eds.), *Material Modeling and Structural Mechanics*,
Advanced Structured Materials 161, https://doi.org/10.1007/978-3-030-97675-0_2

2.1 Introduction

Engineering methods relate to macroeffects captured empirically. With the help of phenomenological criteria one can describe the beginning of yielding, damage or brittle failure of a certain material in a simplified way. The critical state of the sound material is represented only by the stresses, strains, and energetic or power considerations, at which the appropriate limit of a material is reached. Their gradients are not taken into account (Paul, 1968a,b).

In the case of stresses, a limit surface can be suggested in the principal stress space. A corresponding criterion is the mathematical expression taking into account of all points on the limit surface (Feodosjev, 1975; Franklin, 1971; Pisarenko and Lebedev, 1969; Skrzypek, 1993).

In order to formulate such criteria, the equivalent stress concept is typically used (Timoshenko, 1953). Within the concept, arbitrary stress states can be expressed as scalar quantities and compared to uniaxial tensile stress (Fromm, 1931) . Information about stress components and loading path is neglected (Paul, 1968a,b; Wu and Scheublein, 1974).

Uniaxial tensile properties can be readily measured in experiments. These data for different materials are compared in manuals, technical reports, and manufacturer's specifications. Solely, the proper criterion should be selected for design. Because of its simplicity and clarity, the equivalent stress concept found use in engineering applications.

Several criteria have been proposed over the last 150 years. They are summarized in numerous textbooks, see Altenbach et al. (1995); Bertram (2012); Pisarenko and Lebedev (1976); Potapova and Yarzev (2005); Skrzypek (1993); Yagn (1933); Yu (2004); Życzkowski (1981) among others. The amount of introduced criteria is remarkable. Until now, methods for comparison and selection of the most suitable criterion for a particular application are missing, see, for example, Lebedev (2010).

Further, choosing an appropriate criterion remains challenging because of generally incomplete data sets and their inevitable scattering. Trying to fit different criteria is intricate and the optimal evaluation cannot be guaranteed. In order to eliminate the necessity of a specific criterion selection, a general criterion is needed (Rosendahl et al., 2019b), cf. Voigt (1901).

In the present work, the geometric properties of isotropic yield criteria are examined. Global convexity limits of the yield criteria are defined and plausibility assumptions are listed. A general isotropic yield surface should be able to describe possible yield surfaces lying between the lower and the upper bounds of the convexity restrictions. Any known or new criteria can then be viewed as a special case of the general criterion and are, thus, secondary. The use of the general criterion with reasonable restrictions (Kolupaev et al., 2016; Kolupaev, 2018) prevents the risk of inappropriate extrapolations, cf. Życzkowski (1981).

In our work, a nomenclature of criteria based on their geometric properties is introduced. A general schematic for expressing pressure-insensitive yield criteria is provided. Known and new yield criteria are assigned to these schematic. This facilitates the selection of criteria for various applications. Critical gaps in the formulation of criteria are closed. The best known criteria are generalized considering the plausibility assumptions (Appendix 2.7.8). The parameters of the criteria are restricted based on the convexity condition in the π-plane (deviatoric plane).

A universally applicable yield criteria, which describe a single, convex, and C^0- or C^1-continuously surface are proposed. These contain extreme yield figures as the convexity restrictions. Using a I_1-substitution as a function of the trace of the stress tensor, the introduced criteria are applicable to pressure-sensitive materials. They incorporate various conditions to obtain special "theories". The versatility of the introduced criteria is sufficiently high, which may help to stop the growth of the amount of proposed criteria, cf. Habraken (2004).

The present work is organized as follows. Section 2.2 presents methods, requirements, and restrictions in the formulation of yield and strength criteria. In Sect. 2.3, the nomenclature of yield and strength criteria is introduced, which allows their descriptive comparison. In Sect. 2.4, the best known criteria in the authors' opinion are discussed and new criteria proposed. Strength criteria with the shape variation in π-plane are discussed in Sect. 2.5. The most important points of our work are summarized in Sect. 2.6.

2.2 Geometric Properties of Criteria

This section presents methods, requirements, and restrictions in the formulation of yield and strength criteria for isotropic materials. The geometric properties of the surfaces are analyzed and systematized, see also Pisarenko and Lebedev (1969, 1976); Lebedev (2010). Linear, quadratic, and cubic I_1-substitutions are introduced in order to obtain the pressure-sensitive generalization of the yield criteria.

2.2.1 Requirements for Yield and Strength Criteria

Yield surfaces for pressure-insensitive isotropic materials are described by a cylinder or a prism centred around the hydrostatic axis in principal stress space (Paul, 1968a,b)

$$\sigma_{\mathrm{I}} = \sigma_{\mathrm{II}} = \sigma_{\mathrm{III}}, \tag{2.1}$$

where σ_{I}, σ_{II}, and σ_{III} denote the principal stresses (Appendix 2.7.1). Such surfaces do not involve any restriction of hydrostatic stresses (**Fig. 2.1**).

Cross sections orthogonal to the hydrostatic axis are called deviatoric planes or π-planes (de Araújo, 1962; Życzkowski, 1981). Owing to isotropy, the cross sections in the π-plane must be of trigonal, hexagonal or rotational symmetry (**Fig. 2.2**).

Further, based on the DRUCKER postulate (Altenbach, 2018; Betten, 2001; Drucker, 1957, 1959), we require convex yield surfaces. Thus, basic cross sections may be described by a circle or regular polygons of trigonal or hexagonal symmetry

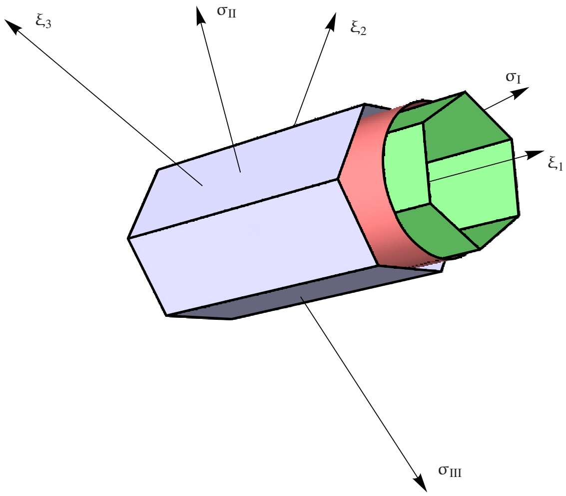

Fig. 2.1 Yield criteria of TRESCA (green), VON MISES (red), and SCHMIDT-ISHLINSKY (violet) in the principal stress space $(\sigma_{\rm I}, \sigma_{\rm II}, \sigma_{\rm III})$ and with coordinates (ξ_1, ξ_2, ξ_3) (Altenbach and Kolupaev, 2014).

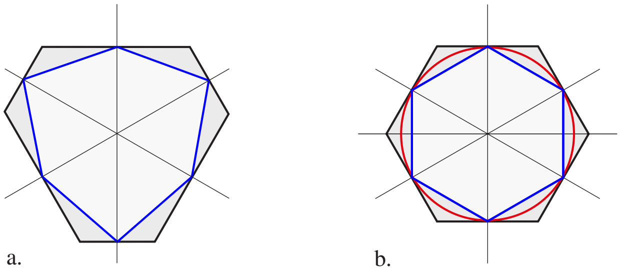

Fig. 2.2: Yield criteria in the π-plane normalized with respect to the appropriate uniaxial tensile limit loading $\sigma_0^{\rm T}$: a. Isogonal (black) and isotoxal (blue) hexagons of trigonal symmetry, b. Regular hexagons of the SCHMIDT-ISHLINSKY (black) and TRESCA (blue) criteria of hexagonal symmetry and the circle of the VON MISES criterion (red) of rotational symmetry (Rosendahl et al., 2019b).

in the π-plane (Rosendahl et al., 2019b, see also Pisarenko and Lebedev (1976); Lebedev (2010)): e.g. triangles, hexagons, enneagons (nine-sided polygons), dodecagons (twelve-sided polygons), among others. Each surface described by a regular polygon in the π-plane has a counterpart, which is obtained by its rotation by π/n in the π-plane about the hydrostatic axis, where n is the number of corners (**Fig. 2.3**).

All materials fail under sufficiently large hydrostatic tensile loading (Gol'denblat and Kopnov, 1971b; Kolupaev, 2018). In this case, the hydrostatic component of loading should be introduced in the yield criterion. Hence, the strength criteria restrict the hydrostatic tensile stress. With the convexity requirement on the meridian of the limit surface it follows

$$3\,\sigma^{\rm TTT} > \sigma_0^{\rm T}.$$

The surface can be open

$$\sigma^{\rm CCC} \to -\infty$$

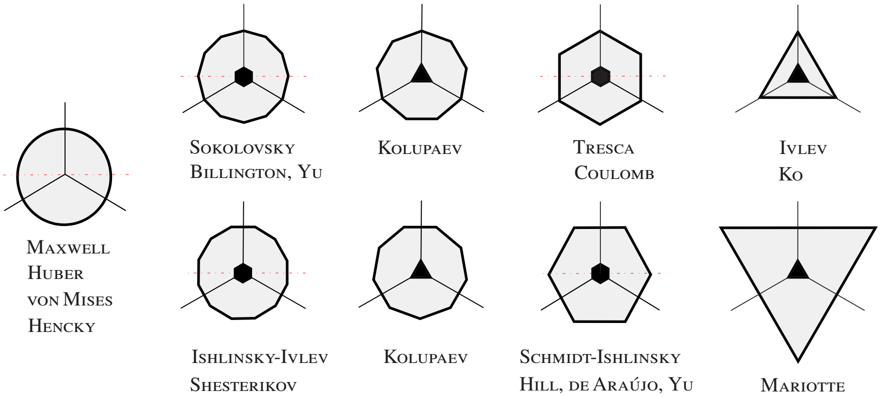

Fig. 2.3: Basic yield figures described by a circle and regular polygons of trigonal or hexagonal symmetry in the π-plane. The symbols of symmetry follow according to Nye (1985).

or closed

$$\sigma^{CCC} = \text{const.} < 0$$

in the direction $I_1 < 0$, where I_1 is the first invariant of the stress tensor (2.107). The superscripts T and C denote uniaxial tensile and compressive limit loading respectively. Accordingly, TTT denotes equitriaxial (hydrostatic) tensile limit loading and CCC - equitriaxial (hydrostatic) compressive limit loading (**Table 2.7**). The subscript 0 in σ_0^T refers to the stress angle $\theta = 0$ (2.112), see **Table 2.7**. Note that, the stress angle at the TTT and CCC loadings is indeterminate.

Criteria discussed in the present work are purely phenomenological. No sufficient conditions for their formulation can be given (Kolupaev, 2018). They are invented and, as a rule, not verified by multiaxial stress states (Wu and Scheublein, 1974). However, the quality of a certain yield or strength criterion may be assessed considering the plausibility assumptions (Appendix 2.7.8). These assumptions are not mandatory, but they allow to select user-friendly criteria for a wide range of applications.

2.2.2 Formulation of Yield and Strength Criteria

Yield and strength criteria for isotropic materials are invariant with respect to an arbitrary rotation of the coordinate system (Mālmeisters et al., 1977; Życzkowski, 1981). Therefore, such criteria are formulated using invariants of the stress tensor discussed in Appendix 2.7.1.

Functions of invariants are also invariants (Appendices 2.7.2-2.7.3). For the formulation of criteria Φ we may also use:

- the principal stresses (principal invariants) σ_{I}, σ_{II}, and σ_{III} (Altenbach et al., 1995; Haigh, 1920; Westergaard, 1920; Życzkowski, 1981)

$$\Phi\left(\sigma_{\mathrm{I}}, \sigma_{\mathrm{II}}, \sigma_{\mathrm{III}}, \sigma_{\mathrm{eq}}\right) = 0, \tag{2.2}$$

- the trace I_1 of the stress tensor and the invariants I_2', I_3' of the stress deviator (2.107) – (2.109) (Backhaus, 1983; Burzyński, 1928; Ottosen and Ristinmaa, 2005; Reuss, 1933; Sawczuk, 1982; Skrzypek, 1993; Yagn, 1931)

$$\Phi\left(\mathrm{I}_1, \mathrm{I}_2', \mathrm{I}_3', \sigma_{\mathrm{eq}}\right) = 0, \tag{2.3}$$

- the cylindrical invariants ξ, ρ, θ (2.110) – (2.112) (Lebedev, 2010; Murzewski, 1957, 1960; Novozhilov, 1951a,b; Ottosen and Ristinmaa, 2005)

$$\Phi\left(\xi, \rho, \theta, \sigma_{\mathrm{eq}}\right) = 0, \tag{2.4}$$

  and
- the spherical invariants ξ, ψ, and θ (2.110), (2.112), (2.113) (Altenbach and Kolupaev, 2014; Kolupaev, 2018; Lagzdin' and Tamuzh, 1971; Lebedev, 2010)

$$\Phi\left(\xi, \psi, \theta, \sigma_{\mathrm{eq}}\right) = 0. \tag{2.5}$$

In the formulations (2.4)–(2.5), the invariant ξ (2.110) is the scaled invariant I_1 and describes the coordinate of the loading on the hydrostatic axis, the radius ρ in the π-plane (2.111) is the scaled root of the second invariant I_2', and θ (2.112) is the corresponding stress angle in the π-plane. The radius ρ may be replaced by the stress triaxiality factor ψ (2.113) or (2.114), which yields a description of the surface in terms of the spherical invariants.

In addition, a big family of criteria include positive first principal stress

$$\sigma_{\max t} = \frac{1}{2}\left(|\sigma_{\mathrm{I}}| + \sigma_{\mathrm{I}}\right), \tag{2.6}$$

the hydrostatic stress I_1, and the second invariant of stress deviator I_2' to capture mixed mode (brittle and ductile) fracture. Examples are presented in Sdobyrev (1959); Trunin (1965); Hayhurst (1972); Altenbach and Naumenko (1997, 2002) among others. The (non-linear) functions of the maximum tensile stress, the hydrostatic stress and the von Mises equivalent stress is frequently used in damage evolution equations for the creep and creep-fatigue analysis. Examples are presented in Kowalewski et al. (1994); Othman et al. (1994); Dyson and McLean (2001); Altenbach et al. (2000); Naumenko et al. (2011).

All these formulations (2.2)–(2.5) are, from a mathematical point of view, equivalent. Formulation (2.2) has a historical origin and is primarily mentioned in textbooks of strength of materials and theory of plasticity in the discussion of the classical criteria. The Yu strength theory (YST) as a generalization of these classical criteria was firstly expressed in the principal stresses (Yu, 2004) and, later, in the axiatoric-deviatoric invariants (2.3) for visualizations of the meridional cross sections (cross section of the limit surface containing the hydrostatic axis) together with the line of the plane stress state (Kolupaev, 2018). Formulations according to (2.3) were intensively elaborated until the beginning of XXI century. Although such criteria are being developed, they are, as a rule, not user-friendly (Appendix 2.7.8, violated assumptions PP1, PP3, and PM1).

Equations (2.4)–(2.5) allow to manipulate the geometric properties of the surface Φ. Formulation (2.4) seems to be very effective in regard of the applicability and satisfaction of the plausibility assumptions (Appendix 2.7.8). Equation (2.5) has hardly found any practical application and is included for the sake of completeness: it is omitted from our discussions. One or the other of the Eqs. (2.2)–(2.5) may be preferred depending on the didactic targets, modeling concept, consideration the plausibility assumptions or desired application.

When pressure-insensitivity is assumed, the first invariant I_1 does not influence failure / yielding (Mālmeisters et al., 1977; Życzkowski, 1981). For this property, the Eqs. (2.3)–(2.4) can be reduced to

$$\Phi(I_2', I_3', \sigma_{eq}) = 0 \qquad \text{or} \qquad \Phi(\rho, \theta, \sigma_{eq}) = 0. \tag{2.7}$$

Polynomial formulations of $\Phi(I_2', I_3', \sigma_{eq})$ in terms of series of the deviatoric invariants I_2' and I_3' are well elaborated (Kolupaev, 2018) but cannot be recommended for application because of additional outer contours around the physically meaningful surface in the π-plane. As a rule, the equivalent stress σ_{eq} occurs implicitly in such equations.

In order to satisfy the assumption PM1 (Appendix 2.7.8), the equivalent stress σ_{eq} can be specified explicitly:

$$\sigma_{eq} = \Phi(\rho, \theta). \tag{2.8}$$

Such formulations are advantageous for iterative computations, e.g. in FEM codes. We may further postulate a multiplicative split of yield criteria into a function of radius $\Psi(\rho)$ and a function of the stress angle $\Omega(\theta)$ (Życzkowski, 1981)

$$\sigma_{eq} = \Psi(\rho)\,\Omega(\theta). \tag{2.9}$$

To highlight deviations of the shape of the surface in the π-plane from the circle of the VON MISES criterion (**Figs. 2.2** b, red circle, and **2.3**)

$$\sigma_{eq} = \sqrt{3I_2'} \qquad \text{with} \qquad \Omega(\theta) = 1, \tag{2.10}$$

the function of $\Psi(\rho)$ is often replaced by $\sqrt{3I_2'}$ (Giraldo-Londoño and Paulino, 2020; Kolupaev, 2017; Kolupaev et al., 2018; Lebedev, 2010), which yields

$$\sigma_{eq} = \sqrt{3I_2'}\,\Omega(\theta). \tag{2.11}$$

Normalizing criteria with respect to the appropriate uniaxial tensile limit loading, e.g., the tensile yield or strength σ_0^T (**Table 2.7**), leads to the final formulation

$$\sigma_{eq} = \sqrt{3I_2'}\,\frac{\Omega(\theta)}{\Omega(0)}, \tag{2.12}$$

which incorporates several well-known yield criteria and is beneficial for the application.

2.2.3 Pressure-sensitive Extension of Yield Criteria

Reintroducing the first invariant of the stress tensor I_1 in (2.12) using the substitution (Kolupaev, 2018)

$$\sigma_{eq} \to \left[\frac{\sigma_{eq} - \gamma_1\, I_1}{1-\gamma_1}\,\frac{\sigma_{eq} - \gamma_2\, I_1}{1-\gamma_2}\right]^{1/2} \qquad \text{with} \qquad \gamma_1 \in [0,\,1[\tag{2.13}$$

does not violate the assumption PM1 (Appendix 2.7.8). The reciprocal values of the parameters γ_1 and γ_2 describe the intersection of the limit surface with the I_1-axis (scaled space diagonal in the principal stress space). These points are called the hydrostatic nodes TTT and CCC (**Table 2.7**). The parameters γ_1 and γ_2 do not interact with other parameters of the criterion (2.12), and thus do not influence the shape of cross sections in the π-plane.

Therefore, the general equation of a second-order surface of revolution about the hydrostatic axis in the principal stress space can be formulated as a function of the coordinates of the hydrostatic nodes TTT and CCC (Altenbach, 2018; Altenbach and Kolupaev, 2014; Kolupaev, 2018)

$$3I_2' = \frac{\sigma_{eq} - \gamma_1\, I_1}{1-\gamma_1}\,\frac{\sigma_{eq} - \gamma_2\, I_1}{1-\gamma_2}. \tag{2.14}$$

A possibility of an explicit solution of (2.14) with respect to σ_{eq} was a widespread application of this criterion, which is known as the BURZYŃSKI-YAGN criterion.

The meridional cross sections of the rotationally symmetric criteria are shown in **Fig. 2.4**. The surfaces result with rotation of the corresponding line around the I_1-axis. The visualization of the criteria (2.14) in the $(I_1, \sqrt{3I_2'})$–plane (BURZYŃSKI-plane) is then obvious and allows a straightforward comparison with the VON MISES criterion (2.10) (**Fig. 2.4**, red line).

For materials, which do not fail under hydrostatic compression (brass, lead, steel, etc.), the surface Φ has a single hydrostatic node TTT. Based on (2.13) three substitutions are possible:

- linear substitution with $\gamma_1 = \gamma_2$, at which the hydrostatic nodes at the point TTT coincide,

$$\sigma_{eq} \to \frac{\sigma_{eq} - \gamma_1\, I_1}{1-\gamma_1} \qquad \text{with} \qquad \gamma_1 \in [0,\,1[\tag{2.15}$$

  provides straight meridian in the BURZYŃSKI-plane,

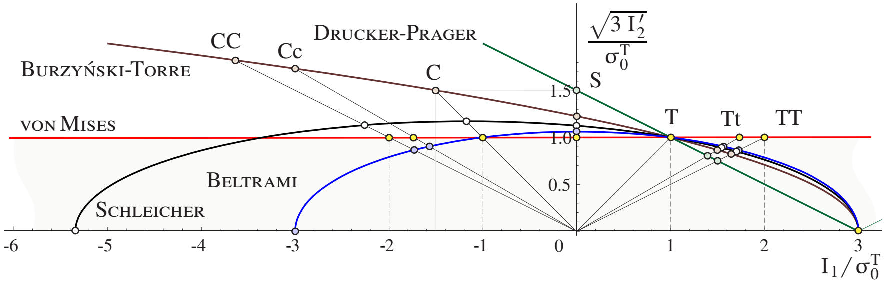

Fig. 2.4: Rotationally symmetric criteria with the setting $\gamma_1 = 1/3$ (point TTT) based on the normal stress hypothesis: cone of DRUCKER-PRAGER with $\gamma_2 = 1/3$, paraboloid of BURZYŃSKI-TORRE with $\gamma_2 = 0$, ellipsoid of SCHLEICHER with $\gamma_2 = (3-\sqrt{17})/6$, and ellipsoid of BELTRAMI with $\gamma_2 = -1/3$ in the BURZYŃSKI-plane $(\mathrm{I}_1, \sqrt{3\mathrm{I}_2'})$. The VON MISES criterion ($\gamma_1 = \gamma_2 = 0$, red line) is shown for comparison.

- the parabolic meridians follow with $\gamma_2 = 0$

$$\sigma_{\mathrm{eq}} \to \left[\frac{\sigma_{\mathrm{eq}} - \gamma_1 \mathrm{I}_1}{1-\gamma_1}\,\sigma_{\mathrm{eq}}\right]^{1/2} \qquad \text{with} \qquad \gamma_1 \in [0, 1[, \tag{2.16}$$

- and the hyperbolic meridians follow with $\gamma_2 \in]0, \gamma_1[$. The second node with the position $1/\gamma_2$ on the hydrostatic axis does not belong to the physically meaningful region of the surface Φ, which is most closed the coordinate origin, cf. Wu (1973); Yagn (1931). Due to this fact, the hyperbolic surfaces are not recommended for applications, cf. Balandin (1937).

For materials, which fail under hydrostatic compression (aerated concrete and ceramics, hard foams, sintered and granular materials, sandstone, etc.) the second hydrostatic node CCC is significant. The parameters in (2.14) are then bounded as follows

$$\gamma_1 \in]0, 1[\qquad \text{and} \qquad \gamma_2 < 0. \tag{2.17}$$

For the yield criteria (2.12), a pressure-sensitive extension (2.13) provides

$$\sqrt{3\mathrm{I}_2'}\,\frac{\Omega(\theta)}{\Omega(0)} = \left[\frac{\sigma_{\mathrm{eq}} - \gamma_1 \mathrm{I}_1}{1-\gamma_1}\,\frac{\sigma_{\mathrm{eq}} - \gamma_2 \mathrm{I}_1}{1-\gamma_2}\right]^{1/2}. \tag{2.18}$$

Suitable approximations are often obtained with the linear I_1-substitution Eq. (2.15)

$$\sqrt{3\mathrm{I}_2'}\,\frac{\Omega(\theta)}{\Omega(0)} = \frac{\sigma_{\mathrm{eq}} - \gamma_1 \mathrm{I}_1}{1-\gamma_1}, \tag{2.19}$$

which leads to conical and pyramidal surfaces in the principal stress space (Lebedev et al., 1979; Lebedev, 2010; Kolupaev et al., 2018; Paul, 1968a,b; Pisarenko and Lebedev, 1976; Rosendahl et al., 2019b; Wronski and Pick, 1977). It is to note, that the linear substitution produces an additional surface beyond of the hydrostatics node TTT (**Fig. 2.4**, DRUCKER-PRAGER cone)

$$\frac{I_1}{\sigma_0^T} \geqslant \frac{1}{\gamma_1}$$

without physical meaning and the apex at the hydrostatic tensile limit loading is C^0-continuously, what contradicts our perceptions and aggravates the computation of gradient of the surface Φ, see Appendix 2.7.8, assumptions PP3 and PG10. This quirk can be fixed by the parabolic I_1-substitution (2.16) or by "rounding off" with the C^1-transition as multisurface criterion (Kolupaev, 2018).

The cubic I_1-substitution in the yield criterion (2.12)

$$\sigma_{eq} \to \sqrt[j+l+m]{\left(\frac{\sigma_{eq} - \gamma_1 I_1}{1 - \gamma_1}\right)^j \left(\frac{\sigma_{eq} - \gamma_2 I_1}{1 - \gamma_2}\right)^l \sigma_{eq}^m} \tag{2.20}$$

with integer and positive powers j, l, and m

$$j + l + m = 3, \qquad j > 0, \qquad l \geqslant 0, \quad \text{and} \quad m \geqslant 0, \tag{2.21}$$

which control the curvature of the meridian, leads to additional fitting possibilities (Kolupaev, 2018). The equation of the criterion can be still resolved analytically with respect to σ_{eq}. As example, the rotationally symmetric criterion

$$\left(3I_2'\right)^{(3/2)} = \left(\frac{\sigma_{eq} - \gamma_1 I_1}{1 - \gamma_1}\right)^j \left(\frac{\sigma_{eq} - \gamma_2 I_1}{1 - \gamma_2}\right)^l \sigma_{eq}^m \quad \text{with} \quad \gamma_1 \in [0, 1[\tag{2.22}$$

can be introduced. The meridian with $l = m = 0$ is a straight line and with $l = 0$ is a parabola. For materials, that fail at hydrostatic compression, it follows $l > 0$ with $\gamma_2 < 0$.

Further I_1-substitutions, e.g. with integer and positive powers

$$j + l + m = 6 \tag{2.23}$$

are conceivable but, in general, can only be treated numerically. If the powers of the I_1-substitution (2.20) are chosen real for refined settings (Fahlbusch, 2015; Fahlbusch et al., 2016), the I_1-substitution with absolute values of the terms

$$\sigma_{eq} \to \sqrt[j+l+m]{\left|\frac{\sigma_{eq} - \gamma_1 I_1}{1 - \gamma_1}\right|^j \left|\frac{\sigma_{eq} - \gamma_2 I_1}{1 - \gamma_2}\right|^l \sigma_{eq}^m} \tag{2.24}$$

for numerical stability is recommended. Such substitutions are excluded from our consideration.

2.3 Designation and Comparison of Yield Criteria

A clear designation of the yield and strength criteria is proposed, what provides overview and simplifies their selection for application. The criteria are systematized in tables and diagrams. A method for comparing of yield criteria is presented, which allows to identify missing criteria.

2.3.1 Nomenclature of Yield Criteria

The mathematical expressions for the yield and strength criteria can be very different (Subsect. 2.2.2), which makes their comparison for the best adjustment not directly possible, cf. Matsuoka and Nakai (1985); Yu (2002); Kolupaev et al. (2009); Zhang et al. (2011); Lagioia and Panteghini (2016); Giraldo-Londoño and Paulino (2020); Xu et al. (2021) among others. A unique nomenclature and consequent designation of the criteria can be performed based on their geometric shapes in the π-plane and meridional cross sections.

Possible shapes of the yield criteria in the π-plane are constrained by the requirement of convexity (Subsect. 2.2.1). The upper and lower convexity limits are referred to as extreme yield figures (Sayir and Ziegler, 1969; Lebedev et al., 1979; Marti, 1980; Bigoni and Piccolroaz, 2004; Lebedev, 2010; Rosendahl et al., 2019b). Extreme yield figures may take the shape of isogonal and isotoxal polygons of trigonal or hexagonal symmetry. Regular polygons are limit cases of the extreme yield figures.

Isogonal polygons are equiangular. An isotoxal polygon is equilateral, that is, all sides are of the same length (Koca and Koca, 2011; Tóth, 1964). In general, isogonal and isotoxal hexagons are of trigonal symmetry (**Fig. 2.2**a). The regular hexagons of the TRESCA and SCHMIDT-ISHLINSKY criteria have an additional symmetry axis and are of hexagonal symmetry (**Figs. 2.2**b and **2.3**, **Table 2.1**). Isogonal and isotoxal dodecagons (twelve-sided polygons) are of hexagonal symmetry, too.

In this work, the basic (regular) yield figures are labeled according to their shapes in the π-plane (**Table 2.1**), cf. Rosendahl et al. (2019b):

- the designation ◯ reflects the VON MISES criterion,
- regular triangles are denoted with 3,
- regular hexagons with 6,
- regular enneagons with 9,
- regular dodecagons with 12,
- regular octadecagon with 18,
- regular icositetragons with 24,
- regular triacontahexagon (Modarres-Motlagh, 1997) with 36, etc.

Further regular polygons with the number of corners divisible by three

- pentadecagons denoted with 15,

- icosihenagons with 21
- icosiheptagons with 27,
- triacontagons with 30,
- triacontatrigons with 33, etc.

are also accepted as yield criteria for isotropic materials, but they has low practical significance. References of them were not found in the literature. These shapes are only mentioned for sake of completeness.

Circumflex ˆ and macron ¯ refer to an upward pointing tip or upward facing flat base of the criterion in the π-plane, respectively (**Fig. 2.3**). The designation of the discussed regular polygons is shown in **Table 2.1**. Further references of the criteria are given in Kolupaev (2018). The aim of the designation is a visual representation of the basic yield figures included in the discussed criteria (**Tables 2.2–2.5**).

Limit surfaces for isotropic materials can be characterized by the regular polygons and the circle in the π-plane they include. For example, the MOHR-COULOMB criterion contains the regular triangle of the RANKINE and regular hexagon of the TRESCA criteria in border cases (**Table 2.4**). The criteria involving less than three of the regular geometries can be considered as special cases of the general formulation and are excluded from our discussion. The limitation to three regular geometries is motivated in Subsect. 2.3.3.

Generalized yield criteria involving three or more basic geometries are significant for application. The number of their parameters should not exceed two. The remained criteria are easily manageable (**Tables 2.2** and **2.5**). However, the assumption, that the criteria should be a single surface in principal stress space, is fulfilled only for criteria marked as equations in **Table 2.2**. Such criteria are functions of the stress angle θ (2.12).

The ordinary pressure-sensitive generalizations of yield criteria, what are of invariable shape in the π-plane, are listed in **Table 2.3**. They are quite simple for real materials. Typical criteria with brittle-ductile transition, obtained as linear combinations of the non-parametric yield criteria of rotational or hexagonal symmetry with the maximum normal stress hypothesis (RANKINE criterion, NSH), are listed in **Table 2.4**, see also Lüpfert (1994). Although such criteria are particular, they are often used because of the lack of measured data. Their approximation with the DRUCKER-PRAGER cone (**Fig. 2.4**) given in some textbooks, is secondary.

In our consideration, further criteria are not effective for application. For example, the LEMAITRE-CHABOCHE yield criterion "intermediary between those of VON MISES and TRESCA" as function of I_2' and I_3' invariants with one parameter additionally to σ_{eq} (Lemaitre and Chaboche, 1985, 1990), see also Altenbach et al. (1995); Altenbach (2018); Jirásek and Bažant (2002); Koval'chuk (1981); Kroon and Faleskog (2013); Takeda et al. (1986) describing the transition

$$\hat{6} - \bigcirc$$

can be replaced with the SZWED criterion with also one parameter (**Table 2.2**)

$$\hat{6} - \bigcirc - \bar{6}.$$

The C^0-yield criterion of Altenbach-Zolochevsky with two parameters (Altenbach et al., 1995; Altenbach, 2001; Altenbach and Kolupaev, 2014)

$$\hat{3} - \hat{6} \,|\, \bigcirc - \bar{3}$$

can be replaced with the modified Altenbach-Zolochevsky C^0-yield criterion with the same number of parameters (Kolupaev, 2017, 2018; Kolupaev et al., 2018; Rosendahl et al., 2019b)

$$\hat{3} - \hat{6} \,|\, \widehat{12} \,|\, \bar{6} - \bar{3}.$$

The symbol | is explained in **Table 2.2**. Here, only one C^1-criterion of von Mises is replaced with the regular dodecagon $\widehat{12}$. The definition range of the modified formulation is significantly larger.

The Leckie-Hayhurst strength criterion (Hayhurst, 1972; Leckie and Hayhurst, 1977) with two parameters

$$\bigcirc + \mathrm{NSH} + \mathrm{I}_1 \quad \text{or, equivalently,} \quad \bigcirc - \bar{3} \to \mathrm{I}_1,$$

where symbol $\to$ denotes the linear I_1-substitution (2.15) and symbol $+$ denotes convex combination, can be substituted with the Sayir pyramid (Kolupaev, 2018) with also two parameters

$$\hat{3} - \bigcirc - \bar{3} \to \mathrm{I}_1$$

but with the larger definition range. However, the Podgórski pyramid with three parameters and significantly larger definition range (**Table 2.5**)

$$\hat{3} - \hat{6} \,|\, \bigcirc - \bar{3} \to \mathrm{I}_1$$

is clearly preferable. Further most important strength criteria are summarized in **Table 2.5**.

The strength criteria with the shape variation in π-plane are discussed in Sect. 2.5. They are not part of the designation and systematization.

2.3.2 Comparison of Yield Criteria

Measured data are normalized by the appropriate tensile limit loading

$$\left(\frac{\sigma_{\mathrm{I}}}{\sigma_0^{\mathrm{T}}}, \frac{\sigma_{\mathrm{II}}}{\sigma_0^{\mathrm{T}}}, \frac{\sigma_{\mathrm{III}}}{\sigma_0^{\mathrm{T}}} \right),$$

so that mechanical properties become unitless. The surfaces Φ for different isotropic materials can be now compared in the same diagrams.

We distinguish pressure-insensitive yield criteria (2.7), which are comprehensively described in the π-plane and pressure-sensitive strength criteria (2.3)–(2.4). Certain types of loading for pressure-insensitive materials coinside in the π-plane

Table 2.1: Basic criteria in the π-plane (Subsect. 2.3.1).

π-plane		 $\hat{3}$ IVLEV	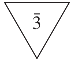 $\bar{3}$ MARIOTTE	 $\hat{6}$ TRESCA	 $\bar{6}$ SCHMIDT-ISHLINSKY
Geometry	r_{15}	$\sqrt{2}/2$	$\sqrt{2}\left(\sqrt{3}-1\right)$	$\sqrt{3/2}\left(\sqrt{3}-1\right)$	$\sqrt{2}\left(\sqrt{3}-1\right)$
	r_{30}	$1/\sqrt{3}$	$2/\sqrt{3}$	$\sqrt{3}/2$	$2/\sqrt{3}$
	r_{60}	1/2	2	1	1
Pdg	β_3	$\{0,1\}$	$\{1,0\}$	$1/2$	–
	η_3	$\{-1,1\}$	$\{-1,1\}$	$\{-1,1\}$	–
Rsn	β_6	–	–	$\{1,0\}$	$\{0,1\}$
	η_6	–	–	$\{1,-1\}$	$\{1,-1\}$
mAZ3	β_3	1	0	$1/2$	$[0,1]$
	α	1	1	1	0
mAZ6	β_6	–	–	1	0
	α	–	–	1	1
References		Ivlev (1959) Cicala (1961) Ko (1963) Bishop (1966) Kolupaev (2018) Rosendahl et al. (2019b)	Mariotte (1718) Shanley (1957) Ivlev (1959) Finnie and Heller (1959) Sayir and Ziegler (1969) Benvenuto (1991)	Coulomb (1776) Tresca (1868) Reuss (1933) Yagn (1933) Prager and Hodge (1954) Życzkowski (1981)	Burzyński (1928) Schmidt (1932) Ishlinsky (1940) Hill (1950); Yu (1961) Haythornthwaite (1961a) de Araújo (1962)

Abbreviation: Pdg – PODGÓRSKI and Rsn – ROSENDAHL criteria, see **Table 2.2**

Table 2.1: Continuation.

		SOKOLOVSKY	ISHLINSKY-IVLEV	ROSENDAHL	ROSENDAHL	VON MISES
π-plane		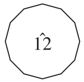	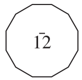	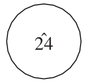	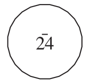	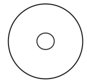
Geometry	r_{15}	$\frac{1}{2}\sqrt{2+\sqrt{3}}$	$\sqrt{2}\left(\sqrt{3}-1\right)$	1	1	1
	r_{30}	1	1	1	1	1
	r_{60}	1	1	1	1	1
Pdg	β_3	–	–	–	–	$[0,1]$
	η_3	–	–	–	–	0
Rsn	β_6	$1/2$	–	–	–	$[0,1]$
	η_6	$\{1,-1\}$	–	–	–	0
mAZ3	β_3	$1/2$	–	–	–	–
	α	$2\sqrt{3}-3$	–	–	–	–
mAZ6	β_6	$1/2$	$[0, 1]$	$1/2$	–	–
	α	1	0	0.4913	–	–
References		Prager (1956) Yu (1961) Pisarenko and Lebedev (1976) Haythornthwaite (1983) Billington (1986) Owen and Hinton (1986)	Ivlev (1960) Shesterikov (1960) Lequeu et al. (1987) Yu (1999) Ishlinsky and Ivlev (2003) Altenbach (2018)	Kolupaev (2018) Rosendahl et al. (2019b)	Rosendahl et al. (2019b) Rosendahl (2020)	Huber (1904) von Mises (1913) Föppl and Föppl (1920) Hencky (1924) Yagn (1933) Skrzypek (1993)

Table 2.2: Designation of the most important yield criteria according Kolupaev (2018); Rosendahl et al. (2019b).

Name	Abbreviation	Designation	Eq.	Parameters	References
Capurso (Ivlev)	-	$\hat{3}-\hat{6}-\bar{3}$	-	1	Capurso (1967); Ivlev (1959); Sayir (1970)
Sayir cubic criterion	CC	$\hat{3}-\bigcirc-\bar{3}$	(2.47)	1	Betten (1976); Sayir (1970); Sayir and Ziegler (1969)
Haythornthwaite	-	$\hat{3}-\bar{6}-\bar{3}$	-	1	Candland (1975); Haythornthwaite (1961b, 1962)
Yu yield criterion	YYC	$\hat{6}-\hat{12}-\bar{6}$	-	1	Yu (2002, 2004, 2017); Yu and Yu (2019)
mod. Yu yield criterion	mYu	$\hat{6}-\hat{12}-\bar{6}$	(2.50)	1	Kolupaev (2017, 2018); Rosendahl et al. (2019b)
Szwed bicubic criterion*	BCC	$\hat{6}-\bigcirc-\bar{6}$	(2.53)	1	Szwed (2000, 2010, 2013)
Multiplicative ansatz criterion	MAC	$\hat{6}-\bar{12}-\bar{6}$	-	1	Kolupaev (2018); Kolupaev and Altenbach (2010); Kolupaev et al. (2013a)
Podgórski**	Pdg	$\hat{3}-\hat{6}\,\vert\,\bigcirc-\bar{3}$	(2.45)	2	Podgórski (1983, 1984); Podgórski (1985, 1986)
Rosendahl	Rsn	$\hat{6}-\hat{12}\,\vert\,\bigcirc-\bar{6}$	(2.50)	2	Rosendahl (2020); Rosendahl et al. (2019b)
C^0-criterion of trig. sym.	C^0-CTS	$\hat{3}-\hat{6}\,\vert\,\hat{12}\,\vert\,\bar{6}-\bar{3}$	(2.65)	2	Kolupaev (2017, 2018); Rosendahl et al. (2019b)
Capurso + Haythornthwaite	C^1-CTS	$\hat{3}-\hat{6}\,\vert\,\bigcirc\,\vert\,\bar{6}-\bar{3}$	-	2	Altenbach et al. (2014); Bolchoun et al. (2011); Kolupaev (2018)
C^0-criterion of hex. sym.	C^0-CHS	$\hat{6}-\hat{12}\,\vert\,\hat{24}\,\vert\,\bar{12}-\bar{6}$	(2.74)	2	Rosendahl (2020); Rosendahl et al. (2019b)
YYC + MAC	C^1-CHS	$\hat{6}-\hat{12}\,\vert\,\bigcirc\,\vert\,\bar{12}-\bar{6}$	-	2	Kolupaev (2018); Kolupaev et al. (2013c)

Comments: * - supplementary sources Barlat et al. (1991); Habraken (2004); Hershey (1954); Hosford (1972, 1979); Karafillis and Boyce (1993); Lagzdin' (1997); Lagzdiņš and Zilaucs (1996); Paul (1968b); Tan (1990) and our references Kolupaev (2018); Kolupaev and Altenbach (2010); ** - supplementary sources Bigoni and Piccolroaz (2003, 2004); Lagioia and Panteghini (2016); Lagioia et al. (2016); Szwed (2000, 2010, 2013) and our investigations Kolupaev (2017, 2018); Rosendahl (2020); Rosendahl et al. (2019b). The symbol | refers the vertical line in the diagrams **Figs. 2.8** and **2.9**.

Table 2.3: Designation of the strength criteria of invariable shape in the π-plane.

Name	Abbreviation	Designation	Eq.	Parameters	References
Drucker-Prager (Mirolyubov)	DP	$\bigcirc \rightarrow I_1$	-	1	Botkin (1940a,b); Drucker and Prager (1952); Mirolyubov (1953)
Burzyński-Yagn	-	$\bigcirc \rightarrow I_1^2$	(2.14)	2	Burzyński (2008); Yagn (1931); Stassi-D'Alia (1967)
Rankine	NSH	$\bar{3} \rightarrow I_1$	(2.135)	1	Ismar and Mahrenholtz (1982); Rankine (1876); de Saint-Venant (1871)
Mariotte-St. Venant	SC	$\bar{3} \rightarrow I_1$	-	1	Benvenuto (1991); Mariotte (1718); Shanley (1957)
Ko (Ivlev) pyramid	-	$\hat{3} \rightarrow I_1$	-	1	Ko (1963); Ivlev (1959); Tschoegl (1971)
Schmidt-Ishlinsky pyramid	-	$\bar{6} \rightarrow I_1$	-	1	Kolupaev (2006, 2018)
Sandel (Drucker) pyramid	-	$\hat{6} \rightarrow I_1$	-	1	Drucker (1953); Sandel (1919, 1925)
Ishlinsky-Ivlev pyramid	-	$\bar{12} \rightarrow I_1$	-	1	-
Sokolovsky pyramid	-	$\hat{12} \rightarrow I_1$	-	1	-

Comments: strain criterion (SC) contains the maximum normal stress hypothesis (NSH) with the setting $\gamma_1 = 1/3$ or, equally, the Poisson's ratio $\nu_+^{\text{in}} = 0$ (Appendix 2.7.6); The symbol $\rightarrow$ denotes the substitutions: I_1 - linear substitution (2.15) and I_1^2 – quadratic substitution (2.13).

Table 2.4: Designation of the strength criteria with the classical properties $r_{60}^{\mathrm{TT}} = 1$ and $r_{60}^{\mathrm{C}} = r_0^{\mathrm{CC}}$ (2.39) obtained with the linear combination based on the criterion of hexagonal or rotational symmetry with the NSH and describing brittle-ductile transition.

Name	Abbreviation	Designation	Eq.	Parameters	References
MOHR-COULOMB (single shear theory)	MC	$\hat{6}+$NSH	-	1	Mohr (1900a,b, 1914); Yu (2002, 2004, 2017)
PISARENKO-LEBEDEV (SDOBYREV)	PL	$\bigcirc+$NSH	-	1	Lebedev (1965); Pisarenko and Lebedev (1976); Sdobyrev (1959)
YU octahedral-shear theory	OST	$\hat{12}+$NSH	-	1	Yu (2002, 2004, 2017, 2018)
YU twin shear theory	TST	$\bar{6}+$NSH	-	1	–"–
-	-	$\bar{12}+$NSH	-	1	-

Comments: symbol + refers linear combination of the respective yield criterion with the NSH (Subsect. 2.3.1).

Table 2.5: Designation of the most important strength criteria. The number of parameters is given additionally to the equivalent stress $\sigma_{\mathrm{eq}} = \sigma_0^{\mathrm{T}}$.

Name	Abbreviation	Designation	Eq.	Parameters	References
PODGÓRSKI pyramid	-	$\hat{3}-\hat{6} \mid \bigcirc - \bar{3} \to I_1$	(2.48)	3	Kolupaev (2017, 2018); Rosendahl et al. (2019b)
ROSENDAHL pyramid	-	$\hat{6}-\hat{12} \mid \bigcirc - \bar{6} \to I_1$	(2.54)	3	Sect. 2.4.2.2
YU strength theory	YST	$\hat{6}-\hat{12}-\bar{6}+$NSH	-	2	Yu (2002, 2004, 2017, 2018)
ROSENDAHL + NSH	-	$\hat{6}-\hat{12} \mid \bigcirc - \bar{6}+$NSH	(2.89)	3	Sect. 2.4.4.1
-	C^0-CTS $\to I_1$	$\hat{3}-\hat{6} \mid \hat{12} \mid \bar{6}-\bar{3} \to I_1$	(2.73)	3	Rosendahl et al. (2019b)
-	C^1-CTS $\to I_1$	$\hat{3}-\hat{6} \mid \bigcirc \mid \bar{6}-\bar{3} \to I_1$	-	3	Kolupaev (2018)
-	C^0-CHS $\to I_1$	$\hat{6}-\hat{12} \mid \hat{24} \mid \bar{12}-\bar{6} \to I_1$	(2.82)	3	Sect. 2.4.3.5
-	C^1-CHS $\to I_1$	$\hat{6}-\hat{12} \mid \bigcirc \mid \bar{12}-\bar{6} \to I_1$	-	3	Sect. 2.4.3.2
extended C^0-YST	C^0-CHS+NSH	$\hat{6}-\hat{12} \mid \hat{24} \mid \bar{12}-\bar{6}+$NSH	-	3	Sect. 2.4.4.1
extended C^0-YST	C^0-CHS+NSH	$\hat{6}-\hat{12} \mid \bigcirc \mid \bar{12}-\bar{6}+$NSH	-	3	Sect. 2.4.4.1
extended C^1-YST	CHS+C^1-NSH	$\hat{6}-\hat{12} \mid \bigcirc - \bar{6}+C^1$-NSH	(2.97)	4	Sect. 2.4.4.2

Comments: symbol | refers the vertical line in the diagrams **Figs. 2.8** and **2.9**; I_1 - linear substitution (2.15), CTS – criterion of trigonal symmetry, CHS – criterion of hexagonal symmetry (**Table 2.2**.)

(**Fig. 2.5**): equal stress angle θ share the same radius ρ (2.111) and collapse onto one point. Introducing the corresponding nomenclature (**Table 2.7**) these are:

- $\theta = 0$: T (uniaxial tension) and CC (equibiaxial compression),
- $\theta = \pi/6$: S (shear), Tt (biaxial tension with $I_3' = 0$), and Cc (biaxial compression with $I_3' = 0$), and
- $\theta = \pi/3$: TT (equibiaxial tension) and C (uniaxial compression).

The values of radii ρ at these stress angles θ are characteristic properties of the yield surface (**Figs. 2.6** and **2.7**).

Pressure-sensitive strength criteria have additional characteristic values because of their I_1-dependence (Subsect. 2.2.3). In order to visualize pressure-sensitive criteria,

- certain cross sections $I_1 = \text{const.}$, e.g. through the particular points T, TT, C, CC, S, Tt, and Cc of the plane stress states (**Table 2.7**) and
- the $(I_1, \sqrt{3I_2'})$-plane (**Fig. 2.4**)

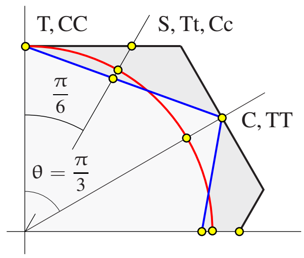

Fig. 2.5 Isogonal (black) and isotoxal (blue) hexagons in the π-plane normalized by the appropriate limit tensile loading σ_0^T (**Fig. 2.2**a): Enlarged detail with the VON MISES criterion (red) and the stress states (T, CC on the 0-meridian, S, Tt, Cc on the $\pi/6$-meridian, and C, TT on the $\pi/3$-meridian) for comparison (Rosendahl et al., 2019b).

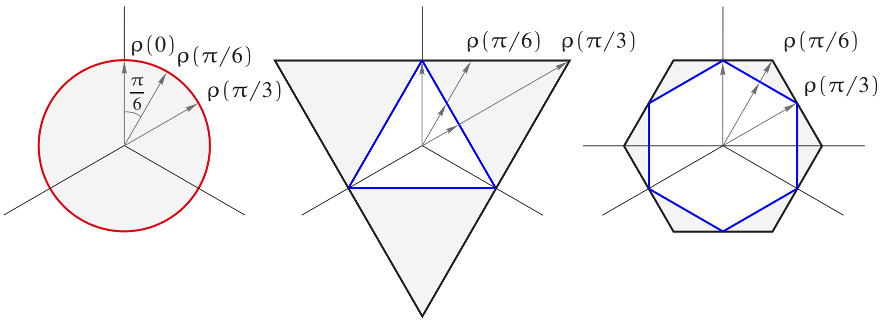

a. $r_{30} = r_{60} = 1$ b. $r_{60} \in \{1/2, 2\}$ c. $r_{60} = 1$

Fig. 2.6: Basic surfaces with the same radius $\rho(0)$ in the π-plane: a. Rotationally symmetric VON MISES criterion (2.10), b. Regular triangles $\hat{3}$ and $\bar{3}$, and c. Regular hexagons $\hat{6}$ and $\bar{6}$. The values r_{30} and r_{60} (2.26) are given for comparison (Rosendahl et al., 2019b).

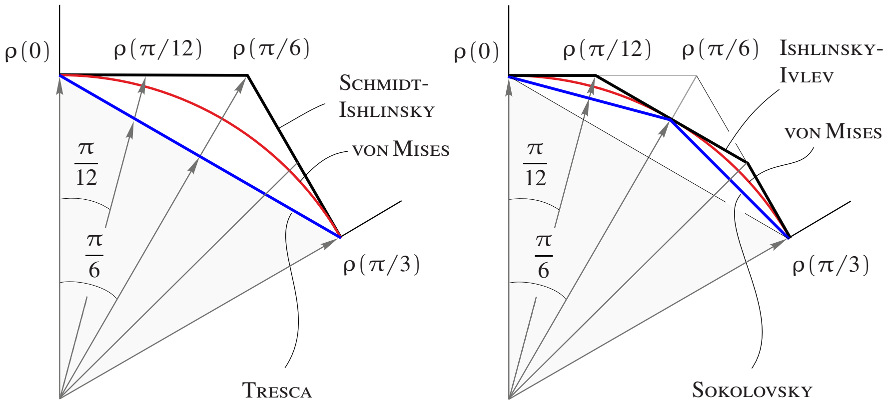

a. $r_{60} = 1$ b. $r_{30} = r_{60} = 1$

Fig. 2.7: Basic surfaces of hexagonal symmetry in the π-plane: a. Regular hexagons $\hat{6}$ and $\bar{6}$ and b. Regular dodecagons $\hat{12}$ and $\bar{12}$ with the VON MISES criterion (2.10). Because of hexagonal symmetry a cut-out of the angle $\theta \in [0, \pi/3]$ is representative (Kolupaev, 2018; Rosendahl et al., 2019b).

with the projection of the meridians $\theta =$ const. and the lines of the plane stress state are needed. Some examples of visualization are given in Altenbach et al. (2014); Kolupaev (2006, 2017, 2018); Kolupaev and Altenbach (2010); Kolupaev et al. (2013b, 2016, 2018); Rosendahl et al. (2019b).

The plane stress $\sigma_{\mathrm{I}} - \sigma_{\mathrm{II}}$ diagram with $\sigma_{\mathrm{III}} = 0$ is not representative for 3D-modeling of the limit surface. However, measured data gained with conventional experimental technique are traditionally shown in this diagram. The meridians $\theta = 0$, $\pi/6$, and $\pi/3$ of the surface Φ can be projected in this diagram. It helps conditionally to check approximations by the fitting to the measured data and to visualize the points of the hydrostatic limit loading by different extrapolations (Kolupaev, 2018). The comparison of approximations in the $\sigma_{11} - \tau_{12}$ diagram is not recommended. Here, numerous effects are invisible.

2.3.3 Shapes of Yield Criteria in the π-plane

Cross sections of pressure-insensitive criteria (2.7) may be described in the π-plane as functions $\rho(\theta)$. Let us introduce geometric properties as relations of radii at the angles

$$\theta = \frac{\pi}{24}, \frac{\pi}{12}, \frac{\pi}{8}, \frac{\pi}{6}, \frac{\pi}{4}, \quad \text{and} \quad \frac{\pi}{3} \tag{2.25}$$

to the radius $\rho(0)$ as

$$\begin{aligned} r_{7.5} &= \frac{\rho(\pi/24)}{\rho(0)}, \; r_{15} = \frac{\rho(\pi/12)}{\rho(0)}, \; r_{22.5} = \frac{\rho(\pi/8)}{\rho(0)}, \\ r_{30} &= \frac{\rho(\pi/6)}{\rho(0)}, \quad r_{45} = \frac{\rho(\pi/4)}{\rho(0)}, \quad r_{60} = \frac{\rho(\pi/3)}{\rho(0)}. \end{aligned} \tag{2.26}$$

The subscript of r

$$7.5, \quad 15, \quad 22.5, \quad 30, \quad 45, \quad \text{or} \quad 60$$

corresponds to the stress angle θ of the respective radius in degree. With these values (2.26), different yield criteria can be easily compared in appropriate diagrams. The chosen angles θ are some fractions of the angle $\pi/3$ between the symmetry axes in the π-plane (**Figs. 2.6** and **2.7**).

Convexity of the polynomial formulated criteria

$$\Phi(I'_2, I'_3, \sigma_{eq}) = 0,$$

e.g. CC and BCC (**Table 2.2**), is most critical at these angles and needs to be checked firstly for parameter restriction, see (Betten, 1979, 2001; Bolchoun et al., 2011; Troost and Betten, 1974). In fact, it is impossible to say, at which other angles the convexity should be checked (Bolchoun et al., 2011). It can be numerically analyzed with small steps, e.g. with $\Delta\theta \leqslant \pi/360$.

All radii of the VON MISES criterion (2.10) are equal (**Fig. 2.6**a)

$$r_{7.5} = r_{15} = r_{22.5} = r_{30} = r_{45} = r_{60} = 1. \tag{2.27}$$

For direct comparison of the yield criteria of trigonal symmetry (**Fig. 2.6**b), the fractions r_{30} and r_{60} are significant. The fractions r_{15} and r_{45} can be used in refined analysis (Rosendahl et al., 2019b).

For the criteria of hexagonal symmetry (**Fig. 2.7**), the radii at the angles $\theta = 0$ and $\pi/3$ are equal $\rho(0) = \rho(\pi/3)$, which yields

$$r_{60} = 1, \tag{2.28}$$

and because $\rho(\pi/12) = \rho(\pi/4)$, we obtain

$$r_{15} = r_{45}. \tag{2.29}$$

In this case, the fractions $r_{7.5}$ and $r_{22.5}$ are sometimes required for the refined comparison of the shapes and, due to hexagonal symmetry, the fractions at the angles $5\pi/24$ and $7\pi/24$ are excluded from consideration.

Figures 2.8 and **2.9** show convexity restrictions for yield criteria of trigonal symmetry in the $r_{60} - r_{30}$ diagram and for yield criteria of hexagonal symmetry in the $r_{15} - r_{30}$ diagram, respectively. These diagrams allow a comparison of all yield criteria for isotropic materials. The yield figures

$$\bigcirc, \quad \hat{12}, \quad \bar{12}, \quad \hat{24}, \quad \text{and} \quad \bar{24}$$

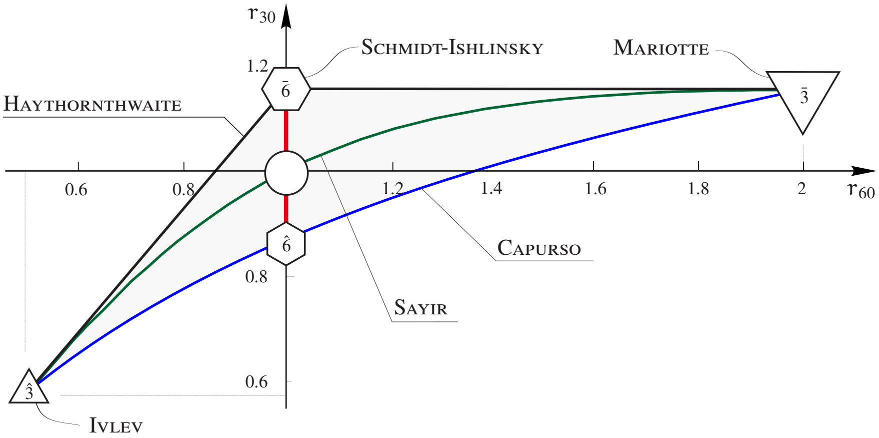

Fig. 2.8: Diagram $\mathrm{r}_{60} - \mathrm{r}_{30}$ for convex yield criteria of trigonal symmetry compared to the VON MISES criterion with $\mathrm{r}_{30} = \mathrm{r}_{60} = 1$ (Kolupaev, 2018). Denotation of criteria follows according to **Tables 2.1** and **2.2**.

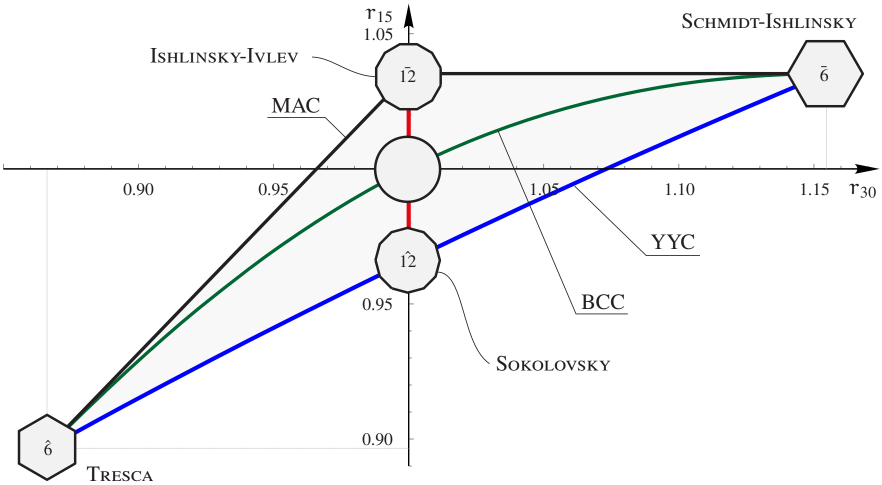

Fig. 2.9: Diagram $\mathrm{r}_{30} - \mathrm{r}_{15}$ for convex yield criteria of hexagonal symmetry ($\mathrm{r}_{60} = 1$) compared to the VON MISES criterion with $\mathrm{r}_{15} = \mathrm{r}_{30} = 1$ (Rosendahl et al., 2019b). Denotation of criteria follows according to **Tables 2.1** and **2.2**.

coincide in the $\mathrm{r}_{60} - \mathrm{r}_{30}$ diagram (**Fig. 2.8**), while the yield figures

$$\bigcirc, \quad \hat{24}, \quad \text{and} \quad \bar{24}$$

coincide in the $r_{15} - r_{30}$ diagram (**Fig. 2.9**). The diagram $r_{7.5} - r_{15}$ for the criteria of hexagonal symmetry with $r_{60} = r_{30} = 1$ is conceivable, but not relevant for engineering application.

Setting

$$I_1 = \text{const.} \tag{2.30}$$

in a particular cross section, the fractions (2.26) can be computed for pressure-sensitive criteria, as well. It is required for the criteria with variable cross sections in the π-plane as function of I_1 (Sect. 2.5). Details on the calculation of the discussed fractions (2.26) for any criterion are given in Appendices 2.7.4 and 2.7.5.

2.3.4 Extreme Yield Figures

Lower and upper bounds of convexity for isotropic criteria in the $r_{60} - r_{30}$ diagram (**Fig. 2.8**) are obtained with extreme yield figures of isotoxal and isogonal hexagons (**Figs. 2.10** and **2.11**). The polynomial formulations (2.7) of these hexagons are known (**Table 2.2**)

- the CAPURSO criterion $\hat{3} - \hat{6} - \bar{3}$ and
- the HAYTHORNTHWAITE criterion $\hat{3} - \bar{6} - \bar{3}$.

However, their polynomial forms feature plane intersections surrounding the physically reasonable shape of the surface Φ, which makes the application involved.

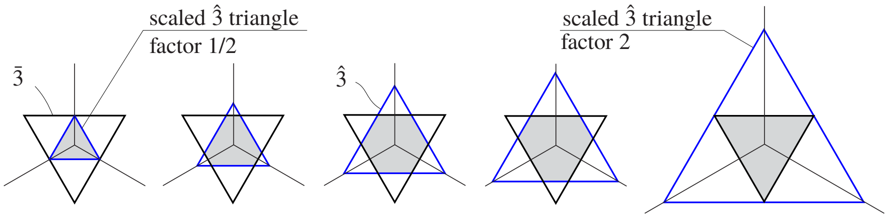

Fig. 2.10: Isogonal (equiangular) hexagons (upper convexity limit, **Fig. 2.8**) formed by the intersection of two triangles in the π-plane: the scaled $\hat{3}$ triangle (blue) and the $\bar{3}$ triangle (black) (Rosendahl et al., 2019b).

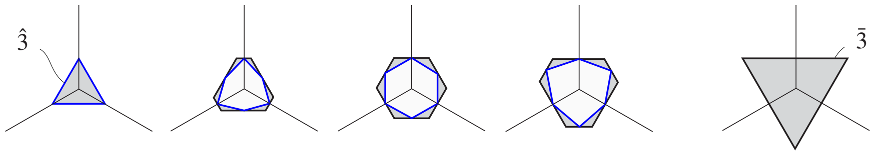

Fig. 2.11: Isotoxal (equilateral, lower convexity limit, blue) and isogonal hexagons (equiangular, upper convexity limit, black) in the π-plane with the $\hat{3}$ (blue) and $\bar{3}$ (black) triangle as limit cases (**Fig. 2.8**) (Rosendahl et al., 2019b).

Isotoxal hexagons (**Fig. 2.8**, lower bound $\hat{3}-\hat{6}-\bar{3}$) as function of stress angle (2.12) can be formulated using the PODGÓRSKI criterion (**Table 2.1** and **2.2**), which describes the geometry of the CAPURSO criterion as a single surface among others. A criterion for isogonal hexagons (**Fig. 2.8**, upper bound $\hat{3}-\bar{6}-\bar{3}$) as function of stress angle without case discrimination is missing (Kolupaev, 2018; Rosendahl et al., 2019b).

Isotoxal and isogonal hexagons degenerate to the same regular triangles $\hat{3}$ and $\bar{3}$ in limit cases (**Figs. 2.6**b and **2.11**) with

$$r_{60} \in \left[\frac{1}{2}, 2\right].$$

These hexagons $\hat{3}-\hat{6}-\bar{3}$ and $\hat{3}-\bar{6}-\bar{3}$ in the π-plane extended with the linear I_1-substitution (2.15) represent pyramids in principal stress space (Subsect. 2.2.3), which are important strength criteria for practical applications. The transition from the hexagon $\hat{6}$ to $\bar{6}$ via $\bigcirc$ is designated with the vertical line

$$\hat{6} | \bigcirc | \bar{6}$$

according to **Fig. 2.8** and can be describe with the modified YU criterion using the ROSENDAHL criterion (**Table 2.2**, mYU).

The lower and upper bounds of the convexity restriction for the yield criteria of hexagonal symmetry in the $r_{30}-r_{15}$ diagram (**Fig. 2.9**) are obtained with extreme yield figures of isotoxal and isogonal dodecagons. Isotoxal dodecagons (lower bound $\hat{6}-\hat{12}-\bar{6}$) as function of the stress angle can be described with the modified YU criterion (**Table 2.2**, mYU). Only a polynomial formulation for isogonal dodecagons (upper bound $\hat{6}-\bar{12}-\bar{6}$) is known (**Fig. 2.9**, MAC, and **Table 2.2**).

Isotoxal and isogonal dodecagons degenerate to the same regular hexagons $\hat{6}$ and $\bar{6}$ in limit cases (**Figs. 2.6**c and **2.7**a) with

$$r_{30} \in \left[\frac{\sqrt{3}}{2}, \frac{2}{\sqrt{3}}\right].$$

Although the I_1-substitution (2.15) is possible here (**Table 2.3**), dodecagons are typically used as pressure-insensitive criteria. The differences between the regular dodecagons $\hat{12}$ and $\bar{12}$ (**Figs. 2.7**b) with $r_{30} = r_{60} = 1$ (**Table 2.1**) are

$$r_{15} \in \left[\frac{1}{2}\sqrt{2+\sqrt{3}}, \sqrt{2}\left(\sqrt{3}-1\right)\right].$$

The deviation between the MAC and YYC including all criteria of hexagonal symmetry (**Fig. 2.9**) is relevant for comparison of the yield criteria.

The differences between the regular icositetragons $\hat{24}$ and $\bar{24}$ are negligible (see **Table 2.1**). These icositetragons are obtained as a result of the generalization of the yield criteria of hexagonal symmetry (**Table 2.1**).

2.3.5 Geometric Properties and Basic Experiments

For comparison of the limit surfaces, test results, approximations, and extrapolations, let us introduce the following limit loading values normalized with respect to the appropriate uniaxial tensile limit loading σ_0^{T}:

$$r_{60}^{\mathrm{C}} = \frac{\sigma_{60}^{\mathrm{C}}}{\sigma_0^{\mathrm{T}}} \qquad \text{and} \qquad r_{60}^{\mathrm{TT}} = \frac{\sigma_{60}^{\mathrm{TT}}}{\sigma_0^{\mathrm{T}}}, \tag{2.31}$$

where σ_{60}^{C} is the uniaxial compressive limit and $\sigma_{60}^{\mathrm{TT}}$ is the limit under equibiaxial tensile loading,

$$r_{30}^{\mathrm{S}} = \sqrt{3}\,\frac{\sigma_{30}^{\mathrm{S}}}{\sigma_0^{\mathrm{T}}}, \qquad r_{30}^{\mathrm{Cc}} = \frac{\sqrt{3}}{2}\,\frac{\sigma_{30}^{\mathrm{Cc}}}{\sigma_0^{\mathrm{T}}}, \qquad \text{and} \qquad r_{30}^{\mathrm{Tt}} = \frac{\sqrt{3}}{2}\,\frac{\sigma_{30}^{\mathrm{Tt}}}{\sigma_0^{\mathrm{T}}}, \tag{2.32}$$

where σ_{30}^{S} is the shear limit, $\sigma_{30}^{\mathrm{Tt}}$ and $\sigma_{30}^{\mathrm{Cc}}$ are the limit loadings of thin-walled tube specimens with closed ends under inner (Tt) and outer pressure (Cc), respectively, and

$$r_0^{\mathrm{CC}} = \frac{\sigma_0^{\mathrm{CC}}}{\sigma_0^{\mathrm{T}}}, \tag{2.33}$$

where σ_0^{CC} is the limit loading under equibiaxial compression (**Table 2.7**). The subscripts of r refer to the stress angles in degree $\theta = 0$, 30, and 60° (2.112). For the VON MISES criterion (2.10), it follows

$$r_{60}^{\mathrm{C}} = r_{60}^{\mathrm{TT}} = r_{30}^{\mathrm{S}} = r_{30}^{\mathrm{Cc}} = r_{30}^{\mathrm{Tt}} = r_0^{\mathrm{CC}} = 1, \tag{2.34}$$

exactly the same as (2.27). It means, all meridians of the cylindrical surface coincide in the BURZYŃSKI-plane and this straight line is parallel to the I_1-axis (**Fig. 2.4**, red line).

While a hydrostatic tensile and compressive test

$$\sigma_{\mathrm{I}} = \sigma_{\mathrm{II}} = \sigma_{\mathrm{III}} > 0$$

and

$$\sigma_{\mathrm{I}} = \sigma_{\mathrm{II}} = \sigma_{\mathrm{III}} < 0$$

until failure can be realized in special cases only (Balandin, 1937; Drass, 2020; Feodosjev, 1975; Kolupaev et al., 2014; Kolupaev, 2018; Paul, 1968a,b; Torre, 1950b), the corresponding properties are important for comparison of extrapolations. We may introduce

$$r^{\mathrm{TTT}} = \frac{\sigma^{\mathrm{TTT}}}{\sigma_0^{\mathrm{T}}} = \frac{1}{3\gamma_1} \qquad \text{and} \qquad r^{\mathrm{CCC}} = -\frac{\sigma^{\mathrm{CCC}}}{\sigma_0^{\mathrm{T}}} = -\frac{1}{3\gamma_2}. \tag{2.35}$$

where σ^{TTT} and σ^{CCC} are the limit loading under hydrostatic tension and compression, respectively. Except for porous and granular media, hydrostatic compressive failure does typically not occur for relevant loadings and

$$\mathrm{r}^{\mathrm{CCC}} \to \infty$$

can be assumed (Subsect. 2.2.3). Based on the NSH (Appendix 2.7.6), a reference value as coordinate TTT on the I_1-axis (**Fig. 2.4**)

$$\frac{1}{\gamma_1} = 3$$

is important for comparison. For porous and granular materials, a reference value as coordinate CCC on the I_1-axis (**Fig. 2.4**)

$$\frac{1}{\gamma_2} = -3\,\mathrm{r}_{60}^{\mathrm{C}}$$

can be used (Kolupaev, 2018).

Now, the values r_0, r_{30}, and r_{60} describe the π-plane shape at a chosen cross section (2.30) and

$$\mathrm{r}_{60}^{\mathrm{C}}, \quad \mathrm{r}_{60}^{\mathrm{TT}}, \quad \mathrm{r}_{30}^{\mathrm{S}}, \quad \mathrm{r}_{30}^{\mathrm{Cc}}, \quad \mathrm{r}_{30}^{\mathrm{Tt}}, \quad \mathrm{r}_{0}^{\mathrm{CC}}, \quad \mathrm{r}^{\mathrm{CCC}}, \quad \text{and} \quad \mathrm{r}^{\mathrm{TTT}}$$

describe corresponding material properties. When $\gamma_1 = \gamma_2 = 0$, pressure-sensitive criteria degenerate to pressure-insensitive criteria: the meridians are parallel to the hydrostatic axis. The values on the same meridians (characterized by the angle θ) coincide:

$$\mathrm{r}_{60} = \mathrm{r}_{60}^{\mathrm{C}} = \mathrm{r}_{60}^{\mathrm{TT}}, \qquad \mathrm{r}_{30} = \mathrm{r}_{30}^{\mathrm{S}} = \mathrm{r}_{30}^{\mathrm{Cc}} = \mathrm{r}_{30}^{\mathrm{Tt}}, \qquad \text{and} \qquad \mathrm{r}_{0}^{\mathrm{CC}} = 1. \tag{2.36}$$

Pressure-insensitive criteria of hexagonal symmetry do not distinguish between tensile and compressive properties

$$\mathrm{r}_{60} = \mathrm{r}_{60}^{\mathrm{C}} = \mathrm{r}_{60}^{\mathrm{TT}} = \mathrm{r}_{0}^{\mathrm{CC}} = 1. \tag{2.37}$$

The meridians $\theta = 0$ and $\pi/3$ coincide in the BURZYŃSKI-plane and together with other meridians are parallel to the I_1-axis.

Classical yield and strength criteria such as VON MISES, TRESCA, SCHMIDT-ISHLINSKY (**Table 2.1**), and the normal stress hypothesis (**Table 2.3**) describe the material behaviour with the property

$$\mathrm{r}_{60}^{\mathrm{TT}} = 1 \tag{2.38}$$

and the linear combinations (**Table 2.4**), e.g. the criteria of MOHR-COULOMB and PISARENKO-LEBEDEV describe the material behaviour with the properties

$$\mathrm{r}_{60}^{\mathrm{TT}} = 1 \qquad \text{and} \qquad \mathrm{r}_{60}^{\mathrm{C}} = \mathrm{r}_{0}^{\mathrm{CC}} \geqslant 1, \tag{2.39}$$

which can be used for the comparison of approximations or for the formulation of fitting restrictions. In the case of missing measured data, it can be assumed, that

$$\mathrm{r}_{60}^{\mathrm{TT}} \in \left]\frac{1}{2}, 1\right[.$$

The low bound follows with the convexity requirement on the meridian $\theta = \pi/3$ and the top bound yields as a conservative restriction of the idealized behavior (2.38).

Special attantion is focused to the value (Birger, 1977; Kolupaev, 2018; Sdobyrev, 1959; Yu, 2004)

$$\mathrm{r}_{60}^{\mathrm{C}} = 2$$

for the criteria in **Table 2.4** and YST (**Table 2.5**), which results as the middle of the restriction $1/\mathrm{r}_{60}^{\mathrm{C}} \in]0, 1]$. We note, if only the value

$$\mathrm{r}_{60}^{\mathrm{C}} \in \left[\frac{1}{2}, 2\right]$$

is known, it is impossible to distinguish between pressure-insensitive and pressure-sensitive material behavior, see the statement in Burzyński (1928) and **Fig. 2.8**. Further measured data is mandatory for any statement. Details on fitting procedures and the parameter identification for pressure-sensitive materials are discussed in Kolupaev et al. (2016); Kolupaev (2017, 2018); Kolupaev et al. (2018); Rosendahl et al. (2019b).

2.4 Yield and Strength Criteria

The phenomenological nature of yield and strength criteria has caused an unmanageable number of possible formulations. Selecting a criterion for a particular application is usually not based on objective arguments. Having to choose an appropriate criterion under basically lack of information can leave engineers confused, see also Lebedev (2010).

Consideration of the plausibility assumptions (Appendix 2.7.8) reduce significantly the number of the criteria suitable for application and minimise risk of inappropriate computation. The aim of this work is the selection of the most effective criteria and their rationale (**Table 2.5**).

2.4.1 Recommended Yield and Strength Criteria

Desired are the C^1-continuous differential criteria (**Table 2.2**)

$$\hat{3} - \hat{6} | \bigcirc | \bar{6} - \bar{3}$$

and

$$\hat{6}-\hat{12}\,|\bigcirc|\,\bar{12}-\bar{6}$$

which fulfil the plausibility assumptions. These criteria should be formulated in the form (2.8) as a functions of two parameters (**Figs. 2.8** and **2.9**). Such criteria are not known so far. Some steps in this direction are proposed below.

In the authors' opinion, the PODGÓRSKI and the ROSENDAHL yield criteria (**Table 2.2**) meet the plausibility assumptions in the best way known and are recommended for application. Unfortunately,

- the PODGÓRSKI criterion does not include isogonal hexagons (**Figs. 2.8** and **2.10**) and
- the ROSENDAHL criterion – isogonal dodecagons (**Fig. 2.9**).

These two criteria are generalized for reliable application (Subsect. 2.4.3). Different ways are examined in order to satisfy the plausibility assumptions.

The C^0-CTS (**Table 2.2**, criterion of trigonal symmetry)

$$\hat{3}-\hat{6}\,|\,\hat{12}\,|\,\bar{6}-\bar{3}$$

and the C^0-CHS (**Table 2.2**, criterion of hexagonal symmetry)

$$\hat{6}-\hat{12}\,|\,\hat{24}\,|\,\bar{12}-\bar{6}$$

as functions of two parameters are derived on the basis of the modified ALTENBACH-ZOLOCHEVSKY criterion (Kolupaev, 2017, 2018; Rosendahl et al., 2019b). Together with the pyramid of PODGÓRSKI (**Table 2.5**)

$$\hat{3}-\hat{6}\,|\bigcirc-\bar{3}\;\rightarrow\;I_1$$

the pressure-sensitive generalization C^0-CTS $\rightarrow I_1$

$$\hat{3}-\hat{6}\,|\,\hat{12}\,|\,\bar{6}-\bar{3}\;\rightarrow\;I_1$$

is a powerful tool for fitting of the measured data. The linear I_1-substitution (2.15) is used here. The quadratic substitution with the parabolic meridians (2.16) can be tried alternatively for approximation. If necessary, these I_1-substitutions can be used for the C^0-CHS

$$\hat{6}-\hat{12}\,|\,\hat{24}\,|\,\bar{12}-\bar{6}\;\rightarrow\;I_1.$$

The YU strength theory (**Table 2.5**, YST)

$$\hat{6}-\hat{12}-\bar{6}+\mathrm{NSH}$$

will be reformulated as function of the stress angle θ without plane intersections and then generalized as the ROSENDAHL + NSH criterion (**Table 2.5**)

$$\hat{6}-\hat{12}\,|\bigcirc-\bar{6}+\mathrm{NSH}$$

for simple applicability. Based on the "rounded off" NSH (Appendix 2.7.6), the modified YST with the properties of real construction materials

$$r_0^{CC} \geqslant r_{60}^{C} \geqslant 1$$

is suggested (Subsect. 2.4.4.2).

The fundamentally different concept of the criteria with variable cross section approach is discussed in Sect. 2.5. These criteria have trigonal symmetry in standard loading region and hexagonal symmetry at high hydrostatic compressive loading, e.g.

$$\hat{6} - \bigcirc - \bar{6} \qquad \text{if} \qquad I_1 \to -\infty.$$

Because of their flexibility, such criteria provide good approximations of experimental data. A general expression is proposed.

With the selected criteria (**Tables 2.2** and **2.5**), it can be checked, whether an optimal approximation of the measured data with the convex shape in the π-plane and the convex meridian is possible. The criteria (**Tables 2.3** and **2.4**) have rather historical and, especially, didactic significance, see also Brandt et al. (1986). Further criteria will be only needed if they fulfil more of the plausibility assumptions compared with the selected criteria.

2.4.2 PODGÓRSKI-*type Shape Functions*

The systematization of the most effective yield criteria (Rosendahl et al., 2019b; Rosendahl, 2020) leads to the shape function

$$\Omega_{3k} = \cos\left[\frac{1}{3k}\left(\pi\,\beta_{3k} - \arccos\left[\eta_0 + \eta_{3k}\cos(3k\theta)\right]\right)\right], \quad k \in \mathbb{N} \tag{2.40}$$

which contains with (**Table 2.2**)

- $k = 1$ – the $\hat{3} - \hat{6} \mid \bigcirc - \bar{3}$ criterion of trigonal symmetry,
- $k = 2$ – the $\hat{6} - \hat{12} \mid \bigcirc - \bar{6}$ criterion of hexagonal symmetry,
- $k = 3$ – the $\hat{9} - \hat{18} \mid \bigcirc - \bar{9}$ criterion of trigonal symmetry,
- $k = 4$ – the $\hat{12} - \hat{24} \mid \bigcirc - \bar{12}$ criterion of hexagonal symmetry.

The parameter η_0 in (2.40) introduced in Bouvet et al. (2002, 2004); Lexcellent (2018); Lexcellent et al. (2006), see also the series of the invariants (Appendix 2.7.7), is redundant and will be discarded

$$\eta_0 = 0.$$

The setting with $k = 1$ in (2.40) is of crucial importance in the formulation of the yield and strength criteria. The setting with $k = 2$ includes many well-known yield criteria of plasticity theory without tension / compression differences (2.28)

$$r_{60} = r_{60}^{C} = 1.$$

The setting with $k = 3$ is the consequence of generalization and only of theoretical significance (Kolupaev, 2006, 2018; Rosendahl et al., 2019b). The setting with $k = 4$ will be used to obtain the $\bar{12}$ criterion for a C^0-generalization (Sect. 2.4.3.5). Further settings with $n \geqslant 5$ are possible, but have not found any application.

Note that, in order to avoid numerical issues, the real part function $\Re$ can be introduced to the shape function Ω_{3k} (2.40)

$$\Omega_{3k} = \Re\left[\cos\left[\frac{1}{3k}\left(\pi\,\beta_{3k} - \arccos\left[\eta_{3k}\cos(3k\theta)\right]\right)\right]\right]. \tag{2.41}$$

Replacing the parameter η_{3k} by

$$\eta_{3k} = \sin\left[\kappa_{3k}\,\frac{\pi}{2}\right] \tag{2.42}$$

yields improved parameter sensitivity and numerical stability. According to Szwed (2000), the parameter β_{3k} can be replaced with

$$\beta_{3k} = \arccos(\chi_{3k}). \tag{2.43}$$

This notion (2.43) will not be pursued here.

2.4.2.1 C^1-criterion $\hat{3} - \hat{6}\,|\,\bigcirc - \bar{3}$

Normalized with respect to the appropriate uniaxial tensile limit loading $\sigma_{eq} = \sigma_0^T$, the PODGÓRSKI criterion (**Table 2.2**) reads

$$\sigma_{eq} = \sqrt{3\,I_2'}\,\frac{\Omega_3(\theta,\beta_3,\eta_3)}{\Omega_3(0,\beta_3,\eta_3)} \tag{2.44}$$

with the shape function of trigonal symmetry, see (2.40) with $k = 1$

$$\Omega_3(\theta,\beta,\eta) = \cos\left[\frac{1}{3}\,(\pi\beta_3 - \arccos[\eta_3\cos 3\theta])\right] \tag{2.45}$$

and the parameter restrictions

$$\beta_3 \in [0,\,1], \quad \eta_3 \in [-1,\,1]. \tag{2.46}$$

It contains the criteria (**Fig. 2.12**, **Tables 2.1** and **2.2**)

- the SAYIR cubic criterion $\hat{3} - \bigcirc - \bar{3}$ with $\beta_3 = \{0, 1\}$,
- the CAPURSO isotoxal hexagons $\hat{3} - \hat{6} - \bar{3}$ with $\eta_3 = \{-1,\,1\}$, and
- the TRESCA-VON MISES transition $\hat{6} - \bigcirc$ with $\beta_3 = 1/2$, $\eta_3 \in [0,\,1]$.

The criterion (2.44)–(2.45) results from the solution of the cubic equation in σ_{eq}

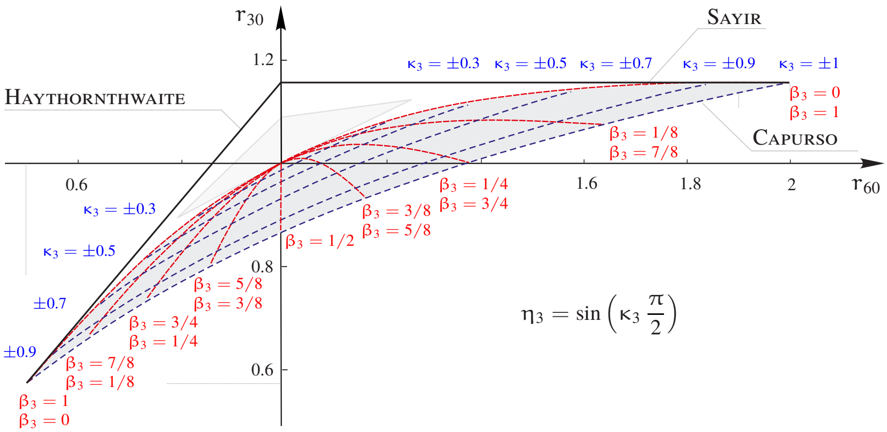

Fig. 2.12: PODGÓRSKI criterion (2.44) in the $r_{60} - r_{30}$ diagram (**Fig. 2.8**). The lines $\beta_3 = \text{const.}$, $\kappa_3 \in [-1, 1]$ (solid red) and $\kappa_3 = \text{const.}$, $\beta_3 \in [0, 1]$ (dashed blue) are shown (Rosendahl et al., 2019b), cf. Podgórski (1984); Podgórski (1985), adapted from Kolupaev (2017, 2018).

$$S'_3 + S'_2\,\sigma_{eq} + S'_1\,\sigma_{eq}^2 = \sigma_{eq}^3 \tag{2.47}$$

for the rational deviatoric series (Appendix 2.7.7, Eq. (2.147)) with the trigonometric identity (Bronstein and Semendjajew, 2007). The number of the basic geometries included in the criterion is sufficient for many applications. The scheme of this C^1-criterion $\hat{3}-\hat{6}\,|\bigcirc-\bar{3}$ is shown in **Fig. 2.13**. The PODGÓRSKI criterion (2.44)–(2.45) has received great recognition from professional community (**Table 2.2**, comments).

The parameter restriction (2.46) is convenient for the practice. The parameters of the criterion β_3 and η_3 can be determined numerically by known values r_{60} and r_{30}.

The isogonal hexagons of the HAYTHORNTHWAITE criterion $\hat{3}-\bar{6}-\bar{3}$ containing the regular hexagon $\bar{6}$ (SCHMIDT-ISHLINSKY criterion) cannot be described with the PODGÓRSKI criterion limiting the application of the criterion in the general case. Although a confined field between the criteria $\hat{3}-\bar{6}-\bar{3}$ and $\hat{3}-\bigcirc-\bar{3}$ can be

Fig. 2.13 Scheme of the PODGÓRSKI criterion of trigonal symmetry (2.44)–(2.45). CC - cubic criterion (**Table 2.2**). Color meaning: black - criteria without any parameters, red – criteria with one parameter, and blue - the criterion with two parameters additionally to σ_{eq}.

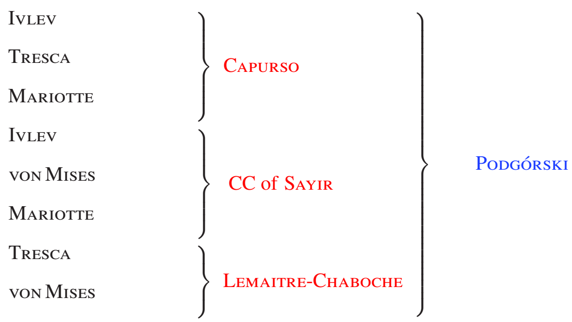

mapped with complex parameters β_3 and η_3 (Kolupaev, 2017, 2018), such approach is not user-friendly.

The PODGÓRSKI pyramid follows with the linear I_1-substitution (2.15) in (2.44) as

$$\frac{\sigma_{eq} - \gamma_1 I_1}{1 - \gamma_1} = \sqrt{3 I_2'} \frac{\Omega_3(\theta, \beta_3, \eta_3)}{\Omega_3(0, \beta_3, \eta_3)} \tag{2.48}$$

and is recommended for use (**Table 2.5**).

2.4.2.2 C^1-criterion $\hat{6} - \hat{12} \,|\, \bigcirc - \bar{6}$

Normalized with respect to the appropriate uniaxial tensile limit loading $\sigma_{eq} = \sigma_0^T$, the ROSENDAHL criterion (**Table 2.2**) reads

$$\sigma_{eq} = \sqrt{3 I_2'} \frac{\Omega_6(\theta, \beta_6, \eta_6)}{\Omega_6(0, \beta_6, \eta_6)} \tag{2.49}$$

with the shape function of hexagonal symmetry

$$\Omega_6(\theta, \beta_6, \eta_6) = \cos\left[\frac{1}{6}\left(\pi\beta_6 - \arccos[\eta_6 \cos 6\theta]\right)\right], \tag{2.50}$$

see (2.40) with $k = 2$, or, equivalently, with (2.118)

$$\Omega_6(\theta, \beta_6, \eta_6) = \cos\left[\frac{1}{6}\left(\pi\beta_6 - \arccos\left[\eta_6 \left(2\cos^2 3\theta - 1\right)\right]\right)\right], \tag{2.51}$$

which may be preferred. The parameter restrictions are

$$\beta_6 \in [0,\, 1], \quad \eta_6 \in [-1,\, 1] \tag{2.52}$$

It contains the criteria (**Fig. 2.14**, **Tables 2.1** and **2.2**)

- the SZWED bicubic criterion $\hat{6} - \bigcirc - \bar{6}$ with $\beta_6 = \{0,\, 1\}$,
- the isotoxal dodecagons $\hat{6} - \hat{12} - \bar{6}$ of the YU yield criterion with $\eta_6 = \{1, -1\}$,
- the SOKOLOVSKY-VON MISES transition $\hat{12} - \bigcirc$ with $\beta_3 = 1/2$, $\eta_6 \in [0, 1]$.

The criterion (2.49)–(2.50) results from the solution of the bicubic equation

$$S_6' + S_4' \sigma_{eq}^2 + S_2' \sigma_{eq}^4 = \sigma_{eq}^6 \tag{2.53}$$

for the rational deviatoric series (Appendix 2.7.7, Eq. (2.147)) with the trigonometric identity, cf. PODGÓRSKI criterion (2.44)–(2.45).

The number of basic geometries included in the criterion is sufficient for many applications. The parameter restriction (2.52) is convenient for the practice, cf. (2.46). This criterion (2.49)–(2.50) is relatively new but suitable for the solutions of several problems in plasticity theory. The scheme of the criterion $\hat{6} - \hat{12} \,|\, \bigcirc - \bar{6}$

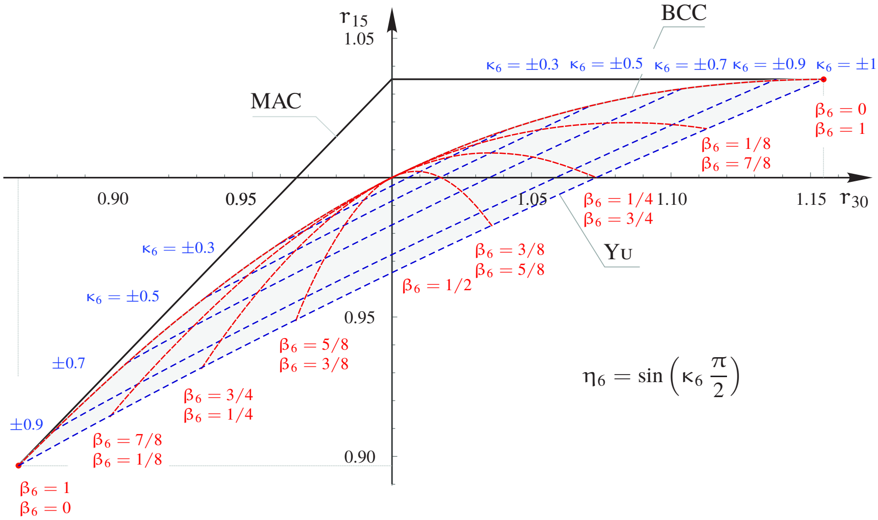

Fig. 2.14: ROSENDAHL criterion (2.50) with $\eta_0 = 0$ in the $r_{30} - r_{15}$ diagram (**Fig. 2.9**). The lines $\beta_6 =$ const., $\kappa_6 \in [-1, 1]$ (solid red) and $\kappa_6 =$ const., $\beta_6 \in [0, 1]$ (dashed blue) are shown, cf. **Fig. 2.12**. BCC – bicubic criterion of SZWED, MAC – multiplicative ansatz criterion (**Table 2.2**).

is shown in **Fig. 2.15**. The parameters of the criterion β_6 and η_6 can be determined numerically by known values r_{30} and r_{15}.

The isogonal dodecagons of the multiplicative ansatz criterion of hexagonal symmetry $\hat{6} - \bar{12} - \bar{6}$ containing the ISHLINSKY-IVLEV criterion (regular dodecagon $\bar{12}$) cannot be described by the ROSENDAHL criterion limiting the application of the criterion in the general case. Although a confined field between the criteria $\hat{6} - \bar{12} - \bar{6}$ and $\hat{6} - \bigcirc - \bar{6}$ can be mapped with complex parameters β_6 and η_6, this approach is not easy-to-use.

The ROSENDAHL pyramid follows with the linear I_1-substitution (2.15) in (2.49) as

$$\frac{\sigma_{eq} - \gamma_1 I_1}{1 - \gamma_1} = \sqrt{3 I_2'} \frac{\Omega_6(\theta, \beta_6, \eta_6)}{\Omega_6(0, \beta_6, \eta_6)} \tag{2.54}$$

and can be recommended for some applications (**Table 2.5**).

2.4.3 Inductive Derivation of Criteria

The deductive derived approaches Φ are seldom possible, see Gurson (1977). An attempt is made to provide a criterion inductively in order to approximate the general forms. This path is not clear. Several ansätze are conceivable, which are fuzzily restricted by the plausibility assumptions (Appendix 2.7.8).

In our opinion, the C^1-criteria containing the transitions

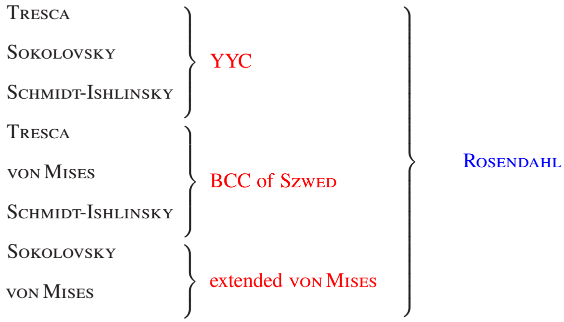

Fig. 2.15 Scheme of the ROSENDAHL criterion of hexagonal symmetry (2.50): YYC - YU yield criterion, BCC - bicubic criterion (**Table 2.2**). The SOKOLOVSKY-VON MISES criterion was not specified until now. Color meaning: black - criteria without any parameters, red – criteria with one parameter, and blue - the criterion with two parameters additionally to σ_{eq}.

$$\hat{3}-\hat{6}|\bigcirc|\bar{6}-\bar{3}$$

and

$$\hat{6}-\hat{12}|\bigcirc|\bar{12}-\bar{6}$$

should be searched considering the plausibility assumptions. Though these criteria are provided in polynomial form as functions of two parameters (**Table 2.2**), their application is not straightforward.

The major problem in the formulation is that the criteria

- the HAYTHORNTHWAITE $\hat{3}-\bar{6}-\bar{3}$ criterion and
- the multiplicative ansatz criterion (MAC) $\hat{6}-\bar{12}-\bar{6}$

as a function of the stress angle θ without case discrimination are unknown. But these criteria can be sufficiently good approximated (Rosendahl et al., 2019b). Two methods are available:

- convex combination of the known criteria (Subsubsect. 2.4.3.1-2.4.3.5) and
- series developments (Subsubsect. 2.4.3.6).

2.4.3.1 Linear Combination of Yield Criteria

The criteria of PODGÓRSKI (Sect. 2.4.2.1) and ROSENDAHL (Sect. 2.4.2.2) have a similar structure. The generalized criterion of trigonal symmetry follows with the linear combination as

$$\sigma_{eq} = \sqrt{3I_2'}\left[\alpha\frac{\Omega_3(\theta,\beta_3,\eta_3)}{\Omega_3(0,\beta_3,\eta_3)} + (1-\alpha)\frac{\Omega_6(\theta,\beta_6,\eta_6)}{\Omega_6(0,\beta_6,\eta_6)}\right], \qquad \alpha\in[0,\,1]. \quad (2.55)$$

For a criterion of hexagonal symmetry we obtain in a analog path

$$\sigma_{eq} = \sqrt{3I_2'}\left[\alpha\frac{\Omega_6(\theta,\beta_6,\eta_6)}{\Omega_6(0,\beta_6,\eta_6)} + (1-\alpha)\frac{\Omega_{12}(\theta,\beta_{12},\eta_{12})}{\Omega_{12}(0,\beta_{12},\eta_{12})}\right], \quad \alpha\in[0,\,1]. \quad (2.56)$$

The advantage of the criteria (2.55) and (2.56) is that the parameter restrictions are known. The disadvantage is, the criteria with five parameters are difficult to manage. The shapes $\hat{6}-\bigcirc$ in (2.55) and $\hat{12}-\bigcirc$ in (2.56) can be describe with each of both terms, what is detrimental by parameter fitting.

The amount of the parameter can be reduced to four:

$$\sigma_{\mathrm{eq}} = \sqrt{3\mathrm{I}_2'}\left[\alpha\,\frac{\Omega_3(\theta,0,\eta_3)}{\Omega_3(0,0,\eta_3)} + (1-\alpha)\,\frac{\Omega_6(\theta,\beta_6,\eta_6)}{\Omega_6(0,\beta_6,\eta_6)}\right], \qquad \alpha \in [0,\,1]. \qquad (2.57)$$

and

$$\sigma_{\mathrm{eq}} = \sqrt{3\mathrm{I}_2'}\left[\alpha\,\frac{\Omega_6(\theta,0,\eta_6)}{\Omega_6(0,0,\eta_6)} + (1-\alpha)\,\frac{\Omega_{12}(\theta,\beta_{12},\eta_{12})}{\Omega_{12}(0,\beta_{12},\eta_{12})}\right], \qquad \alpha \in [0,\,1] \qquad (2.58)$$

but both terms in (2.57) and (2.58) contain the same $\bigcirc$-shape. Such formulations seem intricate and can not be recommended. The number of parameters should be further reduced.

2.4.3.2 C^1-continuous Differential Yield Criteria

The linear combination SAYIR + SZWED of trigonal symmetry (**Table 2.2**)

$$\hat{3}-\bigcirc-\bar{3} \;+\; \hat{6}-\bigcirc-\bar{6}$$

and the linear combination of hexagonal symmetry (C^1-LC-Hex)

$$\hat{6}-\bigcirc-\bar{6} \;+\; \hat{12}-\bigcirc-\bar{12}$$

are the functions of three parameters. The SAYIR + SZWED yield criterion follows with the shape functions (2.45) and (2.50) and with the setting $\beta_3 = \beta_6 = 0$ as

$$\sigma_{\mathrm{eq}} = \sqrt{3\mathrm{I}_2'}\left[\alpha\,\frac{\Omega_3(\theta,0,\eta_3)}{\Omega_3(0,0,\eta_3)} + (1-\alpha)\,\frac{\Omega_6(\theta,0,\eta_6)}{\Omega_6(0,0,\eta_6)}\right], \qquad \alpha \in [0,\,1]. \qquad (2.59)$$

The SAYIR + SZWED pyramid is obtained with the linear I_1-substitution (2.15) as

$$\frac{\sigma_{\mathrm{eq}}-\gamma_1\,\mathrm{I}_1}{1-\gamma_1} = \sqrt{3\mathrm{I}_2'}\left[\alpha\,\frac{\Omega_3(\theta,0,\eta_3)}{\Omega_3(0,0,\eta_3)} + (1-\alpha)\,\frac{\Omega_6(\theta,0,\eta_6)}{\Omega_6(0,0,\eta_6)}\right]. \qquad (2.60)$$

The C^1-LC-Hex yield criterion follows with the SZWED shape functions (2.50) and the PODGÓRSKI-type shape functions (2.40) with $k = 4$. The setting $\beta_6 = \beta_{12} = 0$ yields

$$\sigma_{\mathrm{eq}} = \sqrt{3\mathrm{I}_2'}\left[\alpha\,\frac{\Omega_6(\theta,0,\eta_6)}{\Omega_6(0,0,\eta_6)} + (1-\alpha)\,\frac{\Omega_{12}(\theta,0,\eta_{12})}{\Omega_{12}(0,0,\eta_{12})}\right], \qquad \alpha \in [0,\,1]. \qquad (2.61)$$

The C^1-LS-Hex $\rightarrow \mathrm{I}_1$ pyramid follows with the linear I_1-substitution (2.15) as

$$\frac{\sigma_{eq} - \gamma_1 I_1}{1 - \gamma_1} = \sqrt{3I_2'}\left[\alpha\,\frac{\Omega_6(\theta,0,\eta_6)}{\Omega_6(0,0,\eta_6)} + (1-\alpha)\,\frac{\Omega_{12}(\theta,0,\eta_{12})}{\Omega_{12}(0,0,\eta_{12})}\right]. \tag{2.62}$$

Both criteria (2.59) and (2.61) can be thought of first as replacement for the missing criteria CAPURSO + HAYTHORNTHWAITE (**Table 2.2**)

$$\hat{3} - \hat{6} | \bigcirc | \bar{6} - \bar{3}$$

and YYC+MAC (**Table 2.2**)

$$\hat{6} - \hat{12} | \bigcirc | \bar{12} - \bar{6}.$$

Disadvantage is that both terms in (2.59) and (2.61) can describe the $\bigcirc$-shape. Due to an additional parameter, the shapes between the extreme yield criteria are not uniquely defined.

2.4.3.3 C^0-linear Combinations with Three Parameters

Possible modifications (Subsubsect. 2.4.3.1) as the C^0-linear combination of SAYIR and YYC of trigonal symmetry (**Table 2.2**)

$$\hat{3} - \bigcirc - \bar{3} \; + \; \hat{6} - \hat{12} - \bar{6}$$

or

$$\sigma_{eq} = \sqrt{3I_2'}\left[\alpha\,\frac{\Omega_3(\theta,0,\eta_3)}{\Omega_3(0,0,\eta_3)} + (1-\alpha)\,\frac{\Omega_6(\theta,\beta_6,1)}{\Omega_6(0,\beta_6,1)}\right], \qquad \alpha \in [0,\,1] \tag{2.63}$$

and the linear combination of hexagonal symmetry (C^0-LC-Hex)

$$\hat{6} - \bigcirc - \bar{6} \; + \; \hat{12} - \hat{24} - \bar{12}$$

or

$$\sigma_{eq} = \sqrt{3I_2'}\left[\alpha\,\frac{\Omega_6(\theta,0,\eta_6)}{\Omega_6(0,0,\eta_6)} + (1-\alpha)\,\frac{\Omega_{12}(\theta,\beta_{12},1)}{\Omega_{12}(0,\beta_{12},1)}\right], \qquad \alpha \in [0,\,1] \tag{2.64}$$

are also the functions of three parameters. They can not be recommended for application as over-refined for a C^0-criterion.

These criteria are C^1-criteria with the setting $\eta_6 \approx 0.9999$, $\beta_6 \in [0,\,1]$ in (2.63) and $\eta_{12} \approx 0.9999$, $\beta_{12} \in [0,\,1]$ in (2.64), but it contradicts our aspiration to consider a maximal number of extreme yield figures.

2.4.3.4 C^0-linear Combination $\hat{3} - \hat{6} - \bar{3} + \bar{6}$

A linear combination $\hat{3} - \hat{6} - \bar{3} + \bar{6}$

$$\Phi_3 = \sqrt{3 I_2'} \left[\alpha \frac{\cos\left[\dfrac{1}{3}\,(\pi\,\beta_3 - \arccos\left[\cos 3\,\theta\right])\right]}{\cos\left[\dfrac{1}{3}\,\pi\,\beta_3\right]} + (1-\alpha)\,\cos\left[\frac{1}{6}\arccos\left[\cos 6\,\theta\right]\right]\right] - \sigma_{\mathrm{eq}} \tag{2.65}$$

with the parameter restriction

$$\alpha \in [0,\,1] \qquad \text{and} \qquad \beta_3 \in [0,\,1] \tag{2.66}$$

provides the C^0-criterion $\hat{3}-\hat{6}\,|\,\hat{12}\,|\,\bar{6}-\bar{3}$ of trigonal symmetry. The values are

$$r_{60} = \frac{2}{2-\alpha+\alpha\sqrt{3}\,\tan\left[\dfrac{\pi\,\beta_3}{3}\right]}, \tag{2.67}$$

$$r_{30} = \frac{2}{\sqrt{3}+\alpha\,\tan\left[\dfrac{\pi\,\beta_3}{3}\right]}, \tag{2.68}$$

and

$$r_{15} = \frac{2\sqrt{2}}{1+\sqrt{3}-\alpha\,(1-\sqrt{3})\,\tan\left[\dfrac{\pi\,\beta_3}{3}\right]}. \tag{2.69}$$

We obtain the parameters α and β_3 with known values r_{60} and r_{30} as

$$\alpha = \frac{2\sqrt{3}}{r_{30}} - 1 - \frac{2}{r_{60}}, \tag{2.70}$$

$$\beta_3 = \frac{3}{\pi}\arctan\left[\frac{r_{60}\,(\sqrt{3}\,r_{30}-2)}{(2+r_{60})\,r_{30}-2\sqrt{3}\,r_{60}}\right]. \tag{2.71}$$

The dodecagon $\hat{12}$ with the values $r_{60} = r_{30} = 1$ (**Fig. 2.7** b) follows with

$$\alpha = 2\sqrt{3}-3 \approx 0.4641 \qquad \text{and} \qquad \beta_3 = \frac{1}{2}. \tag{2.72}$$

The criterion Φ_3 (2.65) describes all points in the $r_{60} - r_{30}$ diagram (**Fig. 2.8**). The parameter setting for the basic geometries are given in **Table 2.1**. It is comparable to with the modified ALTENBACH-ZOLOCHEVSKY criterion of trigonal symmetry (Kolupaev, 2017, 2018; Rosendahl et al., 2019b) and is designated as mAZ3.

The equations and restrictions are easy, so this criterion is advocated for the practical application. The function $\cos 6\theta$ can be replaced with (2.118) for uniform presentation of the criterion as function of $\cos 3\theta$. A disadvantage is, that the geometry of the HAYTHORNTHWAITE criterion (**Table 2.2**) cannot be exactly described with the settings

$$\beta_3 = 1 \quad \text{for} \quad \hat{3} - \bar{6}$$

and

$$\beta_3 = 0 \quad \text{for} \quad \bar{6} - \bar{3}$$

of mAZ3, although both criteria coincide in the $r_{60} - r_{30}$ diagram. It is also detrimental that the criterion (2.65) does not include the ◯-criterion.

The C^0-CTS→ I_1 pyramid follows with the linear I_1-substitution (2.15) in (2.65) as

$$\frac{\sigma_{eq} - \gamma_1 I_1}{1 - \gamma_1} = \sqrt{3 I_2'} \left[\alpha \frac{\cos\left[\frac{1}{3}\left(\pi \beta_3 - \arccos\left[\cos 3\theta\right]\right)\right]}{\cos\left[\frac{1}{3}\pi \beta_3\right]} + (1-\alpha) \cos\left[\frac{1}{6}\arccos\left[\cos 6\theta\right]\right]\right] - \sigma_{eq} \tag{2.73}$$

and is also recommended for application (**Table 2.5**).

2.4.3.5 C^0-linear Combination $\hat{6} - \hat{12} - \bar{6} + \bar{12}$

In analogy to mAZ3 (Sect. 2.4.3.4), a linear combination $\hat{6} - \hat{12} - \bar{6} + \bar{12}$

$$\Phi_6 = \sqrt{3 I_2'} \left[\alpha \frac{\cos\left[\frac{1}{6}\left(\pi \beta_6 - \arccos\left[\cos 6\theta\right]\right)\right]}{\cos\left[\frac{1}{6}\pi \beta_6\right]} + (1-\alpha) \cos\left[\frac{1}{12}\arccos\left[\cos 12\theta\right]\right]\right] - \sigma_{eq} \tag{2.74}$$

with the parameter restriction

$$\alpha \in [0, 1] \qquad \text{and} \qquad \beta_6 \in [0, 1] \tag{2.75}$$

provides the C^0-criterion $\hat{6} - \hat{12} | \hat{24} | \bar{12} - \bar{6}$ of hexagonal symmetry. The values are

$$r_{60} = 1, \tag{2.76}$$

$$r_{30} = \frac{2}{2 + \alpha\left(\sqrt{3} - 2 + \tan\left[\frac{\pi \beta_6}{6}\right]\right)}, \tag{2.77}$$

and

$$r_{15} = \frac{2\sqrt{2}}{\sqrt{3}+1+\alpha(\sqrt{3}-1)\tan\left[\dfrac{\pi\beta_6}{6}\right]}. \tag{2.78}$$

We obtain the parameters α and β_6 with known values r_{30} and r_{15} as

$$\alpha = \frac{2+\sqrt{3}}{r_{15}\,r_{30}}\left(2\sqrt{2+\sqrt{3}}\,r_{30} - 2\,r_{15} - \sqrt{3}\,r_{15}\,r_{30}\right), \tag{2.79}$$

$$\beta_6 = \frac{6}{\pi}\arctan\left[\frac{r_{30}\left(\sqrt{2}-\sqrt{6}+r_{15}\right)}{-2\sqrt{2+\sqrt{3}}\,r_{30}+2\,r_{15}+\sqrt{3}\,r_{15}\,r_{30}}\right]. \tag{2.80}$$

The icositetragon $\hat{24}$ with the values $r_{15} = r_{30} = 1$ follows with

$$\alpha = 5\sqrt{2} - 4\sqrt{3} + 3\sqrt{6} - 7 \approx 0.4913 \qquad \text{and} \qquad \beta_6 = \frac{1}{2}. \tag{2.81}$$

The criterion Φ_6 (2.74) describes all points in the $r_{30} - r_{15}$ diagram (**Fig. 2.9**). The parameter settings of this modified ALTENBACH-ZOLOCHEVSKY criterion of hexagonal symmetry (mAZ6) for the basic geometries are given in **Table 2.1**.

The equations are easy, so this criterion is recommended for the practical application. The function $\cos 12\theta$ can be replaced with (2.118) for uniform presentation of the criterion as function of $\cos 3\theta$ or $\cos 6\theta$. The disadvantage is, that the geometry of the MAC (**Table 2.2**) cannot be exactly described with the settings

$$\beta_6 = 1 \quad \text{for} \quad \hat{6} - \bar{12}$$

and

$$\beta_6 = 0 \quad \text{for} \quad \bar{12} - \bar{6}$$

of the mAZ6, although both criteria coincide in the $r_{30} - r_{15}$ diagram. The criterion (2.74) does not include the ◯-criterion and is C^0-continuous, which is detrimental to the yield criteria.

The C^0-CHS→ I_1 pyramid follows with the linear I_1-substitution (2.15) in (2.74) as

$$\frac{\sigma_{eq} - \gamma_1\,I_1}{1-\gamma_1} = \sqrt{3I_2'}\left[\alpha\,\frac{\cos\left[\dfrac{1}{6}\left(\pi\beta_6 - \arccos\left[\cos 6\theta\right]\right)\right]}{\cos\left[\dfrac{1}{6}\,\pi\beta_6\right]} + \right. \tag{2.82}$$
$$\left.(1-\alpha)\cos\left[\frac{1}{12}\arccos\left[\cos 12\theta\right]\right]\right] - \sigma_{eq}$$

and is recommended for application (**Table 2.5**).

2.4.3.6 Series Development

In the next step of the inductive derivations, the series development as sum of cosine is introduced (Bulla and Kolupaev, 2021)

$$\Omega_m = \cos\left[\frac{1}{3\lambda_m}\left(\pi\beta_m - \arccos\left[\eta_0 + \eta_3\cos(3\theta) + \eta_6\cos(6\theta) + \ldots\right]\right)\right] \tag{2.83}$$

with

- $m = 3$ for criteria of trigonal symmetry containing at least one odd term, e.g. η_3 and the even terms with η_6, η_{12}, etc. and
- $m = 6$ for criteria of hexagonal symmetry containing only even terms η_6, η_{12}, etc.

The idea originates with the compete series (2.145) or reduced series (2.146) of the invariants (Appendix 2.7.7).

The problem in (2.83) is the number of parameters which should be reduced for practical application. The associated issue is the necessary restriction of parameters. The functions $\cos 6\theta$, $\cos 12\theta$, etc. can be replaced with (2.118)–(2.119) for uniform presentation. Because of the number of the parameters and related convexity constraints, this shape function (2.83) is not user-friendly.

The next possibility to try it out is a sum of arccosine

$$\Omega_m = \cos\left[\pi\beta_m - \frac{1}{3}\arccos[\eta_3\cos 3\theta] - \frac{1}{6}\arccos[\eta_6\cos 6\theta] + \ldots\right]. \tag{2.84}$$

This formulation also requires further study with the convexity analysis. It can not be directly recommended.

A formally performed linear combination with two parameters

$$\Omega_3 = \cos\left[\alpha\frac{1}{3}\left(\pi\beta_3 - \arccos[\cos 3\theta]\right) - (1-\alpha)\frac{1}{6}\arccos[\cos 6\theta]\right], \tag{2.85}$$

containing $\hat{3} - \hat{6}|\bar{6} - \bar{3}$ with

$$\alpha \in [0, 1] \qquad \text{and} \qquad \beta_3 \in [0, 1] \tag{2.86}$$

yields non-convex geometries for some setting of the parameters (2.86) and can also not be recommended.

We are of the opinion, that these series developments are not effective for practical use because of the number of parameters and the intricate convexity constraints. Maybe further investigations can show the usefulness of this approach.

2.4.4 Modified YU *Strength Theory*

The YU strengh theory (YST) was introduced 2002 and has gained recognition from the community (**Table** 1.5). The word "theory" in relation to the criteria is a tribute to tradition. We adopt this denomination in relation to the YST. The YST can be interpreted as a linear combination of the TRESCA and SCHMIDT-ISHLINSKY criteria containing the SOKOLOVSKY criterion with the normal stress hypothesis (**Fig. 2.16**):

$$\hat{6} - \hat{12} - \bar{6} \quad + \quad \text{NSH}$$

or a convex combination of the equivalent stresses σ_{Tresca}, σ_{SI}, and σ_{I} of these criteria (TRESCA, SCHMIDT-ISHLINSKY, and the maximum normal stress hypothesis) with two parameters (ξ, ζ):

$$\xi\, \sigma_{\text{Tresca}} + \zeta\, \sigma_{\text{SI}} + (1 - \xi - \zeta)\, \sigma_{\text{I}} = \sigma_{\text{eq}} \tag{2.87}$$

and with parameter restrictions to ensure convexity

$$\xi \in [0,\, 1], \qquad \zeta \in [0,\, 1], \qquad \text{and} \qquad \xi + \zeta \leqslant 1. \tag{2.88}$$

The parameters in the formulation (2.87) have no direct physical meaning. This combination (2.87) can be realized in the different ways (Kolupaev, 2017, 2018; Kolupaev et al., 2018; Rosendahl et al., 2019b).

2.4.4.1 C^0-continuous Strength Criterion

Based on the normal stress hypothesis (Appendix 2.7.6) and the ROSENDAHL criterion (2.49), we introduce the linear combination, cf. Kolupaev (2017, 2018); Rosendahl et al. (2019b)

$$\hat{6} - \hat{12} | \bigcirc - \bar{6} \quad + \quad \text{NSH}$$

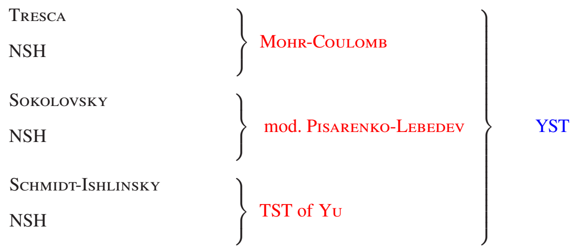

Fig. 2.16 Scheme of the YU strength theory (YST): TST – twin shear theory of YU, NSH – normal stress hypothesis, the SOKOLOVSKY criterion is a C^0-approximation of the VON MISES criterion with a regular dodecagon $\hat{12}$. Color meaning: black - criteria without any parameters, red – criteria with one parameter, and blue - the criterion with two parameters additionally to the equivalent stress σ_{eq}.

or

$$\sigma_{eq} = \frac{1}{r^C_{60}}\,\sigma_{Rsn} + \left(1 - \frac{1}{r^C_{60}}\right)\sigma_{NSH} \tag{2.89}$$

with the parameter restrictions

$$\frac{1}{r^C_{60}} \in]0,\,1], \qquad \beta_6 \in [0,\,1], \qquad \eta_6 \in [-1,\,1]. \tag{2.90}$$

This results in a final equation of the modified YU strength criterion (mYU)

$$\begin{aligned}\sigma_{eq} = {} & \frac{1}{r^C_{60}}\sqrt{3\,I_2'}\,\frac{\cos\left[\frac{1}{6}\left(\pi\,\beta_6 - \arccos\left[\gamma_6\cos 6\theta\right]\right)\right]}{\cos\left[\frac{1}{6}\left(\pi\,\beta_6 - \arccos\left[\gamma_6\right]\right)\right]} \\ & + \frac{1}{3}\left(1 - \frac{1}{r^C_{60}}\right)\left(I_1 + 2\sqrt{3\,I_2'}\cos\theta\right),\end{aligned} \tag{2.91}$$

which contains the criteria shown in **Fig. 2.17**. The modified YU criterion (2.91) describes the limit surface without plane intersections. The value r^S_{30} of the mYU is

$$\begin{aligned} r^S_{30} = 3\,r^C_{60} \times \Bigg[& \sqrt{3}\left(r^C_{60} - 1\right) \\ & + 3\cos\left[\frac{1}{6}\left(\pi\,\beta_6 - \arccos\left[-\gamma_6\right]\right)\right]\sec\left[\frac{1}{6}\left(\pi\,\beta_6 - \arccos\left[\gamma_6\right]\right)\right]\Bigg]^{-1}. \end{aligned} \tag{2.92}$$

The value r^{TTT} for the hydrostatic tensile limit loading results to

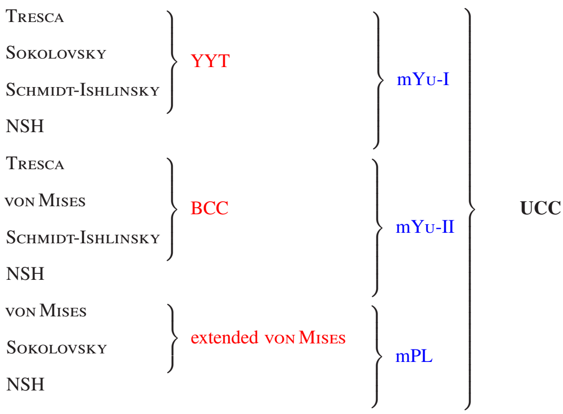

Fig. 2.17 Scheme of the mYU criterion: UCC – unified classical criterion, YYT – YU yield theory, mYU-I and mYU-II – modified YU criteria, mPL – modified PISARENKO-LEBEDEV criterion, BCC – bicubic criterion of SZWED. Color meaning: black - criteria without any parameters, red – criteria with one, blue - with two, and bold black - with three parameters additionally to the equivalent stress σ_{eq}.

$$\mathrm{r}^{\mathrm{TTT}} = \frac{1}{1 - \dfrac{1}{\mathrm{r}^{\mathrm{C}}_{60}}} = \frac{1}{1 - 2\,\nu^{\mathrm{in}}_{+}}. \tag{2.93}$$

The surface Φ of the mYU (2.91) is open in the hydrostatic compression direction ($\mathrm{I}_1 < 0$):

$$\mathrm{r}^{\mathrm{CCC}} \to \infty. \tag{2.94}$$

The inelastic POISSON's ratios at tension and compression are (Kolupaev, 2018)

$$\nu^{\mathrm{in}}_{+} = \frac{1}{2\,\mathrm{r}^{\mathrm{C}}_{60}} \qquad \text{and} \qquad \nu^{\mathrm{in}}_{-} = \frac{\mathrm{r}^{\mathrm{C}}_{60}}{2}, \tag{2.95}$$

as for the MOHR-COULOMB and further criteria in **Table 2.4**.

The TST (**Table 2.4**) cannot be reproduced exactly by this method (2.89). The deviation between $\hat{6} - \bigcirc - \bar{6}$ of the BCC and $\hat{6} - \hat{12} - \bar{6}$ of the YYC is relevant for "very ductile materials" (Christensen, 2019; Kolupaev, 2018; Lemaitre and Chaboche, 1990; von Mises, 1928; Theocaris, 1995)

$$\nu^{\mathrm{in}}_{+} \to \frac{1}{2}. \tag{2.96}$$

The introduced criterion (2.89) is C^0-continuously in the π-plane. The criterion contains a singular peak at the hydrostatic node TTT for pressure-sensitive materials with $\mathrm{r}^{\mathrm{C}}_{60} > 1$, which should be treated separately (**Table 2.11**, PG10). Like the YST, the mYU criterion can be considered as unified classical criterion (UCC) with the properties (2.39).

The modified YU strength criterion (2.89) meet the plausibility assumptions in the best way and is recommended for application as a yield and strength criterion (**Figs. 2.18**, **2.19**, **2.20**, and **2.21** with $\eta_3 = \eta_6 = 1$). Various material properties can be described using this criterion. The implementation in the FEM code is simple due to solely surface in the principal stress space.

Generalization of (2.89) based on the C^0-linear combinations (2.74)

$$\hat{6} - \hat{12}\,|\,\hat{24}\,|\,\bar{12} - \bar{6}$$

or C^1-linear combinations (Sect. 2.4.3.2)

$$\hat{6} - \hat{12}\,|\,\bigcirc\,|\,\bar{12} - \bar{6}$$

and the NSH can be suggested (**Table 2.5**)

$$\hat{6} - \hat{12}\,|\,\hat{24}\,|\,\bar{12} - \bar{6} \qquad + \qquad \mathrm{NSH}$$

or

$$\hat{6} - \hat{12}\,|\,\bigcirc\,|\,\bar{12} - \bar{6} \qquad + \qquad \mathrm{NSH}.$$

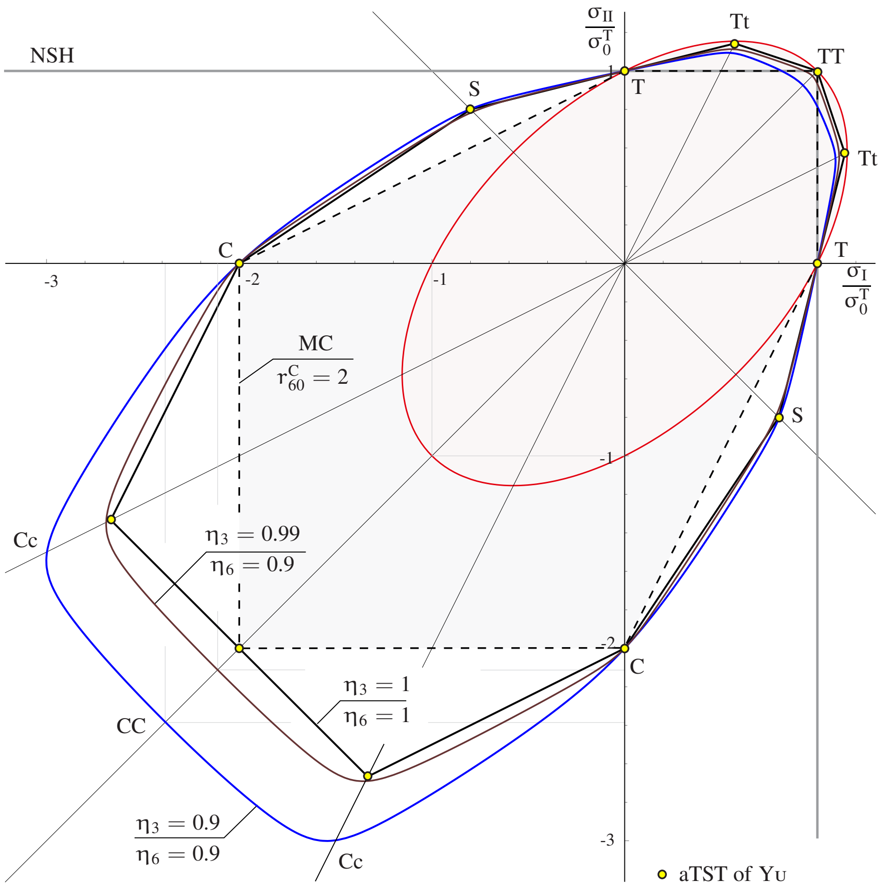

Fig. 2.18: Modified YST (2.98) as function of the parameters η_3 and η_6 with the setting $r^C_{60} = 2$ and $\beta_6 = 0$ in the normalized $\sigma_I - \sigma_{II}$ diagram. The points of the approximated TST (aTST) with $\eta_3 = \eta_6 = 1$ are highlighted. The ellipse of the VON MISES criterion (red) and the MOHR-COULOMB criterion (MC) (dashed line) are shown for comparison.

Such criteria are far from the practical relevance. The additional fitting possibilities with the transition $\hat{2}4|1\bar{2}$-NSH or $\bigcirc|1\bar{2}$-NSH can be only relevant for very ductile material with $r^C_{60} \to 1$ or, equivalently, with (2.96).

2.4.4.2 C^1-continuous Strength Criterion

Linear combination (Sect. 2.4.4.1)

$$\hat{6} - \bigcirc - \bar{6} \quad + \quad \text{NSH}$$

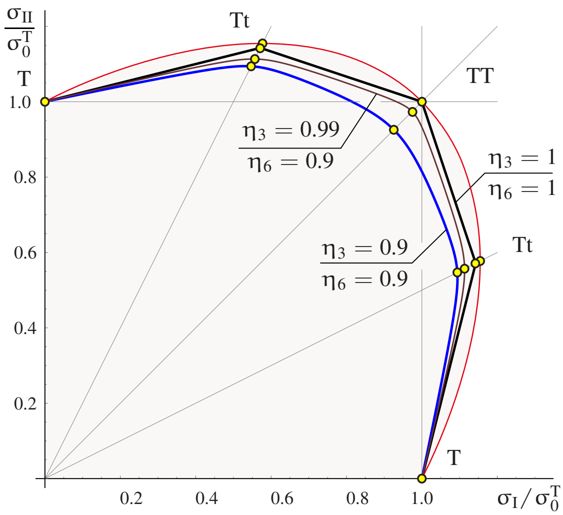

Fig. 2.19 Modified YST (2.98) as function of the parameters η_3 and η_6 with the setting $r^C_{60} = 2$ and $\beta_6 = 0$ in the normalized $\sigma_I - \sigma_{II}$ diagram. The ellipse of the VON MISES criterion (red) is shown for comparison. The first quadrant is enlarged for better visualization.

can be reformulated as linear combination with the linear I_1-substitution (2.15)

$$\hat{6} - \bigcirc - \bar{6} \quad + \quad (\hat{3} \rightarrow I_1), \qquad \gamma_1 = \frac{1}{3}$$

as function of two parameters. The method searched for is a formulation of the C^1-criterion of the above schema in accordance with the YST (**Table 2.5**).

With the equivalent stress σ_{C1} of the C^1-NSH (Appendix 2.7.6) and the ROSENDAHL criterion (2.49) we can write, cf. (2.89)

$$\sigma_{eq} = \frac{1}{r^C_{60}}\,\sigma_{Rsn} + \left(1 - \frac{1}{r^C_{60}}\right)\sigma_{C1} \tag{2.97}$$

or inserted

$$\begin{aligned}\sigma_{eq} = {} & \frac{1}{r^C_{60}}\sqrt{3\,I_2'}\,\frac{\cos\left[\frac{1}{6}\left(\pi\beta_6 - \arccos[\eta_6\cos 6\,\theta]\right)\right]}{\cos\left[\frac{1}{6}\left(\pi\beta_6 - \arccos[\eta_6]\right)\right]} + \\ & \left(1 - \frac{1}{r^C_{60}}\right)\left(\sqrt{3\,I_2'}\,\frac{\cos\left[-\frac{1}{3}\arccos[\eta_3\cos 3\,\theta]\right]}{\cos\left[-\frac{1}{3}\arccos[\eta_3]\right]}(1-\gamma_1) + \gamma_1\,I_1\right)\end{aligned} \tag{2.98}$$

with the substitution (2.138)

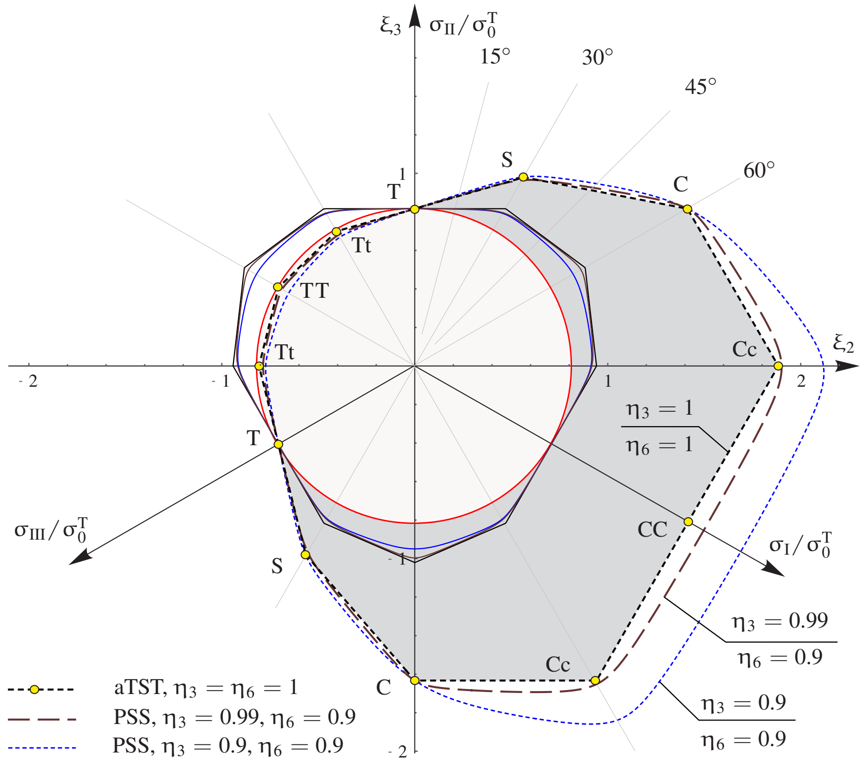

Fig. 2.20: Modified YST (2.98) as function of the parameters η_3 and η_6 with the setting $r^C_{60} = 2$ and $\beta_6 = 0$ in the normalized π-plane. The cross sections orthogonal to the hydrostatic axis at $I_1 = \sigma^T_0/\sqrt{3}$ and the lines of the plane stress state (PSS, dashed lines) are shown. The points of the C^0-approximated TST (aTST) with $\eta_3 = \eta_6 = 1$ are highlighted. The circle of the VON MISES criterion is shown for comparison.

$$\gamma_1(\eta_3) = 1 \Bigg/ \left\{1 + \cos\left[\frac{1}{3}\arccos[\eta_3]\right]\sec\left[\frac{1}{3}\arccos[-\eta_3]\right]\right\} \tag{2.99}$$

as function of four parameters (**Figs. 2.18** and **2.19**)

$$\frac{1}{r^C_{60}} \in [0, 1], \qquad \beta_6 \in [0, 1], \qquad \eta_6 \in [-1, 1], \qquad \eta_3 \in [-1, 1].$$

The fourth parameter can first be set $\eta_3 \in [0.99, 1[$ for the “rounding off” NSH (**Table 2.8**). We obtain with $\eta_6 \in]-1, 1[$ the C^1-continuous strength criterion. The values are

$$\nu^{in}_{+} = \frac{1}{2} - \frac{3}{2}\,\frac{r^C_{60} - 1}{r^C_{60}}\,\gamma_1, \tag{2.100}$$

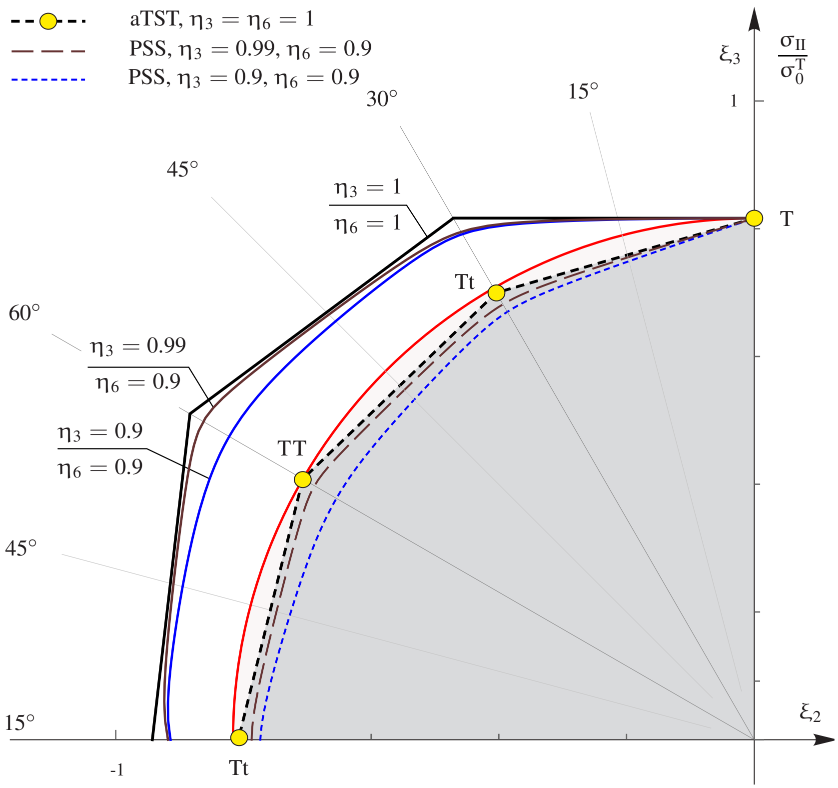

Fig. 2.21: Enlarged cut of the π-plane (**Fig. 2.20**): modified YST (2.98) as function of the parameters η_3 and η_6 with the setting $r^C_{60} = 2$ and $\beta_6 = 0$ in the normalized π-plane. The circle of the VON MISES criterion (red) is shown for comparison.

$$r^{\mathrm{TTT}} = \frac{1}{3}\,\frac{r^C_{60}}{\left(r^C_{60} - 1\right)\gamma_1}, \tag{2.101}$$

and

$$r^{\mathrm{CC}}_0 = \frac{r^C_{60}}{r^C_{60} + 3\gamma_1 - 3\,r^C_{60}\,\gamma_1}. \tag{2.102}$$

Further values are too large and therefore omitted.

Based on the value r^{CC}_0 (2.102), the deviation of the real material properties from the classical assumption with $r^{\mathrm{CC}}_0 = r^C_{60}$ (2.39) can be introduced

$$\delta_{\mathrm{Yu}} = \frac{r^{\mathrm{CC}}_0 - r^C_{60}}{r^C_{60}}. \tag{2.103}$$

And vice versa, the parameter η_3 dependent on the deviation δ_{Yu} of the value r^{CC}_0 from the value r^C_{60} (2.102) can be set (**Table 2.6**).

Table 2.6: Setting of the parameter η_3 dependent on the default deviation $\delta_{\mathrm{Yu}} = 1$ or 2% of the value r_0^{CC} from r_{60}^{C}.

r_{60}^{C}	η_3 at $\delta_{\mathrm{Yu}} = 1\%$	η_3 at $\delta_{\mathrm{Yu}} = 2\%$
1.1	0.963797	0.848176
1.2	0.991328	0.964532
1.5	0.998651	0.994610
2	0.999666	0.998677
5	0.999979	0.999919
10	0.999996	0.999984
12	0.999997	0.999990

This criterion (2.98) can be applied as the yield and strength criterion and is recommended for use. Problems with the derivation become obsolete, but the properties of the classical criteria (2.39) are lost.

The number of parameters seems excessive at first, but can be easily reduced based on the modeling concept:

- Setting $\beta_6 = 0$, $\eta_6 \in [-1, 1]$ for the C^1-transition $\hat{6} - \bigcirc - \bar{6}$ or
- Setting $\beta_6 \in [0, 1]$, $\eta_6 = \{-1, 1\}$ for the C^0-transition $\hat{6} - \hat{12} - \bar{6}$ of the YYC,

with formal or computed setting η_3 (**Table 2.6**). The setting $\eta_3 = 1$ provides the extended C^0-criterion according to YU with the classical properties (Sect. 2.4.4.1). Now, only two parameters remain for definition: (r_{60}^{C}, η_6) or (r_{60}^{C}, β_6).

If the amount of measured data is sufficiently large, the parameter $\eta_3 \in [-1, 1]$ in (2.134) can be used as an extra parameter. The physical background behind the YST is then lost, but fitting quality increases.

2.5 Criterion with Shape Variation in π-plane

Instead of generalizing possible shapes in the π-plane, Pisarenko and Lebedev (1969); Ottosen (1975, 1977, 1980); Ottosen and Ristinmaa (2005); Xiaoping et al. (1989) allowed for shape variation in the π-plane along the hydrostatic axis. Using the PODGÓRSKI shape function Ω_3 (2.45) and the POSENDAHL shape function Ω_6 (2.50), the OTTOSEN idea can be extended as (Rosendahl et al., 2019b)

$$3\,(1-\chi)\,I_2'\left(\frac{\Omega_6(\theta,\,\beta_6,\eta_6)}{\Omega_6(0,\,\beta_6,\eta_6)}\right)^2 + \chi\,\sigma_{\mathrm{eq}}\left[(1-\xi)\sqrt{3\,I_2'}\,\frac{\Omega_3(\theta,\,\beta_3,\eta_3)}{\Omega_3(0,\,\beta_3,\eta_3)} + \xi\,I_1\right] = \sigma_{\mathrm{eq}}^2 \tag{2.104}$$

with the parameters of the convex combinations

$$\chi \in [0, 1] \qquad \text{and} \qquad \xi \in [0, 1]. \tag{2.105}$$

With $\xi \in]0, 1[$, we obtain a surface with cross sections of hexagonal symmetry in the π-plane for $I_1 \to -\infty$. Compared with (2.48), this effect is controlled with an additional parameter χ. Some approximations are obtained for data measured by KUPFER for three types of concrete with $\chi \in [0.9845, 1]$ and $\xi \in [0.3037, 0.3523]$ (Rosendahl et al., 2019b).

The criterion (2.104) can be considered as a generalization of

- the PODGÓRSKI pyramid (2.48) or its corresponding CTS-formulation (2.55) with $\chi = 1$,
- the ROSENDAHL criterion (2.49)–(2.50), which can be replaced with one of the CHS-formulations (2.56) with $\chi = 0$,
- the formulation in accordance with OTTOSEN if $\beta_3 = \beta_6 = \eta_6 = 0, \eta_3 \in [-1, 1]$,
- the strain criterion (**Table 2.3**) with $\chi = 1$ and the regular triangle $\bar{3}$ with $\beta_3 = \{0, 1\}$ and $\eta_3 = \{1, -1\}$. The NSH follows then with the setting $\xi = 1/3$,
- an alternative formulation of the PISARENKO-LEBEDEV criterion (**Table 2.4**) with $\chi \in]0, 1[$, $\beta_3 = \beta_6 = \eta_3 = \eta_6 = 0$, and $\xi = 1/3$,
- the DRUCKER-PRAGER criterion (**Table 2.3**, rotationally symmetric cone) with $\chi = 1$ and $\beta_3 = \beta_6 = \eta_6 = 0$, and
- the BURZYŃSKI-TORRE criterion (rotationally symmetric paraboloid) (Balandin, 1937; Burzyński, 1928; Torre, 1947; Yagn, 1931) with $\beta_3 = \beta_6 = \eta_3 = \eta_6 = 0$, $\chi \in]0, 1[$ and $\xi = 1$.

The criterion (2.104) fulfils some plausibility assumptions (Appendix 2.7.8) quite well and can be recommended for application. The variable cross section approach according OTTOSEN is different from the fixed cross section approach. Because of the greater flexibility, the criterion (2.104) provides very good approximations of experimental data but such criteria require increased numerical effort in the application.

Some measurements regarding the change of the cross section as function of I_1 are given in Launay et al. (1970); Launay and Gachon (1971, 1972). Approximations are shown in Gol'dman (1994); Fahlbusch (2015); Kolupaev (2018); Rosendahl et al. (2019b), among others.

2.6 Summary

In this work, a nomenclature of the yield criteria Φ is introduced. The regular polygons of trigonal and hexagonal symmetry in the π-plane are represented schematically based on the number of their edges and the orientation in the π-plane. The rotationally symmetric VON MISES criterion is denoted as a circle (Subsect. 2.3.1).

Known plausibility assumptions of the yield and strength criteria are summarized (Appendix 2.7.8). They limit the variety of the criteria on the basis of applicability. The relevant assumptions in the authors' opinion are highlighted, which are used for selection of the recommended criteria (**Table 2.2** and **2.5**, criteria with the equation number). It is posited, that only the yield criteria involving three or more regular (basic) geometries (**Table 2.1**) are significant for application. This viewing reduces the number of the suitable criteria. Further criteria are particular and can be easily approximated with these specified criteria.

The earlier strength criteria are presented in **Tables 2.3** and **2.4**. Some missing criteria are introduced according to the pattern. These criteria are too simple for design with current requirements but the introduced schematics can be primary used as support in didactic.

Nowadays the most effective yield criteria are the criteria of PODGÓRSKI-type with $k = 1$ and 2 (Subsect. 2.4.2). They meet the plausibility assumptions in the best way known. However, they do not include all relevant yield criteria at once. Thus, their application is associated with restrictions. Two ways for the formulation of the generalized yield criteria are discussed (Subsect. 2.4.3):

- convex combination of the known criteria (Subsects. 2.4.3.1–2.4.3.5) and
- series development as "arccosine of the sum" and "sum of arccosines" (Subsect. 2.4.3.6).

The first schema has proven for practical use. The second way is still being investigated.

Several ways can be envisaged for the linear combinations (Subsect. 2.4.3.1) with the PODGÓRSKI-type shape functions (2.40). The disadvantage of the proposed formulations is that the number of the parameters increases. Both terms in the linear combinations (Subsect. 2.4.3.1) can describe the same geometries: TRESCA and VON MISES criteria in (2.55) and SOKOLOVSKY and VON MISES criteria in (2.56). These criteria are modified according to ALTENBACH-ZOLOCHEVSKY in order to reduce the number of parameters (Subsects. 2.4.3.4 and 2.4.3.5). The resulting C^0-criteria extended with I_1-substitution can be easily applied for fitting of measured data.

Open question remains the formulation of the HAYTHORNTHWAITE and MAC criteria as a function of the stress angles without case discrimination (**Table 2.2**). If such criteria will be derived, the formulations (Subsect. 2.4.3) are no longer required.

The YU strength theory (Subsect. 2.4.4) is of crucial importance for practice. The C^0-generalization without plane intersections (Subsect. 2.4.4.1) provides decisive advantages compared to the original YU's formulation. The C^1-generalization (Subsect. 2.4.4.2) is a powerful tool that includes the YST and is recommended for use.

The yield and strength criteria can be easily compared based on the introduced relations (Subsects. 2.3.2 and 2.3.5). Different approximations can be visualized in the diagrams $r_{60} - r_{30}$ (**Fig. 2.8**) or $r_{30} - r_{15}$ (**Fig. 2.9**), π-plane, and the BURZYŃSKI-plane. Additional requirements can be set for the parameters to reduce their number, e.g. the classical properties (2.39) or, based on the NSH, the position of the node TTT with $\gamma_1 = 1/3$ in order to obtain the special "theories".

The study of the yield and strength criteria remains in focus of professional community (Altenbach, 2010). Further development of the equivalent stress concept can be seen in consideration of the adjusted plausibility assumptions, which should be accompanied with restriction of the parameters. The number of parameters should be kept to a minimum.

Acknowledgements The authors thank Dr.-Ing. Philipp L. Rosendahl, TU-Darmstadt, for critical reading of the manuscript, suggestions for improvement, and discussions. Dr. rer. nat. Alexandre Bolchoun, ISG Industrielle Steuerungstechnik GmbH, Stuttgart, is sincerely thanked for plausibility check, numerous comments, and discussions.

2.7 Appendix

2.7.1 Invariants of Stress Tensor

Stress based criteria Φ for isotropic materials should be invariant with respect to the symmetric second-rank stress tensor $\boldsymbol{\sigma}$ (Życzkowski, 1981). Therefore, the criteria are built up using the invariants of this tensor. As a result of the eigenvalue problem, the principal values (principal stresses) are obtained and denoted by σ_{I}, σ_{II}, and σ_{III} (Altenbach et al., 1995; Altenbach and Kolupaev, 2014). The following order is assumed

$$\sigma_{\mathrm{I}} \geqslant \sigma_{\mathrm{II}} \geqslant \sigma_{\mathrm{III}}. \tag{2.106}$$

The invariants of the stress tensor play an important role in the formulation of the equivalent stress expressions (Sect. 2.2). Three stress invariants: the trace (axiator) I_1 of the stress tensor and the invariants I_2', I_3' of the stress deviator as functions of the principal stresses (Życzkowski, 1981; Altenbach et al., 1995; Altenbach and Kolupaev, 2014)

$$\mathrm{I}_1 = \sigma_{\mathrm{I}} + \sigma_{\mathrm{II}} + \sigma_{\mathrm{III}}, \tag{2.107}$$

and

$$\begin{aligned} \mathrm{I}_2' &= \frac{1}{6}\left[(\sigma_{\mathrm{I}} - \sigma_{\mathrm{II}})^2 + (\sigma_{\mathrm{II}} - \sigma_{\mathrm{III}})^2 + (\sigma_{\mathrm{III}} - \sigma_{\mathrm{I}})^2\right] = \\ &= \frac{1}{2}\left[\left(\sigma_{\mathrm{I}} - \frac{1}{3}\mathrm{I}_1\right)^2 + \left(\sigma_{\mathrm{II}} - \frac{1}{3}\mathrm{I}_1\right)^2 + \left(\sigma_{\mathrm{III}} - \frac{1}{3}\mathrm{I}_1\right)^2\right], \end{aligned} \tag{2.108}$$

$$\begin{aligned} \mathrm{I}_3' &= \left(\sigma_{\mathrm{I}} - \frac{1}{3}\mathrm{I}_1\right)\left(\sigma_{\mathrm{II}} - \frac{1}{3}\mathrm{I}_1\right)\left(\sigma_{\mathrm{III}} - \frac{1}{3}\mathrm{I}_1\right) = \\ &= \frac{1}{3}\left[\left(\sigma_{\mathrm{I}} - \frac{1}{3}\mathrm{I}_1\right)^3 + \left(\sigma_{\mathrm{II}} - \frac{1}{3}\mathrm{I}_1\right)^3 + \left(\sigma_{\mathrm{III}} - \frac{1}{3}\mathrm{I}_1\right)^3\right] \end{aligned} \tag{2.109}$$

are often used in modeling, see (2.3).

2.7.2 Scalar Functions of Invariants

Scalar functions of the invariants (2.107) - (2.109) are also invariants (Mālmeisters et al., 1977), e. g.

- the scaled axiator I_1 of the stress tensor (De Boer, 2000; Kolupaev, 2018)

$$\xi_1 = I_1/\sqrt{3} \tag{2.110}$$

  describes the coordinate of loading on the hydrostatic axis (**Fig. 2.1**, axis ξ_3),
- the root of the scaled second invariant of the stress deviator

$$\rho_{HW} = \sqrt{2\,I_2'} \tag{2.111}$$

  as radius in the HAIGH-WESTERGAARD coordinates (De Boer, 2000; Kolupaev, 2018),
- the stress angle θ in the π-plane (plane with the cross section $I_1 = \text{const.}$) (Novozhilov, 1951b; Życzkowski, 1981; Chen and Zhang, 1991; Ottosen and Ristinmaa, 2005)

$$\cos 3\theta = \frac{3\sqrt{3}}{2}\frac{I_3'}{\left(I_2'\right)^{3/2}}, \qquad \theta \in \left[0, \frac{\pi}{3}\right], \tag{2.112}$$

  and
- the elevation ψ (Hencky, 1943; Życzkowski, 1981; Altenbach and Kolupaev, 2014)

$$\tan\psi = \frac{\sqrt{3\,I_2'}}{I_1}, \qquad \psi \in [0, \pi] \tag{2.113}$$

  or a stress triaxiality factor (Yagn and Vinogradov, 1954; Davis and Connelly, 1959; Lebedev et al., 1979; Kolupaev, 2006; Lebedev, 2010; Kolupaev, 2018)

$$\eta = \frac{1}{\tan\psi}. \tag{2.114}$$

These invariants (2.110) - (2.113) are sometimes preferred because of the geometric interpretation of the loading in the stress space. Other invariants are given in Altenbach et al. (1995); Altenbach and Kolupaev (2014); Yagn and Vinogradov (1954); Życzkowski (1981) for instance.

2.7.3 Modified Invariants

The radius (2.111) can be also introduced based on the VON MISES hypothesis (von Mises, 1913, 1928) as

$$\rho = \sqrt{3\,\mathrm{I}_2'} \tag{2.115}$$

for normalization of the measured data with respect to the appropriate uniaxial tensile limit loading

$$\sigma_{\mathrm{I}} = \sigma_0^{\mathrm{T}}, \qquad \sigma_{\mathrm{II}} = \sigma_{\mathrm{III}} = 0 \tag{2.116}$$

and uniform visualization (Subsects. 2.3.2 and 2.3.5).

The deviatoric invariant I_3' (2.108) can be expressed as a function of ρ and $\cos 3\theta$ (Szwed, 2000, 2013)

$$\mathrm{I}_3' = \frac{2}{3\sqrt{3}} \sqrt{\left(\mathrm{I}_2'\right)^3} \cos 3\theta = \frac{2}{3^3}\, \rho^3 \cos 3\theta, \tag{2.117}$$

what is used in Appendix 2.7.7 for deployment of the series of invariants.

With a double-angle function (Bronstein and Semendjajew, 2007) we obtain further invariants (Jemioło and Szwed, 1999; Szwed, 2000, 2013), see also Życzkowski (1981)

$$\cos 6\theta = 2\cos^2 3\theta - 1 = 2\, \frac{3^3}{2^2} \frac{\left(\mathrm{I}_3'\right)^2}{\left(\mathrm{I}_2'\right)^3} - 1 \tag{2.118}$$

and

$$\cos 12\theta = 2\cos^2 6\theta - 1 = 2\left(2\cos^2 3\theta - 1\right)^2 - 1 = 2\left(2\, \frac{3^3}{2^2} \frac{\left(\mathrm{I}_3'\right)^2}{\left(\mathrm{I}_2'\right)^3} - 1\right)^2 - 1, \tag{2.119}$$

which are used as “building blocks” in the formulation of the phenomenological criteria $\Phi(\rho, \theta)$ (Appendix 2.7.7).

2.7.4 Particular Points on Limit Surface

Particular points on the limit surface Φ can be obtained with the setting of the corresponding elevation ψ (2.113) and the stress angle θ (2.112)

$$\frac{\sqrt{3\,\mathrm{I}_2'}}{\mathrm{I}_1} = \tan\psi \qquad \text{and} \qquad \frac{3\sqrt{3}}{2} \frac{\mathrm{I}_3'}{\left(\mathrm{I}_2'\right)^{3/2}} = \cos 3\theta \tag{2.120}$$

normalized with

$$\sqrt{3\,\mathrm{I}_2'} = 1.$$

Typical settings follows, among others, with

$$\tan\psi = \infty,\, \pm\sqrt{3} \pm 1,\, \pm\frac{1}{\sqrt{3}},\, \pm\frac{1}{2},\, \pm\left(2-\sqrt{3}\right),\, \pm\left(\sqrt{6}-\sqrt{3}+\sqrt{2}-2\right), \ldots$$

for the angle

$$\psi = \frac{\pi}{2}, \pm\frac{\pi}{3}, \pm\frac{\pi}{4}, \pm\frac{\pi}{6}, \pm 0.4636, \pm\frac{\pi}{12}, \pm\frac{\pi}{24}, \dots$$

and the meridians (Subsect. 2.3.3), e.g.

$$\theta = 0, \frac{\pi}{12}, \frac{\pi}{6}, \frac{\pi}{4}, \frac{\pi}{3}.$$

For example, we obtain with $I_1 = 0$ and

$$\begin{aligned}
&\text{meridian} \quad \theta = 0: && \sigma_{\mathrm{I}} = \frac{2}{3}\, r_0^{\mathrm{Tcc}}\, \sigma_0^{\mathrm{T}}, && \sigma_{\mathrm{II}} = \sigma_{\mathrm{III}} = -\frac{1}{2}\,\sigma_{\mathrm{I}},\\
&\text{meridian} \quad \theta = \frac{\pi}{6}: && \sigma_{\mathrm{I}} = -\sigma_{\mathrm{II}} = \frac{1}{\sqrt{3}}\, r_{30}^{\mathrm{S}}\, \sigma_0^{\mathrm{T}}, && \sigma_{\mathrm{III}} = 0,\\
&\text{meridian} \quad \theta = \frac{\pi}{3}: && \sigma_{\mathrm{I}} = -\frac{2}{3}\, r_{60}^{\mathrm{ttC}}\, \sigma_0^{\mathrm{T}}, && \sigma_{\mathrm{II}} = \sigma_{\mathrm{III}} = -\frac{1}{2}\,\sigma_{\mathrm{I}}.
\end{aligned}$$

The meridians of VON MISES criterion coincide in the BURZYŃSKI-plane and it follows

$$r_0^{\mathrm{Tcc}} = r_{30}^{\mathrm{S}} = r_{60}^{\mathrm{ttC}} = 1.$$

The seven points of the plane stress states and the points of the hydrostatic loading are chosen for the analysis and comparison of the limit surfaces (**Table 2.7**). These loading cases have established definition and can be considered as the basic tests (Bulla and Kolupaev, 2021; Kolupaev, 2006, 2018).

2.7.5 Values for Comparison

In the following, details on the stress computation for comparison of geometric properties of the yield criteria Φ are given (Subsects. 2.3.2 and 2.3.5). These normalized stresses of the plane stress state are obtained with the setting

$$3\, I_2' = 1 \qquad \text{and} \qquad \sigma_{\mathrm{III}} = 0. \tag{2.121}$$

The value r_{15} is obtained setting

$$\cos\left[3\,\frac{\pi}{12}\right] = \frac{\sqrt{2}}{2}$$

with

$$\sigma_{\mathrm{I}} = \sqrt{\frac{2}{3}}, \qquad \sigma_{\mathrm{II}} = -\frac{1}{\sqrt{2}} + \frac{1}{\sqrt{6}}, \tag{2.122}$$

Table 2.7: Basic stress states with the corresponding stress angle θ and the dimensionless invariants η, cos 3θ, cos 6θ, cos 9θ, and cos 12θ (Kolupaev, 2018).

Label	CCC	CC	Cc	C	S	T	Tt	TT	TTT
$\frac{\sigma_{I}}{\sigma_0^T}$	$-r^{CCC}$	$-r_0^{CC}$	$-\frac{2}{\sqrt{3}}r_{30}^{Cc}$	$-r_{60}^{C}$	$\frac{1}{\sqrt{3}}r_{30}^{S}$	1	$\frac{2}{\sqrt{3}}r_{30}^{Tt}$	r_{60}^{TT}	r^{TTT}
$\frac{\sigma_{II}}{\sigma_0^T}$	$-r^{CCC}$	$-r_0^{CC}$	$-\frac{1}{\sqrt{3}}r_{30}^{Cc}$	0	$-\frac{1}{\sqrt{3}}r_{30}^{S}$	0	$\frac{1}{\sqrt{3}}r_{30}^{Tt}$	r_{60}^{TT}	r^{TTT}
$\frac{\sigma_{III}}{\sigma_0^T}$	$-r^{CCC}$	0	0	0	0	0	0	0	r^{TTT}
θ	-	0	$\frac{\pi}{6}$	$\frac{\pi}{3}$	$\frac{\pi}{6}$	0	$\frac{\pi}{6}$	$\frac{\pi}{3}$	-
η	$-\infty$	-2	$-\sqrt{3}$	-1	0	1	$\sqrt{3}$	2	∞
$\cos 3\theta$	-	1	0	-1	0	1	0	-1	-
$\cos 6\theta$	-	1	-1	1	-1	1	-1	1	-
$\cos 9\theta$	-	1	0	-1	0	1	0	-1	-
$\cos 12\theta$	-	1	1	1	1	1	1	1	-

Comments: C - uniaxial compression, Cc - biaxial compression in the stress relation 1:2, CC - equibiaxial compression, CCC - hydrostatic compression, S or TC - shear, T - uniaxial tension, Tt - biaxial tension in the stress relation 1:2, TT - equibiaxial tension, TTT - hydrostatic tension.

$$\sigma_{I} = -\sqrt{\frac{2}{3}}, \qquad \sigma_{II} = -\sqrt{\frac{2}{3} + \frac{1}{\sqrt{3}}} \tag{2.123}$$

or

$$\sigma_{I} = \sqrt{\frac{2}{3} + \frac{1}{\sqrt{3}}}, \qquad \sigma_{II} = \sqrt{\frac{2}{3} - \frac{1}{\sqrt{3}}}. \tag{2.124}$$

The value r_{30} is obtained setting

$$\cos\left[3\,\frac{\pi}{6}\right] = 0 \qquad \text{and} \qquad \sigma_{I} = -\sigma_{II}$$

with

$$\sigma_{I} = \frac{1}{\sqrt{3}}. \tag{2.125}$$

The value r_{45} is obtained setting

$$\cos\left[3\,\frac{\pi}{4}\right] = -\frac{\sqrt{2}}{2}$$

with

$$\sigma_{I} = \sqrt{\frac{2}{3}}, \qquad \sigma_{II} = \frac{1}{\sqrt{2}} + \frac{1}{\sqrt{6}} \tag{2.126}$$

or

$$\sigma_{\mathrm{I}} = \pm\sqrt{\frac{2}{3}}, \qquad \sigma_{\mathrm{II}} = \sqrt{\frac{2}{3} \pm \frac{1}{\sqrt{3}}}. \tag{2.127}$$

The value r_{60} is obtained setting

$$\cos\left[3\,\frac{\pi}{3}\right] = -1 \qquad \text{and} \qquad \sigma_{\mathrm{II}} = 0$$

with

$$\sigma_{\mathrm{I}} = -1. \tag{2.128}$$

The value $r_{7.5}$ is obtained setting (Weisstein, 2021)

$$\cos\left[3\,\frac{\pi}{24}\right] = \frac{1}{2}\sqrt{2+\sqrt{2}}$$

with

$$\sigma_{\mathrm{I}} = \pm\sqrt{\frac{1}{3}\left(2+\sqrt{2}\right)}, \qquad \sigma_{\mathrm{II}} = \pm\sqrt{\frac{1}{3}\left(2 \mp \sqrt{2 \pm \sqrt{3}}\right)} \tag{2.129}$$

or

$$\sigma_{\mathrm{I}} = -\sqrt{\frac{1}{3}\left(2-\sqrt{2+\sqrt{3}}\right)}, \qquad \sigma_{\mathrm{II}} = \sqrt{\frac{1}{3}\left(2+\sqrt{2-\sqrt{3}}\right)}. \tag{2.130}$$

And the value $r_{22.5}$ is obtained setting (Weisstein, 2021)

$$\cos\left[3\,\frac{\pi}{8}\right] = \frac{1}{2}\sqrt{2-\sqrt{2}}$$

with

$$\sigma_{\mathrm{I}} = \pm\sqrt{\frac{1}{3}\left(2-\sqrt{2}\right)}, \qquad \sigma_{\mathrm{II}} = \sqrt{\frac{1}{3}\left(2 \pm \sqrt{2 \pm \sqrt{3}}\right)} \tag{2.131}$$

or

$$\sigma_{\mathrm{I}} = -\sqrt{\frac{1}{3}\left(2+\sqrt{2+\sqrt{3}}\right)}, \qquad \sigma_{\mathrm{II}} = -\sqrt{\frac{1}{3}\left(2-\sqrt{2-\sqrt{3}}\right)}. \tag{2.132}$$

Further values of the plane stress state (Sect. 2.3.5)

$$r^{\mathrm{S}}_{30}, \quad r^{\mathrm{Tt}}_{30}, \quad r^{\mathrm{TT}}_{60}, \quad r^{\mathrm{C}}_{60}, \quad r^{\mathrm{Cc}}_{30}, \quad \text{and} \quad r^{\mathrm{CC}}_{0}$$

for pressure-sensitive criteria are given in Rosendahl et al. (2019b). The values for hydrostatic tensile limit loading (Subsect. 2.3.5) is

$$\mathrm{r}^{\mathrm{TTT}} = \frac{\sigma^{\mathrm{TTT}}}{\sigma_0^{\mathrm{T}}} = \frac{1}{3\gamma_1}$$

and hydrostatic compressive limit loading is

$$\mathrm{r}^{\mathrm{CCC}} = \frac{\sigma^{\mathrm{CCC}}}{\sigma_0^{\mathrm{T}}} = -\frac{1}{3\gamma_2},$$

which follow with $3\,\mathrm{I}_2' = 0$. Accordingly, $\cos 3\theta$ (2.112) is indeterminate in these two points.

2.7.6 Modified Normal Stress Hypothesis

Based on the PODGORSKI criterion (2.44) with (2.45), we obtain a conical (pyramidal at the border of the parameter η_3) criterion with the linear I_1-substitution (2.15)

$$\sqrt{3\,\mathrm{I}_2'}\,\frac{\Omega_3(\theta,0,\eta_3)}{\Omega_3(0,0,\eta_3)} = \frac{\sigma_{\mathrm{eq}} - \gamma_1\,\mathrm{I}_1}{1-\gamma_1} \qquad \text{with} \qquad \gamma_1 \in [0,1[, \qquad \eta_3 \in [-1,1] \tag{2.133}$$

or resolved with respect of the equivalent stress σ_{eq}

$$\sigma_{\mathrm{eq}} = \sqrt{3\,\mathrm{I}_2'}\,\frac{\cos\left[-\dfrac{1}{3}\arccos[\eta_3\cos 3\theta]\right]}{\cos\left[-\dfrac{1}{3}\arccos[\eta_3]\right]}(1-\gamma_1) + \gamma_1\,\mathrm{I}_1. \tag{2.134}$$

This criterion is named the SAYIR cone $\hat{3} - \bigcirc - \bar{3} \to \mathrm{I}_1$ (Kolupaev, 2018). The maximum normal stress hypothesis (NSH) follows with the setting

$$\gamma_1 = \frac{1}{3} \qquad \text{and} \qquad \eta_3 = 1$$

or after substitution (Chen and Zhang, 1991; Kolupaev, 2018; Rosendahl et al., 2019b)

$$\sigma_{\mathrm{NSH}} = \frac{1}{3}\left(\mathrm{I}_1 + 2\sqrt{3\,\mathrm{I}_2'}\cos\theta\right) \tag{2.135}$$

which results in the most important properties of the NSH (**Fig. 2.22**, **Table 2.8**)

$$\mathrm{r}_{60}^{\mathrm{C}} \to \infty, \qquad \nu_+^{\mathrm{in}} = 0, \qquad \mathrm{r}_{30}^{\mathrm{S}} = \sqrt{3}, \qquad \mathrm{r}_{60}^{\mathrm{TT}} = \mathrm{r}^{\mathrm{TTT}} = 1.$$

Restrictive is that the derivation at the corners of the surface Φ is discontinuous (Lagioia and Panteghini, 2016). These corners in the π-plane can be "rounded off" with the parameter $\eta_3 \in [0.99, 1[$ depending on the required computation accuracy (**Fig. 2.22**, **Table 2.8**).

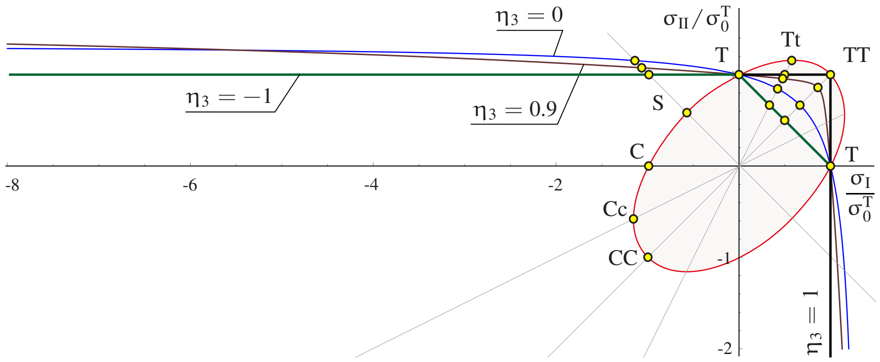

Fig. 2.22: Modified normal stress hypothesis (2.134) as function of the parameter η_3 (2.138) in the normalized $\sigma_{\text{I}} - \sigma_{\text{II}}$ diagram. The ellipse of the VON MISES criterion (red line) and the NSH (thick black line) are shown for comparison.

Table 2.8: Settings of the parameter $\eta_3 \in [-1, 1]$ and corresponding values for the modified normal stress hypothesis (2.134) with the property $r^{\text{C}}_{60} \to \infty$ (2.138).

η_3	γ_1	ν^{in}_{+}	r^{S}_{30}	r^{Tt}_{30}	r^{TT}_{60}	r^{TTT}	π-plane
1	1/3	0	$\sqrt{3}$	$\sqrt{3}/2$	1	1	$\bar{3}$
0.999999	0.3335	-0.0003	1.7325	0.8659	0.9995	0.9995	-
0.99999	0.3339	-0.0009	1.7335	0.8657	0.9982	0.9982	-
0.9999	0.3351	-0.0027	1.7368	0.8648	0.9946	0.9946	-
0.999	0.3390	-0.0085	1.7468	0.8623	0.9832	0.9832	-
0.99	0.3510	-0.0265	1.7773	0.8542	0.9496	0.9496	-
0.9	0.3870	-0.0804	1.8623	0.8284	0.8614	0.8614	-
0	1/2	-1/4	2	$\sqrt{3}-1$	2/3	2/3	○
-1	2/3	-1/2	$\sqrt{3}$	$1/\sqrt{3}$	1/2	1/2	$\hat{3}$

The value r^{C}_{60} for the criterion (2.134) can be computed as

$$r^{\text{C}}_{60} = 1 \Big/ \left[(1-\gamma_1) \cos\left[\frac{1}{3} \arccos[-\eta_3]\right] \sec\left[\frac{1}{3} \arccos[\eta_3]\right] - \gamma_1 \right] \tag{2.136}$$

and the property $r^{\text{C}}_{60} \to \infty$ follows with the denominator

$$(1-\gamma_1) \cos\left[\frac{1}{3} \arccos[-\eta_3]\right] \sec\left[\frac{1}{3} \arccos[\eta_3]\right] - \gamma_1 = 0. \tag{2.137}$$

The parameter $\gamma_1(\eta_3)$ results in

$$\gamma_1(\eta_3) = 1 \Big/ \left[1 + \cos\left[\frac{1}{3}\arccos[\eta_3]\right] \sec\left[\frac{1}{3}\arccos[-\eta_3]\right]\right]. \tag{2.138}$$

This means that the $\pi/3$-meridian is parallel to the straight line $I_1 = -\sqrt{3\,I_2'}$ in the BURZYŃSKI-plane (Kolupaev, 2018). Inserted Eq. (2.138) in Eq. (2.134) results in the values of the modified normal stress hypothesis (C^1-NSH):

$$r_{30}^{S} = \frac{2}{\sqrt{3}\,(1-\gamma_1)} \cos\left[\frac{1}{3}\arccos[\eta_3]\right] \tag{2.139}$$

or

$$r_{30}^{S} = \frac{2}{\sqrt{3}} \left[\cos\left[\frac{1}{3}\arccos[-\eta_3]\right] + \cos\left[\frac{1}{3}\arccos[\eta_3]\right]\right], \tag{2.140}$$

$$r_{30}^{Tt} = \frac{2}{\sqrt{3}\left[2\gamma_1 + (1-\gamma_1)\sec\left[\frac{1}{3}\arccos[\eta_3]\right]\right]} \tag{2.141}$$

or

$$r_{30}^{Tt} = 2\sqrt{3}\,\frac{\cos\left[\frac{1}{3}\arccos[-\eta_3]\right] + \cos\left[\frac{1}{3}\arccos[\eta_3]\right]}{3 + 6\cos\left[\frac{1}{3}\arccos[-\eta_3]\right]}, \tag{2.142}$$

$$r_{60}^{TT} = \frac{1}{3\gamma_1}, \tag{2.143}$$

and the inelastic POISSON's ratio at tension follows with

$$\nu_{+}^{in} = \frac{1}{2}\,(1 - 3\gamma_1). \tag{2.144}$$

This formulation (2.134) with (2.138) is used to derive a C^1-continuous strength criterion according to YST (Subsect. 2.4.4).

The C^1-continuous normal stress hypothesis (C^1-NSH) can be applied in the whole range of the parameter $\eta_3 \in [-1, 1]$ for better approximation of measured data (**Table 2.8**). Although the property $r_{60}^{C} \to \infty$ is retained (**Fig. 2.22**), physical background of the normal stress hypothesis is then lost.

2.7.7 Series of Invariants

The general structure of the yield criterion Φ is unknown and can not be deduce based on theoretical considerations (Subsect. 2.4.3). It is known that the criteria Φ are functions of the stress invariants (Subsect. 2.2.2), which can be grouped into the number of series. One of possibilities is to construct the deviatoric series of the same powers of the radius ρ (2.115) and increasing powers of $\cos 3\theta$.

The complete deviatoric series S_n'

$$S'_n = \rho^n \left(b_n + c_{n1} \cos 3\theta + c_{n2} \cos^2 3\theta + \ldots\right), \qquad n \in \mathbb{N} \tag{2.145}$$

contains several parameters b_n and c_{ni}, which should be restricted based on the theoretical considerations and later fitted to the test data. The terms with fractional exponents (Chen and Han, 1993)

$$(I'_3)^{1/3}, \qquad (I'_3)^{2/3}, \qquad (I'_3)^{4/3}, \qquad \text{etc.}$$

or, what is the same,

$$\rho\,(\cos 3\theta)^{1/3}, \qquad \rho^2\,(\cos 3\theta)^{2/3}, \qquad \rho^4\,(\cos 3\theta)^{4/3}, \qquad \text{etc.}$$

are excluded from these series because they lead to non-convex surfaces, see Altenbach et al. (1995); Gol'denblat and Kopnov (1968, 1971b); Spitzig et al. (1975); Spitzig and Richmond (1979) and cf. Desai (1980); Desai and Faruque (1984b,a); Jemioło (1992); Wojewódzki et al. (1995).

The applicability of the complete series (2.145) in a criterion is controversial because of the large number of parameters. The method is sought for restriction of this number in order to formulate the effective criteria according to the plausibility assumptions (Appendix 2.7.8).

We obtain the reduced deviatoric series if only the invariants ρ (2.115), I'_3 in the form $\rho^3 \cos 3\theta$ (2.117), and their products of the same power n of ρ are taken:

$$\begin{aligned}
S'_1 &= b_1\,\rho,\\
S'_2 &= b_2\,\rho^2,\\
S'_3 &= (b_3 + c_3 \cos 3\theta)\,\rho^3,\\
S'_4 &= (b_4 + d_{13} \cos 3\theta)\,\rho^4,\\
S'_5 &= (b_5 + d_{23} \cos 3\theta)\,\rho^5,\\
S'_6 &= (b_6 + d_{33} \cos 3\theta + c_6 \cos^2 3\theta)\,\rho^6,\\
S'_7 &= (b_7 + d_{43} \cos 3\theta + d_{16} \cos^2 3\theta)\,\rho^7,\\
S'_8 &= (b_8 + d_{53} \cos 3\theta + d_{26} \cos^2 3\theta)\,\rho^8,\\
S'_9 &= (b_9 + d_{63} \cos 3\theta + d_{36} \cos^2 3\theta + c_9 \cos^3 3\theta)\,\rho^9,\\
S'_{10} &= (b_{10} + d_{91} \cos 3\theta + d_{46} \cos^2 3\theta + d_{19} \cos^3 3\theta)\,\rho^{10},\\
S'_{11} &= (b_{11} + d_{83} \cos 3\theta + d_{56} \cos^2 3\theta + d_{29} \cos^3 3\theta)\,\rho^{11},\\
S'_{12} &= (b_{12} + d_{93} \cos 3\theta + d_{66} \cos^2 3\theta + d_{39} \cos^3 3\theta + c_{12} \cos^4 3\theta)\,\rho^{12},\\
&\ldots
\end{aligned} \tag{2.146}$$

The parameters b_n weight the invariant ρ and the parameters c_n weight the invariant $\rho^3 \cos 3\theta$ of the appropriate powers n. The parameter d_{kl} weights the product of the invariants $(\rho)^k$ and $(\rho^3 \cos 3\theta)^l$ of the powers $n = k + l$.

The terms $b_n \rho^n$ with odd powers and the terms with the parameters d_{kl} for odd k are often neglected in the modeling. The reason for this lies in the structure of the polynomial criteria formulated as the intersection of three, six, nine, or twelve planes in the principal stress space. Such formulations contain only terms with ρ^2, $\rho^3 \cos 3\theta$ or, what the same, positive integer powers of the invariants I'_2 and I'_3 (2.117) and their products (Kolupaev, 2018). The rational deviatoric series follows with

$$
\begin{aligned}
S'_2 &= b_2 \rho^2, \\
S'_3 &= c_3 \cos 3\theta \, \rho^3, \\
S'_4 &= b_4 \rho^4, \\
S'_5 &= d_{23} \cos 3\theta \, \rho^5, \\
S'_6 &= (b_6 + c_6 \cos^2 3\theta) \, \rho^6, \\
S'_7 &= d_{43} \cos 3\theta \, \rho^7, \\
S'_8 &= (b_8 + d_{26} \cos^2 3\theta) \, \rho^8, \\
S'_9 &= d_{63} \cos 3\theta + c_9 \cos^3 3\theta) \, \rho^9, \\
S'_{10} &= (b_{10} + d_{46} \cos^2 3\theta) \, \rho^{10}, \\
S'_{11} &= (d_{83} \cos 3\theta + d_{29} \cos^3 3\theta) \, \rho^{11}, \\
S'_{12} &= (b_{12} + d_{66} \cos^2 3\theta + c_{12} \cos^4 3\theta) \, \rho^{12}, \\
&\dots
\end{aligned}
\tag{2.147}
$$

The highest art in the formulation of the phenomenological yield criteria Φ is to select the appropriate terms S'_i, which are relevant for the considered material behavior. As this is hardly possible, various formulations are tried out and tested for the fulfillment of the plausibility assumptions (Appendix 2.7.8). The relevant formulations are obtained with:

- cosine ansatz criterion (Altenbach and Kolupaev, 2009; Kolupaev, 2018; Kolupaev and Altenbach, 2010)
- quadratic, bi-, tri-, and sextaquadratic equations (Kolupaev, 2018), and
- cubic (2.47), bicubic (2.53), tri-, and quadracubic equations (Sect. 2.4.2),

which are the explicit functions of σ_{eq} (2.12). Further formulation possibilities are shown in Subsect. 2.4.3.6.

2.7.8 Plausibility Assumptions

Several requirements on the yield and strength criteria Φ (Sect. 2.2) were pronounced in the past, which can be interpreted as plausibility assumptions. These requirements are not mandatory but the quality of the criteria may be assessed considering the plausibility assumptions, which are formally separated in physical, mathematical, geometric, and ”subjective“ assumptions (Tables **2.9-2.12**). Their relevance is shown in the authors’ opinion.

Two assumptions PM14 and PS1 are in contradiction with the known statements. PM14 is immediately justified when an elasticity theory of higher order is considered and the number of parameters increases. Contradiction to PS1 comes from the past as lack of tools was vindicated by lack of necessity.

The desires PS14 and PS15 disagree with the idea of the phenomenology. In engineering methods the microstricture is homogenized. There are no physical principles, e.g. balance equations in Continuum Mechanics (Altenbach, 2018), underlying such a formulation. The criteria should only not contradict the physical principles.

PS18 is problematic because the term “failure mode of isotropic material” is in progress, see (Cuntze and Freund, 2004; Cuntze, 2006, 2013, 2021). If the polynomial criteria Φ (2.3) of power three or greater in the stress are considered, different failure modes can be set in the “global fitting” and the additional parameters can be interpreted as “interaction parameters”. Furthermore, the mastery of convexity in the criteria of the failure mode concept is not clear.

Table 2.9: Physical plausibility assumptions.

Label	Content	References	Relevance
PP1	possess only one root for any given radial load path	Bower and Koedam (1997); Torre (1947); Wu (1973)	✓
PP2	nonintersecting of limit surfaces in dependence of the parameters	Brandt et al. (1986); Gol'denblat and Kopnov (1968), Gol'denblat and Kopnov (1971a)	✓
PP3	single surface in principal stress space without any additional outer contours and plane intersections	Lagioia et al. (2016); Rosendahl (2020); Rosendahl et al. (2019b) Wu (1973); Wu and Scheublein (1974)	✓
PP4	restriction of hydrostatic tensile stress	Balandin (1937); Filonenko-Boroditsch (1961) Gol'denblat and Kopnov (1971a); Kolupaev (2018); Skrzypek (1993)	✓
PP5	limit condition in any stress states	Brandt et al. (1986)	
PP6	time and temperature should be explicitly taken into account	Brandt et al. (1986); Gol'denblat and Kopnov (1968), Lüpfert (1994); Pisarenko and Lebedev (1976)	
PP7	consideration of stress gradients	Gol'denblat and Kopnov (1968); Pisarenko and Lebedev (1976)	
PP8	criteria for isotropic materials should be the consequence of the criteria for anisotropic materials	Banabic et al. (2000); Bazhanov et al. (1970); Christensen (2013) Cuntze and Freund (2004); Cuntze (2013); Habraken (2004) Labossière and Neale (1987); Mittelstedt and Becker (2016) Mittelstedt (2021); Wilczynski (1992); Wu (1973)	
PP9	formulation in the stress and strain space	Wilczynski (1992); Rosendahl et al. (2019a); Wu (1973)	

Table 2.10: Mathematical plausibility assumptions.

Label	Content	References	Relevance
PM1	explicit solvability of the criterion w.r.t. the equivalent stress σ_{eq}	Kolupaev (2018); Rosendahl et al. (2019b)	✓
PM3	homogeneous function of stresses	Kolupaev (2018)	
PM4	dependence of the criterion on all three invariants	Altenbach and Kolupaev (2014); Gol'denblat and Kopnov (1971a) Lagioia et al. (2016); Lebedev (2010); Kolupaev (2018)	
PM5	maximum power of the stress n in the equation with the polynomial formulations not higher than 12	Altenbach and Kolupaev (2014); Kolupaev (2018)	
PM6	separate definition of the meridional and deviatoric sections	Lagioia et al. (2016)	
PM7	invariants I_1 and I_3' in odd and even powers	Brandt et al. (1986); Gol'denblat and Kopnov (1968), Gol'denblat and Kopnov (1971a); Kolupaev (2018)	
PM8	reality of the limit state of stress (reality of the root of Φ)	Gol'denblat and Kopnov (1971a)	✓
PM9	no case discrimination	Rosendahl et al. (2019b)	
PM10	unique assignment of the limit surface to parameters of the criterion	Rosendahl et al. (2019b)	
PM11	restrictions imposed on the inelastic POISSON's ratio at tension ν_{+}^{in} and compression ν_{-}^{in} even for the strength criteria	Altenbach et al. (2014); Kolupaev (2018)	
PM12	provision of an explicit expression for the equivalent stress σ_{eq}	Rosendahl (2020)	
PM13	parameter restrictions as $[0, 1]$ or $[-1, 1]$	-	
PM14	no analogies with the linear elasticity theory regards the amount of parameters	Christensen (2013); Cuntze (1999); Cuntze and Freund (2004)	
		Cuntze (2013)	
PM15	statistical nature of the modeled process	Lebedev (2010); Pisarenko and Lebedev (1969, 1976), Lebedev et al. (1979)	
PM16	numerically robust in the application	Mittelstedt and Becker (2016)	

Table 2.11: Geometric plausibility assumptions.

Label	Content	References	Relevance
PG1	clear geometric background	Balandin (1937); Lebedev et al. (1979); Kolupaev (2018) Pisarenko and Lebedev (1969, 1976)	
PG2	smooth surface	Gol'denblat and Kopnov (1971a); Lebedev (2010) Labossière and Neale (1987); Wu (1973)	
PG3	convexity, convexity restrictions for yield and strength criteria	Brandt et al. (1986); Franklin (1971); Wu (1973) Murzewski and Mendera (1963); Torre (1950a)	
PG3.1	C^1-continuous differential criteria	Balandin (1937); Murzewski and Mendera (1963) Puck (1996); Rosendahl (2020); Torre (1947)	
PG3.2	C^2-continuous differential criteria	Lagioia et al. (2016); Torre (1949); Zhang et al. (2021)	
PG4	convexity in the meridional plane	Kolupaev (2018)	
PG5	C^1 continuous differentiability of the criterion in the π-plane except at the border of the convexity limits	Altenbach and Kolupaev (2014); Abbo and Sloan (1995) Rosendahl et al. (2019b)	
PG6	convex restrictions in the parameter space	Kolupaev (2018)	
PG7	continuous differentiable change of the cross section of the surface in the π-plane as function of the invariant I_1	Altenbach and Kolupaev (2014); Kolupaev (2018)	
PG8	wide range of possible convex shapes in the π-plane	Altenbach and Kolupaev (2014); Rosendahl et al. (2019b)	
PG9	wide range of possible convex shapes in the meridian cross section	Rosendahl et al. (2019b)	
PG10	no singularity at the apex	Altenbach and Kolupaev (2014); Abbo and Sloan (1995), Franklin (1971); Kolupaev (2018); Lagioia et al. (2016), Theocaris (1995); Zhang et al. (2021)	
PG11	classical strength hypotheses, reduction to known criteria in limit cases	Altenbach and Kolupaev (2014); Brandt et al. (1986) Gol'denblat and Kopnov (1968); Kolupaev (2018) Rosendahl (2020); Wilczynski (1992)	✓
PG12	the surface cannot contain the zero point of the origin	Torre (1950a)	

Table 2.12: Subjective plausibility assumptions (application requirements).

Label	Content	References	Relevance
PS1	maximum generality	Brandt et al. (1986); Ponomarev et al. (1957); Rosendahl (2020)	
PS2	reliability and trustworthiness of predictions	Balandin (1937); Burzyński (2008); Pisarenko and Lebedev (1969)	
PS3	simple and confident application	Burzyński (2008); Pisarenko and Lebedev (1969); Sendeckyj (1972)	
PS5	easy to understand for mechanical engineers	Habraken (2004); Mittelstedt and Becker (2016); Ponomarev et al. (1957)	
PS6	easy to implement in FE-code	Banabic et al. (2000); Barlat et al. (1991); Habraken (2004)	
PS7	minimum number of parameters	Boehler and Delafin (1982); Burzyński (2008); Murzewski and Mendera (1963)	
PS8	independence and uniqueness of the parameters	Rosendahl et al. (2019b); Rosendahl (2020)	
PS9	dimensionless parameters	Asteris (2013); Altenbach and Kolupaev (2014); Kolupaev (2018)	
PS10	easy parameter identification	Habraken (2004); Balandin (1937); Collins (1993); Hashin (1980)	
PS11	elegance in the formulation	Christensen (2013); Cohen et al. (2009); Puck (1996); Yoshimine et al. (2004)	
PS12	geometrical meaning of the parameters	Kolupaev (2018)	
PS13	derivation (origin) of the formula	Christensen (2013)	
PS14	reference to the microstructure	Pisarenko and Lebedev (1976)	
PS15	physical background	Lebedev et al. (1979); Ponomarev et al. (1957); Puck (1996)	✓
PS16	clear advantages in the application	–	
PS17	clear parameter restriction	–	
PS18	reference to the failure mode	Christensen (2013); Cuntze et al. (1997); Cuntze (1999, 2021)	
PS19	parameters as material properties	Christensen (2013)	
PS20	mechanical sense of the single terms	Burzyński (2008)	
PS21	meaning of behavior resulting from approximation	Kirkpatrick (1954)	

References

Abbo AJ, Sloan SW (1995) A smooth hyperbolic approximation to the Mohr-Coulomb yield criterion. Computers & Structures 54(3):427–441

Altenbach H (2001) A generalized limit criterion with application to strength, yielding, and damage of isotropic materials. In: Lemaitre J (ed) Handbook of Materials Behaviour Models. Academic Press, San Diego, pp 175–186

Altenbach H (2010) Strength hypotheses - a never ending story. Czasopismo Techniczne Mechanika (Technical Transactions Mechanics) Wydawnictwo Politechniki Krakowskiej 107(20):5–15

Altenbach H (2018) Continuum Mechanics: Introduction to Material-independend and Material-dependend Equations (in German: Kontinuumsmechanik: Einführung in die material-unabhängigen und materialabhängigen Gleichungen), 4th edn. Springer, Vieweg, Berlin, Heidelberg

Altenbach H, Kolupaev VA (2009) Fundamental forms of strength hypotheses. In: Indeitcev DA, Krivtsov AM (eds) Proc. of XXXVI Summer School Advanced Problems in Mechanics, Institute for Problems in Mechanical Engineering RAS, St. Petersburg, pp 32–45

Altenbach H, Kolupaev VA (2014) Classical and non-classical failure criteria. In: Altenbach H, Sadowski T (eds) Failure and Damage Analysis of Advanced Materials, Springer, Wien, Heidelberg, Int. Centre for Mechanical Sciences CISM, Courses and Lectures Vol. 560, pp 1–66

Altenbach H, Naumenko K (1997) Creep bending of thin-walled shells and plates by consideration of finite deflections. Computational Mechanics 19(6):490–495

Altenbach H, Naumenko K (2002) Shear correction factors in creep-damage analysis of beams, plates and shells. JSME Int J Series A Solid Mechanics and Material Engineering, The Japan Society of Mechanical Engineers 45(1):77–83

Altenbach H, Altenbach J, Zolochevsky A (1995) Advanced Deformation Models and Failure Criteria in Material Mechanics (in German: Erweiterte Deformationsmodelle und Versagenskriterien der Werkstoffmechanik). Deutscher Verlag für Grundstoffindustrie, Stuttgart

Altenbach H, Kolarow G, Morachkovsky O, Naumenko K (2000) On the accuracy of creep-damage predictions in thinwalled structures using the finite element method. Computational Mechanics 25(1):87–98

Altenbach H, Bolchoun A, Kolupaev VA (2014) Phenomenological yield and failure criteria. In: Altenbach H, Öchsner A (eds) Plasticity of Pressure-Sensitive Materials, Springer, Berlin Heidelberg, Engineering Materials, pp 49–152

de Araújo FC (1962) Elasticidade e Plasticidade. Imprensa Portuguesa, Porto

Asteris PG (2013) Unified yield surface for the nonlinear analysis of brittle anisotropic materials. Science Letters A Mathematics, Physics and Mechanics 4(2):46–56

Backhaus G (1983) Deformationsgesetze. Akademie-Verlag, Berlin

Balandin PP (1937) On the strength hypotheses (in Russ.: K voprosu o gipotezakh prochnosti). Vestnik inzhenerov i tekhnikov 1:19–24

Banabic D, Bunge HJ, Pöhlandt K, Tekkaya AE (2000) Formability of Metallic Materials: Plastic Anisotropy, Formability Testing, Forming Limits. Springer, Berlin

Barlat F, Lege DJ, Brem JC (1991) A six-component yield function for anisotropic materials. Int J of Plasticity 7(7):693–712

Bazhanov VL, Gol'denblat II, Kopnov VA, Pospelov AD, Sinjukov AM (1970) Plates and Shells Made of Fiberglass Plastics (In Russ. Plastinki o obolochki iz stekloplastikov). Visshaja Shkola, Moscow

Benvenuto E (1991) An Introduction to the History of Structural Mechanics. Springer, New York

Bertram A (2012) Elasticity and Plasticity of Large Deformations. Springer, Berlin

Betten J (1976) Plastische Anisotropie und Bauschinger-Effekt; allgemeine Formulierung und Vergleich mit experimentell ermittelten Fließortkurven. Acta Mechanica 25(1-2):79–94

Betten J (1979) Über die Konvexität von Fließkörpern isotroper und anisotroper Stoffe. Acta Mech 32:233–247

Betten J (2001) Kontinuumsmechanik. Springer, Berlin
Bigoni D, Piccolroaz A (2003) A new yield function for geomaterials. In: Viggiani C (ed) Constitutive Modeling and Analysis of Boundary Value Problems in Geotechnical Engineering, Hevelius Edizioni, Benevento, Italy, pp 266–281
Bigoni D, Piccolroaz A (2004) Yield criteria for quasibrittle and frictional materials. Int J of Solids and Structures 41(11):2855–2878
Billington EW (1986) Introduction to the Mechanics and Physics of Solids. Adam Hilger Ltd., Bristol
Birger IA (1977) On a criterion for fracture and plasticity (in Russ.: Ob odnom kriterii razrushenija i plastichnosti). Mekhanika tverdogo tela, Izvestija Akademii Nauk SSSR 9(4):143–150
Bishop AW (1966) The strength of soils as engineering materials. Geotechnique 16(2):91–130
Boehler JP, Delafin M (1982) Failure criteria for unidirectional fiber-reinforced composites under confining pressure. In: Boehler JP (ed) Mechanical Behavior of Anisotropic Solids / Nr. 295 – Comportment Méchanique des Solides Anisotropes, Proceedings of the Euromech Colloquium 115, Villard-de-Lans, June 19–22, 1979, Springer, pp 449–470
Bolchoun A, Kolupaev VA, Altenbach H (2011) Convex and non-convex flow surfaces (in German: Konvexe und nichtkonvexe Fließflächen). Forschung im Ingenieurwesen 75(2):73–92
Botkin AI (1940a) Equilibrium of granular and brittle materials (in Russ.: O ravnovesii sypuchikh i khrupkikh materialov). Transactions of the Scientific Research Institute of Hydrotechnics, Izvestija NIIG, Leningrad 28:189–211
Botkin AI (1940b) Theories of elastic failure of gramelar and of brittle materials (in Russ.: O prochnosti sypuchikh i khrupkikh materialov). Transactions of the Scientific Research Institute of Hydrotechnics, Izvestija NIIG, Leningrad 26:205–236
Bouvet C, Calloch S, Lexcellent C (2002) Mechanical behavior of a Cu-Al-Be shape memory alloy under multiaxial proportional and nonproportional loadings. J Engng Materials and Technology 124(2):112–124
Bouvet C, Calloch S, Lexcellent C (2004) A phenomenological model for pseudoelasticity of shape memory alloys under multiaxial proportional and nonproportional loadings. European J of Mechanics-A/Solids 23(1):37–61
Bower MV, Koedam DH (1997) Tensor polynomial failure criterion: Coefficient limits based on convexity requirements. J of Reinforced Plastics and Composites 16(5):435–477
Brandt AM, Dzieniszewski W, Jendo S, Marks W, Owczarek S, Wasiutyński Z (1986) Criteria and Methods of Structural Optimization. Martinus Nijhoff Publishers, PWN - Polish Scientific Publishers, Dordrecht, Warszawa
Bronstein IN, Semendjajew KA (2007) Handbook of Mathematics. Springer, Berlin
Bulla M, Kolupaev VA (2021) Stress analysis in design with plastics: Accessible method with huge impact. Kautschuk, Gummi Kunststoffe KGK, Hüthig GmbH 74(6):60–67
Burzyński W (1928) Study on Material Effort Hypotheses, (in Polish: Studjum nad Hipotezami Wytężenia). Akademia Nauk Technicznych, Lwów
Burzyński W (2008) Theoretical foundations of the hypotheses of material effort, Wlodzimierz Burzyński (1900-1970), Czasopismo Techniczne (1929) 47, 1–41, Lwów, (in Polish: Teoretyczne podstawy hipotez wytężenia). Engineering Transactions, Polish Academy of Sciences 56 (Special Issue):9–45
Candland CT (1975) Implications of macroscopic failure criteria which are independent of hydrostatic stress. Int J of Fracture 11(3):540–543
Capurso M (1967) Yield conditions for incompressible isotropic and orthotropic materials with different yield stress in tension and compression. Meccanica 2(2):118–125
Chen WF, Han DJ (1993) Failure criteria for concrete materials. In: Boehler JP (ed) Failure Criteria of Structured Media, Balkema, Rotterdam, pp 375–384
Chen WF, Zhang H (1991) Structural Plasticity - Theory, Problems, and CAE Software. Springer, New York
Christensen R (2019) Failure criteria for fiber composite materials, the astonishing sixty year search, definitive usable results. Composites Science and Technology 182:107,718
Christensen RM (2013) The Theory of Materials Failure. University Press, Oxford

Cicala P (1961) Presentazione geometrica delle relazioni fondamentali d'elastoplasticità. Giornale del Genio Civile 99:125–137

Cohen T, Masri R, Durban D (2009) Analysis of circular hole expansion with generalized yield criteria. Int J of Solids and Structures 46(20):3643–3650

Collins JA (1993) Failure of Materials in Mechanical Design: Analysis, Prediction, Prevention. Wiley, New York

Coulomb CA (1776) Essai sur une application des regles des maximis et minimis a quelques problemes de statique relatifs, a la architecture. Mem Acad Roy Div Sav 7:343–387

Cuntze R, Deska R, Szelinski B, Jeltsch-Fricker R, Meckbach S, Huybrechts D, Kopp J, Kroll L, Gollwitzer S, Rackwitz R (1997) Neue Bruchkriterien und Festigkeitsnachweise für unidirektionalen Faserkunststoffverbund unter mehrachsiger Beanspruchung: Modellbildung und Experimente, BMBF-Förderkennzeichen: 03N8002, Abschlussbericht Nr. 506. 5: Grund- und Werkstoffe, VDI-Verlag, Düsseldorf

Cuntze RG (1999) The Failure Mode Concept - A new comprehensive 3D-strength analysis concept for any brittle and ductile behaving material. In: Europ. Conf. on Spacecraft Structures, Materials and Mechan. Testing, ESTEC, Noordwijk, no. ESA SP-428 in ESA-CNES-DLR-DGLR, pp 269–287

Cuntze RG (2006) Failure conditions for isotropic materials, unidirectional composites, woven fabrics-their visualization and links. In: Busse G, Kröplin B (eds) Conf. on Damage in Composite Materials CDCM, 18th-19th of September 2006, Stuttgart

Cuntze RG (2013) Strength failure conditions of isotropic materials. Industrieausschuss Strukturberechnungsunterlagen (IASB), HSB Handbuch Struktur Berechnung 51101-01-730C, Augsburg

Cuntze RG (2021) Failure Mode Concept (FMC) and Strength Mechanics Building: A Physical and Theoretical Material Symmetry. Manuscript, Augsburg

Cuntze RG, Freund A (2004) The predictive capability of failure mode concept-based strength criteria for multidirectional laminates. Composites Science and Technology 64(3):343–377

Davis EA, Connelly FM (1959) Stress distribution and plastic deformation in rotating cylinders of strainhardening material. Transactions of the ASME, J of Applied Mechanics 26:25–30

De Boer R (2000) Theory of Porous Media: Highlights in Historical Development and Current State. Springer, Berlin

Desai CS (1980) A general basis for yield, failure and potential functions in plasticity. Int J for Numerical and Analytical Methods in Geomechanics 4(4):361–375

Desai CS, Faruque MO (1984a) A generalized basis for modelling plastic behavior of materials. In: Desai CS, Gallagher RH (eds) Mechanics of Engineering Materials, Wiley, Chichester, pp 211–230

Desai CS, Faruque O (1984b) Constitutive model for (geological) materials. J of Engineering Mechanics 110(9):1391–1408

Drass M (2020) Constitutive Modelling and Failure Prediction for Silicone Adhesives in Façade Design, Diss., FB 13 Bauingenieurwesen, Technical University of Darmstadt, Mechanik, Werkstoffe und Konstruktion im Bauwesen, vol 55. Springer Vieweg, Wiesbaden

Drucker DC (1953) Limit analysis of two and three dimensional soil mechanics problems. J of the Mechanics and Physics of Solids 1(4):217–226

Drucker DC (1957) A definition of stable inelastic material. Techn. Report No. 2 AD143756, Nonr-562(20)/2, Division of Engineering, Brown University, Providence, Rhode Island

Drucker DC (1959) A definition of stable inelastic material. J of Applied Mechanics, Transactions of the ASME 26(1):101–106

Drucker DC, Prager W (1952) Soil mechanics and plastic analysis or limit design. Quarterly of Appl Mathematics 10:157–165

Dyson BF, McLean M (2001) Micromechanism-quantification for creep constitutive equations. In: Murakami S, Ohno N (eds) IUTAM Symposium on Creep in Structures, Kluwer, Dordrecht, pp 3–16

Fahlbusch NC (2015) Entwicklung und Analyse mikromechanischer Modelle zur Beschreibung des Effektivverhaltens von geschlossenzelligen Polymerschäumen. Diss., Fachbereich Maschinenbau der Technischen Universität Darmstadt

Fahlbusch NC, Kolupaev VA, Becker W (2016) Generalized limit surfaces – with an example of hard foams. In: Naumenko K, Aßmus M (eds) Advanced Methods of Continuum Mechanics for Materials and Structures, Springer Science + Business Media, Singapore, Advanced Structured Materials, vol 60, pp 337–365

Feodosjev VI (1975) Ten Lecture-conversations on Strength of Materials (in Russ.: Desjat' lekzij-besed po soprotivleniju materialov). Nauka, Moscow

Filonenko-Boroditsch MM (1961) Mechanical Theories of Strength (in Russ.: Mechanicheskie teorii prochnosti). Izdatel'stvo Moskovskogo Universiteta MGU, Moscow

Finnie I, Heller WR (1959) Creep of Engineering Materials. McGraw-Hill, New York

Föppl A, Föppl L (1920) Drang und Zwang: Eine höhere Festigkeitslehre für Ingenieure. R. Oldenbourg, München

Franklin JA (1971) Triaxial strength of rock materials. Rock Mechanics 3(2):86–98

Fromm H (1931) Grenzen des elastischen Verhaltens beanspruchter Stoffe. In: Auerbach F, Hort W (eds) Statik und Dynamik elastischer Körper nebst Anwendungsgebieten. II. Teil. Zum Gebrauch für Ingenieure, Physiker und Mathematiker, vol 4, Barth-Verlag, Leipzig, pp 359–435

Giraldo-Londoño O, Paulino GH (2020) A unified approach for topology optimization with local stress constraints considering various failure criteria: von Mises, Drucker-Prager, Tresca, Mohr-Coulomb, Bresler-Pister and Willam-Warnke. Proceedings of the Royal Society A 476(2238):20190,861

Gol'denblat II, Kopnov VA (1968) Yield and Strength Criteria for Structural Materials (in Russ.: Kriterii prochnosti i plastichnosti konstrukzionnych materialov). Mashinostroenie, Moscow

Gol'denblat II, Kopnov VA (1971a) General criteria of the strength of isotropic media. Polymer Mechanics 7(2):251–261

Gol'denblat II, Kopnov VA (1971b) General theory of criteria of strength for isotropic and anisotropic materials. Strength of Materials 3(2):184–188

Gol'dman AY (1994) Prediction of the Deformation Properties of Polymeric and Composite Materials. ACS Professional Reference Book, American Chemical Society, Washington

Gurson AL (1977) Continuum theory of ductile rupture by void nucleation and growth: Part I - yield criteria and flow rules for porous ductile media. J of Engineering Materials and Technology 99(1):2–15

Habraken AM (2004) Modelling the plastic anisotropy of metals. Archives of Computational Methods in Engineering 11(1):3–96

Haigh BP (1920) The strain-energy function and the elastic limit. Engineering 109:158–160

Hashin Z (1980) Failure criteria for unidirectional fiber composites. J of Applied Mechanics pp 329–334

Hayhurst DR (1972) Creep rupture under multi-axial states of stress. J of the Mechanics and Physics of Solids 20(6):381–390

Haythornthwaite RM (1961a) The range of the yield condition in stable, ideally plastic solids. Technical report, ORA Project 04403, University of Michigan, College of Engineering, Department of Engineering Mechanics, Detroit

Haythornthwaite RM (1961b) Range of yield condition in ideal plasticity. Proc ASCE J Eng Mech Division EM6 87:117–133

Haythornthwaite RM (1962) Range of yield condition in ideal plasticity. Transactions ASCE 127(1):1252–1269

Haythornthwaite RM (1983) Piecewise linear yield criteria in invariant form. J of Engineering Mechanics 109(4):1016–1022

Hencky H (1924) Zur Theorie plastischer Deformationen und der hierdurch im Material hervorgerufenen Nachspannungen. ZAMM 4(4):323–334

Hencky H (1943) Ermüdung, Bruch, Plastizität. Stahlbau 16(23/24):95–97

Hershey AV (1954) The plasticity of an isotropic aggregate of anisotropic face-centered cubic crystals. J of Applied Mechanics 21(3):241–249

Hill R (1950) LXVI. On the inhomogeneous deformation of a plastic lamina in a compression test. The London, Edinburgh, and Dublin Philosophical Magazine and J of Science, Series 7 41(319):733–744

Hosford WF (1972) A generalized isotropic yield criterion. Transactions of the ASME, J of Applied Mechanics 39(June):607–609

Hosford WF (1979) On yield loci of anisotropic cubic metals. In: 7th North American Metalworking Research, SME, Proc. NAMRC, Dearborn, 7, pp 191–196

Huber MT (1904) Specific strain work as a measure of material effort (in Polish: Właściwa praca odkształcenia jako miara wytężenia materyału). Czasopismo Techniczne, Lwów, Organ Towarzystwa Politechnicznego we Lwowie 22:34–40, 49–50, 61–62, 80–81

Ishlinsky AY (1940) Hypothesis of strength of shape change (in Russ.: Gipoteza prochnosti formoizmeneniya). Uchebnye Zapiski Moskovskogo Universiteta, Mekhanika 46:104–114

Ishlinsky AY, Ivlev DD (2003) Mathematical Theory of Plasticity (in Russ.: Matematicheskaya teoriya plastichnosti). Fizmatlit, Moscow

Ismar H, Mahrenholtz O (1982) Über Beanspruchungshypothesen für metallische Werkstoffe. Konstruktion 34:305–310

Ivlev DD (1959) The theory of fracture of solids (in Russ.: K teorii razrushenija tverdykh tel). J of Applied Mathematics and Mechanics 23(3):884–895

Ivlev DD (1960) On extremum properties of plasticity conditions (in Russ.: Ob ekstremal'nykh svojstvakh uslovij plastichnosti). J of Applied Mathematics and Mechanics 24(5):1439–1446

Jemioło S (1992) Rational formulation of yield conditions for isotropic materials, (in Polish: O racjonalnym formułowaniu warunków plastyczności dla materiału izotropowego). Prace Naukowe Politechniki Warszawskiej, Budownictwo 120:51–62

Jemioło S, Szwed A (1999) Application of convex isotropic functions in failure theory for isotropic materials: Yield criteria for metals, (in Polish: O zastosowaniu funkcji wypukłych w teorii wytężenia materiałów izotropowych: Propozycja warunków plastyczności metali). Prace Naukowe Politechniki Warszawskiej, Budownictwo 133:5–52

Jirásek M, Bažant ZP (2002) Inelastic Analysis of Structures. Wiley, London and New York

Karafillis AP, Boyce MC (1993) A general anisotropic yield criterion using bounds and a transformation weighting tensor. J of the Mechanics and Physics of Solids 41(12):1859–1886

Kirkpatrick WM (1954) The behaviour of sands under three dimensional stress systems. PhD thesis, Department of Civil and Mechanical Engineering at the Royal Technical College, University of Glasgow

Ko WL (1963) Application of the finite elastic theory to the behavior of rubber-like materials. PhD thesis, California Institute of Technology, Pasadena

Koca M, Koca NO (2011) Quasi regular polygons and their duals with Coxeter symmetries D_n represented by complex numbers. In: J. of Physics: Conference Series, Group 28: Physical and Mathematical Aspects of Symmetry, IOP Publishing, vol 284, pp 1–10

Kolupaev VA (2006) 3D-Creep Behaviour of Parts Made of Non-Reinforced Thermoplastics (in German: Dreidimensionales Kriechverhalten von Bauteilen aus unverstärkten Thermoplasten). Diss., Martin-Luther-Universität Halle-Wittenberg, Halle-Saale

Kolupaev VA (2017) Generalized strength criteria as functions of the stress angle. J of Eng Mechanics 143(9):04.017.095

Kolupaev VA (2018) Equivalent Stress Concept for Limit State Analysis. Springer, Cham

Kolupaev VA, Altenbach H (2010) Considerations on the Unified Strength Theory due to Mao-Hong Yu (in German: Einige Überlegungen zur Unified Strength Theory von Mao-Hong Yu). Forschung im Ingenieurwesen 74(3):135–166

Kolupaev VA, Bolchoun A, Altenbach H (2009) Unified representation and evaluation of the strength hypotheses. In: Elboujdaini M, Tyson B, Patnaik P (eds) 12th Int. Conference on Fracture ICF 12, 10 p., National Research Council Canada, Ottawa

Kolupaev VA, Bolchoun A, Altenbach H (2013a) Yield criteria for incompressible materials in the shear stress space. In: Öchnser A, Altenbach H (eds) Experimental and Numerical Investigation of Advanced Materials and Structures, Springer, pp 107–119

Kolupaev VA, Yu MH, Altenbach H (2013b) Visualisation of the Unified Strength Theory. Archive of Applied Mechanics 83(7):1061–1085

Kolupaev VA, Yu MH, Altenbach H (2013c) Yield criteria of hexagonal symmetry in the π-plane. Acta Mechanica 224(7):1527–1540

Kolupaev VA, Becker W, Massow H, Dierkes D (2014) Design of test specimens from hard foams for the investigation of biaxial tensile strength (in German: Auslegung von Probekörpern aus Hartschaum zur Ermittlung der biaxialen Zugfestigkeit). Forschung im Ingenieurwesen 78(3-4):69–86

Kolupaev VA, Yu MH, Altenbach H (2016) Fitting of the strength hypotheses. Acta Mechanica 227(6):1533–1556

Kolupaev VA, Yu MH, Altenbach H, Bolchoun A (2018) Comparison of strength criteria based on the measurements on concrete. J of Eng Mechanics (ASCE) 144(6)

Koval'chuk BI (1981) Criterion for the limiting state of some hull steels under combined strain at room and elevated temperatures. Strength of Materials 13(5):548–554

Kowalewski ZL, Hayhurst DR, Dyson BF (1994) Mechanisms-based creep constitutive equations for an aluminium alloy. J of Strain Analysis for Engineering Design 29(4):309–316

Kroon M, Faleskog J (2013) Numerical implementation of a J_2- and J_3-dependent plasticity model based on a spectral decomposition of the stress deviator. Computational Mechanics 52(5):1059–1070

Labossière P, Neale KW (1987) Macroscopic failure criteria for fiber-reinforced composite materials. Solid Mechanics Archives, 439–450 12(2):65–95

Lagioia R, Panteghini A (2016) On the existence of a unique class of yield and failure criteria comprising Tresca, von Mises, Drucker-Prager, Mohr-Coulomb, Galileo-Rankine, Matsuoka-Nakai and Lade-Duncan. Proceedings of the Royal Society of London, Series A 472:20150713(2185):1–21

Lagioia R, Panteghini A, Puzrin AM (2016) The I_3 generalization of the Galileo-Rankine tension criterion. Proceedings of the Royal Society A: Mathematical, Physical and Engineering Sciences 470:20140568(2172):1–23

Lagzdin' A (1997) Smooth convex limit surfaces in the space of symmetric second-rank tensors. Mechanics of Composite Materials 33(2):119–127

Lagzdin' AZ, Tamuzh VP (1971) Construction of a phenomenological theory of the fracture of an anisotropic medium (in Russ.: K postroeniju fenomenologicheskoj teorii razrushenija anizotropnoj sredy). Mekhanika Polimerov 7(4):563–571

Lagzdiņš A, Zilaucs A (1996) Constructing convex limit surfaces in material mechanics. Mechanics of Composite Materials 32(3):233–241

Launay P, Gachon H (1971) Strain and ultimate strength of concrete under triaxial stress. In: Proceedings of the First Int. Conference on Structural Mechanics in Reactor Technology, Berlin, September 20-24, 1971. Commission of the European Communities, Brussels (EUR-4820), Vol. 3, paper Hl/3, pp 23–40

Launay P, Gachon H (1972) Strain and ultimate strength of concrete under triaxial stress, Paper SP 34-13. In: Kesler CE (ed) Concrete for Nuclear Reactors, Bundesanstalt für Materialprüfung in Berlin, Oct. 5-9, 1970, ACI Publication SP-34, American Concrete Institute, Detroit, pp 269–282

Launay P, Gachon H, Poitevin P (1970) Déformation et résistance ultime du béton sous étreinte triaxiale. Annales de l'institut Technique du Batiment et de Travaux Publics, Série: Essais et Mesures (123) 269(5):21–48

Lebedev AA (1965) Generalized criterion for the fatigue strength (in Russ.: Obobshhennyj kriterij dlitel'noj prochnosti). In: Thermal Strength of Materials and Structure Elements (in Russ.: Termoprochnost' materialov i konstrukcionnykh elementov), vol 3, Naukova Dumka, Kiev, pp 69–76

Lebedev AA (2010) Development of the theories of strength in the mechanics of materials. Strength of Materials 42(5):578–592

Lebedev AA, Koval'chuk BI, Lamashevsky VP, Giginjak FF (1979) Computation of Complex Stress State: Determining of Equivalent Stresses. Akademija Nauk Ukrainskoj SSR, Institut Problem Prochnosti, Kiew

Leckie FA, Hayhurst DR (1977) Constitutive equations for creep rupture. Acta Metallurgica 25(9):1059–1070

Lemaitre J, Chaboche JL (1985) Mécanique des Matériaux Solides. Dunod, Paris

Lemaitre J, Chaboche JL (1990) Mechanics of Solid Materials. Cambridge University Press, Cambridge

Lequeu PH, Gilormini P, Montheillet F, Bacroix B, Jonas JJ (1987) Yield surfaces for textured polycrystals. Acta Metall 35(2):439–451, 1159–1174

Lexcellent C (2018) Linear and Non-linear Mechanical Behavior of Solid Materials. Springer, Cham

Lexcellent C, Boubakar ML, Bouvet C, Calloch S (2006) About modelling the shape memory alloy behaviour based on the phase transformation surface identification under proportional loading and anisothermal conditions. Int J of Solids and Structures 43(3-4):613–626

Lüpfert HP (1994) Beurteilung der statischen Festigkeit und Dauerfestigkeit metallischer Werkstoffe bei mehrachsiger Beanspruchung. Dt. Verl. für Grundstoffindustrie, Leipzig

Mālmeisters A, Tamužs V, Teters G (1977) Mechanik der Polymerwerkstoffe. Akademie-Verlag, Berlin

Mariotte E (1718) Traité du Mouvement des Eaux et des Autres Corps Fluides. J. Jambert, Paris

Marti P (1980) Zur plastischen Berechnung von Stahlbeton, Institut für Baustatik und Konstruktion, vol 104. Birkhäuser, Basel, Diss. ETH Zürich

Matsuoka H, Nakai T (1985) Relationship among Tresca, Mises, Mohr-Coulomb and Matsuoka-Nakai failure criteria. Soils and Foundations 25(4):123–128

Mirolyubov IN (1953) On the generalization of the strengt theory based on the octaedral stresses in the case of brittle materials (in Russ.: K voprosu ob obobshhenii teorii prochnosti oktaedricheskikh kasatelnykh naprjazhenij na khrupkie materialy). Trudy Leningradskogo Technologicheskogo Instituta pp 42–52

von Mises R (1913) Mechanik des festen Körpers im plastischen deformablen Zustand. Nachrichten der Königlichen Gesellschaft der Wissenschaften Göttingen, Mathematisch-physikalische Klasse pp 582–592

von Mises R (1928) Mechanik der plastischen Formänderung von Kristallen. J of Applied Mathematics and Mechanics, ZAMM 8:161–185

Mittelstedt C (2021) Structural Mechanics in Lightweight Engineering. Springer, Cham

Mittelstedt C, Becker W (2016) Struckturmechanik ebener Laminate. Studienbereich Mechanik, Technische Universität Datmstadt, Lasertype GmbH, Darmstadt

Modarres-Motlagh A (1997) Lower bound to collapse load for structures. PhD thesis, School of Mechanical and Manufacturing Engineering, Faculty of Engineering, University of New South Wales UNSW

Mohr O (1900a) Welche Umstände bedingen die Elastizitätsgrenze und den Bruch eines Materials. Zeitschrift des VDI 45:1524–1530

Mohr O (1900b) Welche Umstände bedingen die Elastizitätsgrenze und den Bruch eines Materials. Zeitschrift des VDI 46:1572–1577

Mohr O (1914) Abhandlungen aus dem Gebiete der technischen Mechanik. Wilhelm & Sohn, Berlin

Murzewski J (1957) Une theorie statistique du corps fragile quasihomogene. In: IXe Congrès International de Mécanique Appliquée, ICAM-1956, Université de Bruxelles, vol 5, pp 313–320

Murzewski J (1960) A probabilistic theory of plastic and brittle behaviour of quasi-homogeneous materials. Archiwum Mechaniki Stosowanej 3(12):203–227

Murzewski J, Mendera Z (1963) Yield surface of steel determined by semi-empirical method. Bulletin de L'Academie Polonaise des Sciences, Serie des Sciences Techniques XI(7):35–42

Naumenko K, Altenbach H, Kutschke A (2011) A combined model for hardening, softening, and damage processes in advanced heat resistant steels at elevated temperature. Int J of Damage Mechanics 20(4):578–597

Novozhilov VV (1951a) On the connection between stresses and strains in a nonlinear-elastic continuum (in Russ.: O svjazi mezhdu naprjazhenijami i deformazijami v nelinejno-uprugoj srede). Prikladnaja Matematika i Mekhanika XV(2):183–194

Novozhilov VV (1951b) On the principles of the statical analysis of the experimental results for isotropic materials (in Russ.: O prinzipakh obrabotki rezultatov staticheskikh ispytanij izotropnykh materialov). Prikladnaja Matematika i Mekhanika XV(6):709–722

Nye JF (1985) Physical Properties of Cristals: Their Representation by Tensors and Matrices. Oxford University Press, Oxford

Othman AM, Dyson BF, Hayhurst DR, Lin J (1994) Continuum damage mechanics modelling of circumferentially notched tension bars undergoing tertiary creep with physically-based constitutive equations. Acta Metallurgica et Materialia 42(3):597 – 611

Ottosen NS (1975) Failure and elasticity of concrete. Report Risø-M-1801, Danish Atomic Energy Commission, Research Establishment Risö, Engineering Department, Roskilde

Ottosen NS (1977) A failure criterion for concrete. J of the Engineering Mechanics Division 103(4):527–535

Ottosen NS (1980) Nonlinear finite element analysis of concrete structures. Tech. rep., Forskningscenter Risoe. Risoe-R, No. 411, Roskilde: Risø National Laboratory

Ottosen NS, Ristinmaa M (2005) The Mechanics of Constitutive Modeling. Elsevier Science, London

Owen DRJ, Hinton E (1986) Finite Elements in Plasticity, Theory and Practice. Pineridge Press Limited, Swansea

Paul B (1968a) Generalized pyramidal fracture and yield criteria. Int J of Solids and Structures 4(2):175–196

Paul B (1968b) Macroscopic plastic flow and brittle fracture. In: Liebowitz H (ed) Fracture: An Advanced Treatise, vol II, Academic Press, New York, pp 313–496

Pisarenko GS, Lebedev AA (1969) Deformation and Fracture of Materials under Combined Stress (in Russ.: Soprotivlenie materialov deformirovaniju i razrusheniju pri slozhnom naprjazhennom sostojanii). Naukowa Dumka, Kiev

Pisarenko GS, Lebedev AA (1976) Deformation and Strength of Materials under Complex Stress State (in Russ.: Deformirovanie i prochnost' materialov pri slozhnom naprjazhennom sostojanii). Naukowa Dumka, Kiev

Podgórski J (1983) Ogólny warunek stanu granicznego dla materiałów izotropowych. Prace IPPT PAN, IFTR Reports, Instytut Podstawowych Probłemów Techniki Polskiej Akademii Nauk 17:4–21

Podgórski J (1984) Limit state condition and the dissipation function for isotropic materials. Archives of Mechanics 36(3):323–342

Podgórski J (1985) General failure criterion for isotropic media. J of Engineering Mechanics 111(2):188–201

Podgórski J (1986) Critical states in bodies with internal friction, (in Polish: Stany krytyczne w ciałach z tarciem wewnętrznym). Praca doctorska, Prace IPPT, IFTR Reports, Instytut Podstawowych Problemów Techniki Polskiej Akademii Nauk, 25, Warszawa

Ponomarev SD, Biderman VL, Likharev KK, Makushin VM, Malinin NN, Feodosjev VI (1957) Strength Analysis in Mechanical Engineering (in Russ.: Raschety na prochnost' v mashinostroenii), vol 1. Gosudarstvennoe nauchno-technicheskoe izdatel'stvo mashinostroitel'noj literatury, Moskow

Potapova LB, Yarzev VP (2005) Mechanics of Materials under Complex Stress State. How Predict the Limit Stresses? (in Russ.: Mekhanika materialov pri slozhnom naprjazhennom sostojanii. Kak prognozirujut predel'nye naprjazhenija?). Mashinostroenie-1, Moscow

Prager W (1956) A new methods of analyzing stresses and strains in work hardening plastic solids. J of Applied Mechanics (ASME) 23:493–496

Prager W, Hodge P (1954) Theorie ideal plastischer Körper. Springer, Wien

Puck A (1996) Festigkeitsanalyse von Faser-Matrix-Laminaten: Modelle für die Praxis. Hanser, München

Rankine WJM (1876) Manual of Applied Mechanics. Griffin, London

Reuss A (1933) Vereinfachte Beschreibung der plastischen Formänderungsgeschwindigkeiten bei Voraussetzung der Schubspannungsfließbedingung. ZAMM 13(5):356–360
Rosendahl PL (2020) From bulk to structural failure: Fracture of hyperelastic materials. Diss., Fachgebiet Strukturmechanik, Technische Universität Darmstadt
Rosendahl PL, Drass M, Felger J, Schneider J, Becker W (2019a) Equivalent strain failure criterion for multiaxially loaded incompressible hyperelastic elastomers. Int J of Solids and Structures 166:32–46
Rosendahl PL, Kolupaev VA, Altenbach H (2019b) Extreme yield figures for universal strength criteria. In: Altenbach H, Öchsner A (eds) State of the Art and Future Trends in Material Modeling, Advanced Structured Materials, Springer Nature, Cham, 100, pp 259–324
de Saint-Venant AJCB (1871) Theorie du mouvement non permanent des eaux, avec application aux crues des rivieres et a l'introduction de marees dans leurs lits. Comptes Rendus des Séances de L'Académie des Sciences 73:237–240
Sandel GD (1919) Ueber die Festigkeitsbedingungen: Ein Beitrag zur Lösung der Frage der zulässigen Anstrengung der Konstruktionsmaterialen. Diss., Technische Hochschule zu Stuttgart
Sandel GD (1925) Über die Festigkeitsbedingungen: Ein Beitrag zur Lösung der Frage der zulässigen Anstrengung der Konstruktionsmaterialen. Jänecke, Leipzig
Sawczuk A (1982) Introduction to Mechanics of Plastic Structures (in Polish: Wprowadzenie do mechaniki konstrukcji plastycznych). Panstwowe Wydawnictwo Naukowe PWN, Warszawa
Sayir M (1970) Zur Fließbedingung der Plastizitätstheorie. Ingenieur-Archiv 39(6):414–432
Sayir M, Ziegler H (1969) Der Verträglichkeitssatz der Plastizitätstheorie und seine Anwendung auf räumlich unstetige Felder. Zeitschrift für angewandte Mathematik und Physik ZAMP 20(1):78–93
Schmidt R (1932) Über den Zusammenhang von Spannungen und Formänderungen im Verfestigungsgebiet. Ingenieur-Archiv 3(3):215–235
Sdobyrev VP (1959) Criterion for the long term strength of some heat-resistant alloys at a multiaxial loading (in Russ.: Kriterij dlitelnoj prochnosti dlja nekotorykh zharoprochnykh splavov pri slozhnom naprjazhennom sostojanii). Izvestija Akademii Nauk SSSR, Otdelenie Tekhnicheskikh Nauk, Mekhanika i Mashinostroenie 1(6):93–99
Sendeckyj GP (1972) A brief survey of empirical multiaxial strength criteria for composites. In: Corten HT (ed) Composite Materials: Testing and Design (Second Conference), ASTM STP 497, ASTM International, Philadelphia, pp 41–51
Shanley FR (1957) Strength of Materials. McGraw-Hill, New York
Shesterikov SA (1960) On the theory of ideal plastic solid (in Russ.: K postroeniju teorii ideal'no plastichnogo tela). Prikladnaja Matematika i Mekhanika, Otdelenie Tekhnicheskikh Nauk Akademii Nauk Sojusa SSR, Russian Academy of Science 24(3):412–415
Skrzypek JJ (1993) Plasticity and Creep: Theory, Examples and Problems. CRC Press, Boca Raton
Spitzig W, Sober R, Richmond O (1975) Pressure dependence of yielding and associated volume expansion in tempered martensite. Acta Metallurgica 23(7):885–893
Spitzig WA, Richmond O (1979) Effect of hydrostatic pressure on the deformation behavior of polyethylene and polycarbonate in tension and in compression. Polymer Engineering & Science 19(16):1129–1139
Stassi-D'Alia F (1967) Flow and fracture of materials according to a new limiting condition of yelding. Meccanica 2(3):178–195
Szwed A (2000) Strength hypotheses and constitutive relations of materials including degradation effects, (in Polish: Hipotezy wytężeniowe i relacje konstytutywne materiałów z uwzględnieniem efektów degradacji). Praca doctorska, Wydział Inżynierii Lądowej Politechniki Warszawskiej, Warszawa
Szwed A (2010) General strengh criterion for incompressible materials. In: Szcześniak WE, Zbiciak A (eds) Theoretical Foundations of Civil Engineering : Polish-Ukraïnian-Lithuanian Transactions, Oficyna Wydawnicza Politechniki Warszawskiej, Warsaw, 18, pp 313–318
Szwed A (2013) Construction of the deviatoric shape function for the cross-sections of the limit surfaces, (in Polish: Konstrukcja funkcji kształtu przekrojów dewiatorowych powierzchni

granicznych). In: Jemioło S, Szwed A (eds) Seria Monografie Zakładu Wytrzymałości Materiałów, Teorii Sprężystości i Plastyczności ZWMTSiP, Deformacje i Wytrzymałość Materiałów i Elementów Konstrukcji, Wydział Inżynierii Lądowej Politechniki Warszawskiej, Warszawa, 3, pp 51–66

Takeda T, Kikuchi S, Nasu Y (1986) Experimental evaluation of yield condition containing third invariant of deviatoric stresses. In: Proceedings of the Thirtieth Japan Congress on Materials Research, Society of Materials Science, Japan, Kyoto, pp 13–18

Tan JJ (1990) Unified form of yield criteria for metallic materials. Chinese Science Bulletin 35(7):555–557

Theocaris PS (1995) Failure criteria for isotropic bodies revisited. Eng Fracture Mechanics 51(2):239–264

Timoshenko SP (1953) History of Strength of Materials: With a Brief Account of the History of Theory of Elasticity and Theory of Structure. McGraw-Hill, New York

Torre C (1947) Einfluß der mittleren Hauptnormalspannung auf die Fließ- und Bruchgrenze. Österreichisches Ingenieur-Archiv I(4/5):316–342

Torre C (1949) Die Grenzzustände statisch beanspruchter Stoffe. Schweizer Archiv für angewandte Wissenschaft und Technik pp 116–121, 145–158

Torre C (1950a) Die Mechanik der Grenzbeanspruchungen. Österreichisches Ingenieur-Archiv IV(1):93–108

Torre C (1950b) Grenzbedingung für spröden Bruch und plastisches Verhalten bildsamer Metalle. Österreichisches Ingenieur-Archiv IV(2):174–189

Tóth LF (1964) Regular Figures. Pergamon Press, Oxford

Tresca H (1868) Mémoire sur l'ecoulement des corps solides. Mémoires Pres par Div Savants 18:733–799

Troost A, Betten J (1974) Zur Frage der Konvexität von Fließbedingungen bei plastischer Inkompressibilität und Kompressibilität. Mechanics Research Communications 1:73–78

Trunin II (1965) Failure criteria under creep conditions in multiaxial stress state (in Russ.: Kriterii prochnosti v usloviyakh polzuchesti pri slozhnom napryazhennom sostoyanii). Prikl Mekhanika 1(7):77–83

Tschoegl NW (1971) Failure surfaces in principial stress space. J of Polymer Science, Part C - Polymer Symposium 32:239–267

Voigt W (1901) Zur Festigkeitslehre. Annalen der Physik, Leipzig 309(3):567–591

Weisstein EW (2021) Trigonometry Angles – Pi/8. https://mathworld.wolfram.com/ TrigonometryAnglesPi8.html

Westergaard HM (1920) On the resitance of ductile materials to combined stress in two or three directions perpendicular to one another. J of the Franklin Institute 189:627–640

Wilczynski AP (1992) Some relationships and limitations of tensorial polynomials strength theories. Composites Science and Technology 44(3):209–213

Wojewódzki W, Jemioło S, Lewiński P, Szwed A (1995) On constitutive relationships modelling the mechanical properties of concrete (in Polish: O relacjach konstytutywnych modelujących własności mechaniczne betonu). Prace Naukowe Politechniki Warszawskiej, Budownictwo 128:1–150

Wronski AS, Pick M (1977) Pyramidal yield criteria for epoxides. J of Materials Science 12(1):28–34

Wu EM (1973) Phenomenological anisotropic failure criterion. In: Broutman LJ, Krock RH, Sendeckyi GP (eds) Treatise on Composite Materials, Academic Press, New York, vol 2, pp 353–431

Wu EM, Scheublein JK (1974) Laminate strength - a direct characterization procedure. In: Berg CA, McGarry FJ, Elliott SY (eds) Composite Materials: Testing and Design (Third Conference), ASTM International, Special Technical Publication 546, Philadelphia

Xiaoping V, Ottosen NS, Thelandersson S, Nielsen MP (1989) Review of constructive models for concrete, EUR 12394 EN. Final Report Ispra, Reactor Safety Programme 1985-1987, Commission of the European Communities, Nuclear Science and Technology, Contract No. 3301-87-12 ELISPDK, Luxembourg

Xu P, Sun Z, Shao S, Fang L (2021) Comparative analysis of common strength criteria of soil materials. Materials 14(15):4302
Yagn YI (1931) New methods of strength prediction (in Russ.: Novye metody pascheta na prochnost'). Vestnik inzhenerov i tekhnikov 6:237–244
Yagn YI (1933) Strength of Materials: Theory and Problems (in Russ.: Soprotivlenie materialov: teorja i zadachnik). Kubuch, Leningrad
Yagn YI, Vinogradov IN (1954) Influence of the shape of the stress deviator upon the strength of metals at plastic deformations (in Russ.: Vlijanie vida deviatora naprjazhenij na soprotivlenie metallov plasticheskomy deformierovaniju). Doklady Akademii Nauk SSSR (Moskva) 96(3):515–517
Yoshimine M, Yu MH, He LN, Iwatate T (2004) The beauty of strength criteria. In: Kleibner M, Legocki A (eds) Int. Symposium on Developments in Plasticity and Fracture, Centenary of M. T. Huber Criterion, August 12–14, 2004, Cracow, Poland, p 1
Yu MH (1961) General behaviour of isotropic yield function (in Chinese). Scientific and Technological Research Paper of Xi'an Jiaotong University pp 1–11
Yu MH (1999) Engineering Strength Theory (in Chinese). Higher Education Press, Beijing
Yu MH (2002) Advances in strength theories for materials under complex stress state in the 20th century. Applied Mechanics Reviews 55(5):169–218
Yu MH (2004) Unified Strength Theory and its Applications. Springer, Berlin
Yu MH (2017) Unified strength theory (UST). In: Feng XT (ed) Rock Mechanics and Engineering, Volume 1: Principles, CRC Press, Balkema, Leiden, pp 425–452
Yu MH (2018) Unified Strength Theory and its Applications. Springer, Singapore
Yu MH, Yu SQ (2019) Introduction to Unified Strength Theory. CRC Press/Balkema, London
Zhang J, Zhang ZX, Huang CP (2011) Representation based classification of strength theories of concrete. In: Advanced Materials Research, vol 168, pp 74–77
Zhang N, Li X, Wang D (2021) Smoothed classic yield function for C2 continuities in tensile cutoff, compressive cap, and deviatoric sections. Int J of Geomechanics 21(3):04021,005
Życzkowski M (1981) Combined Loadings in the Theory of Plasticity. PWN-Polish Scientific Publ., Warszawa